



**POLYMERIC HYDROGEL CONTAINING LIDOCAINE LOADED  
POLYELECTROLYTE COMPLEX FOR  
DRY SOCKET WOUND DRESSING**



**A DISSERTATION SUBMITTED IN PARTIAL FULFILLMENT  
OF THE REQUIREMENTS FOR  
THE DEGREE OF DOCTOR OF PHILOSOPHY IN PHARMACY  
COLLEGE OF PHARMACY**

**GRADUATE SCHOOL, RANGSIT UNIVERSITY  
ACADEMIC YEAR 2022**



สารประกอบเชิงซ้อนพอลิอิเล็กโตรไลต์บรรจุลิโดเคน  
ในรูปแบบเจลเพื่อการรักษาบาดแผล



ดุษฎีนิพนธ์ฉบับนี้เป็นส่วนหนึ่งของการศึกษาตาม  
หลักสูตรปรัชญาดุษฎีบัณฑิต สาขาวิชาเภสัชศาสตร์  
วิทยาลัยเภสัชศาสตร์

บัณฑิตวิทยาลัย มหาวิทยาลัยรังสิต

ปีการศึกษา 2565

Dissertation entitled

**POLYMERIC HYDROGEL CONTAINING LIDOCAINE LOADED  
POLYELECTROLYTE COMPLEX FOR  
DRY SOCKET WOUND DRESSING**

by

NUTTAWUT SUPACHAWAROJ

was submitted in partial fulfillment of the requirements  
for the degree of Doctor of Philosophy in Pharmacy

Rangsit University  
Academic Year 2022

---

Assoc.Prof.Watcharee Khunkitti, Ph.D.  
Examination Committee Chairperson

Assoc.Prof.Pienkit Damprasert, Ph.D.  
Member

---

Asst.Prof.Orawan Theanphong, Ph.D.  
Member

Apirada Sucontphunt, Ph.D.  
Member

---

Asst.Prof.Sucharat Limsithichaikoon, Ph.D.  
Member and Advisor

Approved by Graduate School

(Asst.Prof.Pl.Off. Vanee Sooksatra, D.Eng.)

Dean of Graduate School

September 23, 2022

คุณฉันทิพนธ์เรือง

สารประกอบเชิงซ้อนพอลิโพลีโทไลท์บรจุลิโดเคน  
ในรูปแบบเจลเพื่อการรักษาบาดแผล

โดย  
ฉันทิพนธ์ สุภชา วิจารณ์

ได้รับการพิจารณาให้เป็นส่วนหนึ่งของการศึกษาตามหลักสูตร  
ปริญญาปรัชญาดุษฎีบัณฑิต สาขาวิชาเภสัชศาสตร์

มหาวิทยาลัยรังสิต  
ปีการศึกษา 2565

รศ.ดร.ภญ.วัชรวิ คุณกิตติ  
ประธานกรรมการสอบ

รศ.ดร.เพ็ชรกิจ แดงประเสริฐ  
กรรมการ

ผศ.ดร.ภญ. อรวรรณ เขียวมณีพงษ์  
กรรมการ

ดร.ภญ.เอภีรดา สุคนธ์พันธุ์  
กรรมการ

ผศ.ดร.ภญ. สุชารัตน์ ลิ้มสิทธิชัยกุล  
กรรมการและอาจารย์ที่ปรึกษา

บัณฑิตวิทยาลัยรับรองแล้ว

(ผศ.ร.ต.หญิง ดร.วรรณิ์ สุขสาตร)

คณบดีบัณฑิตวิทยาลัย

23 กันยายน 2565

## Acknowledgments

I would like to acknowledge and thanks my supervisor Asst. Prof. Dr. Sucharat Limsiththichaikoon, for completing this thesis possible. Her guidance and support me through every moment of my project. I would like to thank committee members for making my defense a great experience, as well as for your in interested suggestions and recommendations for develop my research.

I would also like to give special thanks to my family as a whole for their continuous support and understanding when undertaking my research and writing my thesis. My family's encouragement has been the driving force behind my achievement.

Nuttawut Supachawaroj

Researcher



## กิตติกรรมประกาศ

ข้าพเจ้าขอขอบพระคุณอาจารย์ที่ปรึกษา ผศ.ดร.ภญ. สุจารัตน์ ลีมีสิทธิชัยกุล ที่ทำวิทยานิพนธ์ฉบับนี้เกิดขึ้นมาได้รวมถึงได้ให้คำแนะนำและสนับสนุนตลอดทุกช่วงเวลาของการทำงานวิจัย. ข้าพเจ้าขอขอบพระคุณกรรมการทุกท่านที่ทำให้ได้พบกับประสบการณ์ที่ดีในการสอบปกป้องวิทยานิพนธ์ตลอดจนคำแนะนำและข้อเสนอแนะที่น่าสนใจเพื่อนำไปใช้ในการพัฒนาวิจัยต่อไป

ข้าพเจ้าขอขอบคุณเป็นพิเศษกับครอบครัวของฉันสำหรับ ความเข้าใจและการสนับสนุนอย่างต่อเนื่องในช่วงระหว่างทำการวิจัยและเขียนโครงการวิจัยของฉัน. ครอบครัวของฉันก็เป็นกำลังใจที่คอยผลักดันจนประสบความสำเร็จ

ณัฐวุฒิ สุขชาวโรจน์  
ผู้วิจัย

มหาวิทยาลัยรังสิต Rangsit University

6006467 : Nuttawut Supachawaroj  
 Dissertation Title : Polymeric Hydrogel Containing Lidocaine Loaded Polyelectrolyte  
 Complex for Dry Socket Wound Dressing  
 Program : Doctor of Philosophy in Pharmacy  
 Dissertation Advisor : Asst.Prof.Sucharat Limsitthichaikoon, Ph.D.

### Abstract

This study aimed to invent a thermoresponsive hydrogel containing lidocaine hydrochloride (LH) loaded in polyelectrolyte complex (PEC) used in dry socket wound treatment. The PEC, composed of chitosan (CS)–pectin (PC)–hyaluronic (HA), was created by varying the ratio of LH and HA according to 2<sup>3</sup> full factorial experiments. Nine formulations (LC) were assessed, and their physicochemical properties and *in vitro* cytotoxicity were determined. The results showed that the ratio of CS:PC:HA affected particle size, zeta potential, %entrapment efficiency, and cytotoxicity of the LC formulation. The ratio of 0.3:0.1:1.5 and 10% LH provided suitable characteristics of the PEC and was chosen for further investigation. The LC was incorporated into thermoresponsive gel formed from poloxamer407 (P407) in a ratio of 1:1. The effects of LH concentration loaded in PEC were observed in comparison to the LH in P407. All formulations observed that the gelation temperature was in the range of 27-28°C and the gelation time around 2-3 min which is all accepted range in dental routine work. The gels provided good characterization and texture profile analysis which revealed the gel hardness associated with the syringeability, and mucoadhesion. Rheology showed a pseudo-plastic flow behavior, and the LH released from hydrogel indicated sustained drug release by polymeric matrix drug delivery. The gels were 50% degraded in artificial saliva within 48 hours implying biodegradability. The hydrogel provided significantly faster onset and higher pain score reduction compared to standard benzocaine gel in clinical trials without allergy or other side effects. The LH-loaded PEC in the thermoresponsive gel was successfully developed, which could be further used in a dental application.

(Total 97 pages)

Keywords: Dry Socket Wound, Lidocaine Hydrochloride, Polyelectrolyte Complex, Poloxamer 407, Thermoresponsive Hydrogel

Student's Signature ..... Dissertation Advisor's Signature .....

## Table of Contents

		<b>Page</b>
<b>Acknowledgments</b>		<b>i</b>
<b>Abstracts</b>		<b>iii</b>
<b>Table of Contents</b>		<b>v</b>
<b>List of Tables</b>		<b>viii</b>
<b>List of Figures</b>		<b>ix</b>
<b>Abbreviations</b>		<b>xiii</b>
<b>Chapter 1</b>	<b>Introduction</b>	<b>1</b>
	1.1 Background	1
	1.2 Research Objectives	4
	1.3 Research hypothesis	5
	1.4 Research Framework	6
	1.5 Definition of Terms	10
<b>Chapter 2</b>	<b>Literature Review</b>	<b>12</b>
	2.1 Dry socket	12
	2.1.1 Incidence	12
	2.1.2 Patho physiology	13
	2.1.3 Review in treatments	15
	2.2 Lidocaine Hydrochloride (LH)	18
	2.3 Hyaluronic Acid (HA)	20
	2.4 Chitosan	21
	2.5 Pectin	22
	2.6 Polyelectrolyte complexes	23
	2.7 <i>In situ</i> gel	24
	2.8 Poloxamer 407	25



## Table of Contents (Cont.)

		<b>Page</b>
<b>Chapter 3</b>	<b>Research Methodology</b>	<b>26</b>
	3.1 Materials	26
	3.2 Product Development	26
	3.2.1 Development of lidocaine hydrochloride and hyaluronic acid loaded chitosan-pectin polyelectrolyte complex carrier (LC)	26
	3.2.2 Characterizations of LC formulations	28
	3.2.3 <i>In vitro</i> study of cytotoxicity and wound healing	30
	3.2.4 Development of LC incorporated in thermoresponsive polymeric hydrogel (LTP)	31
	3.3 Clinical research in anesthetic efficacy	36
	3.3.1 Inclusion and exclusion criteria	36
	3.3.2 Irritating and allergy tests	37
	3.3.3 Onset and Effective time	38
	3.3.4 Anesthetic efficacy	39
	3.4 Data Analysis	40
<b>Chapter 4</b>	<b>Research Results</b>	<b>41</b>
	4.1 Development of lidocaine hydrochloride and hyaluronic acid loaded chitosan pectin polyelectrolyte complex carrier (LC)	41
	4.1.1 Formulation development	41
	4.1.2 Physicochemical characterization	42
	4.1.3 Morphology observation	51
	4.1.4 Optimization: Factorial analysis and validation	52
	4.2 <i>In vitro</i> study of cytotoxicity and wound healing	55
	4.2.1 Cell viability	55
	4.2.2 Scratch wound assay	59

## Table of Contents (Cont.)

	<b>Page</b>
4.3 Development of lidocaine hydrochloride loaded polyelectrolyte complex incorporated in a thermoresponsive hydrogel.	59
4.3.1 Formulation development	59
4.3.2 The interaction of thermoresponsive gel formation	64
4.3.3 Effects of lidocaine hydrochloride loaded thermoresponsive gel formation on texture profile analysis	66
4.3.4 Drug content	68
4.3.5 <i>In vitro</i> drug release	69
4.3.6 Drug safety	71
4.3.7 <i>In vitro</i> degradation	71
4.3.8 Stability	72
4.4 Clinical research in anesthetic efficacy	73
4.4.1 Irritating and allergy tests	73
4.4.2 Onset and efficacy time	73
4.4.3 Comparison of anesthetic efficacy	73
<b>Chapter 5 Conclusion</b>	<b>75</b>
5.1 Conclusion	75
5.2 Further study	76
<b>References</b>	<b>77</b>
<b>Appendices</b>	<b>86</b>
<b>Appendix A</b> HPLC condition and validation of LH	87
<b>Appendix B</b> Document of clinical research	90
<b>Biography</b>	<b>97</b>

## List of Tables

<b>Tables</b>	<b>Page</b>
1.1 Research Framework	6
3.1 Factors and levels used in 2 <sup>3</sup> Full factorial Designs of independent variables of LH and HA.	27
3.2 Nine different formulations composed of chitosan (CS), pectin (PC), lidocaine hydrochloride (LH) and hyaluronic acid (HA) in various concentrations.	27
3.3 The composition of LTP by varying P407 concentration range 14-18 %w/w	31
3.4 Composition of concentration loaded PEC and unloaded PEC hydrogel	33
4.1 Full factorial design 2 factors 3 levels for optimization of lidocaine hydrochloride (LH) and hyaluronic acid (HA) loaded in chitosan pectin polyelectrolyte complex.	42
4.2 Drug release for 2 hr which the coefficient of correlation (r <sup>2</sup> ) demonstrated in zero-order, first-order, and Higuchi release model	48
4.3 Preliminary study of gelation temperature and gelation time of LC9 incorporated in poloxamer 407 by varying the poloxamer concentration.	60
4.4 Gelation temperature, gelation time, drug content, and stability	62
4.5 TPA of the 4 formulations That present in Hardness, Syringibility	68
4.6 Drug release over 8 hours according to zero-order, first-order, and Higuchi release models, including the coefficient of correlation (r <sup>2</sup> ), slope (k), and intercept.	71

## List of Figures

<b>Figures</b>	<b>Page</b>
1.1 Dry socket wound after right lower wisdom tooth surgical removal	1
2.1 Pathophysiology of tooth socket and dry socket and pain pattern	13
2.2 Pathway of dry socket	14
2.3 Kinin pathway modified from	14
2.4 (a) gauze strip and cotton pallet, (b) clove oil, (c) gauze soak clove oil for dry socket wound dressing.	17
2.5 (a) Alvogyl <sup>®</sup> , (b) Pack Alvogyl <sup>®</sup> into the socket to treat dry socket	18
2.6 Structure of lidocaine hydrochloride retrieved from	19
2.7 Structure of hyaluronic acid	21
2.8 Structure of chitosan structure	21
2.9 Pectin structure	23
2.10 Model of polyelectrolyte complex structure, (a) Ladder-like, (b) Scrambled-egg	24
2.11 Structure of poloxamer 407	25
3.1 Flow consort diagram of the irritating and allergy tests	37
3.2 Flow consort diagram of the anesthetic human trials; (a) Onset of anesthesia ( $T_{on}$ ) the effective time ( $T_{eff}$ ) of LCT; (b) Comparison efficacy of this split-mouth randomized trial between LG and BG	38
3.3 Box table of pinprick test at the palate and random table	39
4.1 The development of polyelectrolyte complexes and the three different polymeric structures Chitosan, pectin, hyaluronic acid, and polyelectrolyte complex chemical structures.	42

## List of Figures (Cont.)

Figures	Page
<p>4.2 The comparison of particle size (gray columns) and polydispersity index (PDI) (red dot) (a) and zeta potential of LC formulations varied using a 32factorial design (b), with white columns representing the zeta potential of freshly prepared LC (day 0) and grey columns representing zeta potential values after 3 months of LC storage at room temperature. The error bars represent standard deviations (n = 6); the symbols indicate significant changes at <math>p &lt; 0.05</math>: *when compared to freshly prepared and (3 months) stored LCs, using Student's t-test.</p>	43
<p>4.3 Comparison in viscosity of the formulation (white columns) and % mucoadhesiveness at 0 (red line), 15 (yellow line), 30 (blue line) and 60 min (green line). Error bars represent standard deviations (SD) (n = 6).</p>	45
<p>4.4 Comparison of percentage of entrapment efficiency (white column) and viscosity of freshly prepared LC formulations (red line). Error bars represent standard deviations (SD) (n = 6).</p>	46
<p>4.5 Comparison of percentage of cumulative drug-release of 9 formulations of LC varied in 32 factorial designs at 24 hr. which data are average % cumulative amount <math>\pm</math> SD (n = 6). Error bars represent standard deviations (SD) (n = 6).</p>	49
<p>4.6 At room temperature, the stability of LC1 to LC9 formulations was tested (a) immediately after preparation, (b) 15 minutes later, and (c) three months later. When compared to freshly prepared, LC1–LC3 particles began to separate quickly within 15 minutes, but LC4–LC7 took three months to fully separate. These PEC formulations were stable, as evidenced by the homogeneous solutions of LC8 and LC9.</p>	50

### List of Figures (Cont.)

Figures	Page
4.7 SEM images of LC5 (a), LC8 (b), and transmission electron microscopy (TEM) images of LC5 (c) and LC8 (d), all at 25,000 magnification, show molecular dispersions of LH in PEC form between 50 and 100 nm. PEC particles are indicated by the red arrows, while polymeric micelles are indicated by the white arrows.	52
4.8 Response surface plot and contour plot of independent variables LH (lidocaine hydrochloride) and HA (hyaluronic acid) on (a) particle size, (b) zeta potential, (c) entrapment efficiency, and (d) drug release at 5 min.	54
4.9 Percentage of cell viability by MTT assay (n = 8) at 24 hr of control in blank DMEM as negative control, HA (-), HA (0), HA (+), DMEM with FBS for positive control, chitosan-pectin-hyaluronic polyelectrolyte complex (PEC) and Zinc phosphate (Zn) (a) in comparison with cells viability of formulation LS, LC3, LC6 and LC9 in a concentration of 50-1000 $\mu\text{g/ml}$ . Error bars represent standard deviations; symbols indicate significant differences at $p < 0.05$ : * compared to the negative controls (DMEM), and # compared between LS and LC at the same concentration, using student <i>t</i> -test.	56
4.10 (a) Representative images from <i>in vitro</i> scratch wound healing assays demonstrating that cell migration into gap is accelerated in LC3, LC6, LC9 when compared to controls (DMEM) and accelerated healing condition (DMEM FBS). (b) Summary bar graph of wound distance at indicated time points during the scratch.	58
4.11 LTPs at 4°C were presented in solution phase	60
4.12 LTPs at 37°C temperature, LTP1 were presented in solution phase and LTP2 and 3 in gel phase.	61
4.13 Gelation temperature and gelation time of LTP (F1, F2, F3 and F4)	62
4.14 Rheology of four formulations and blank. (a) Shear stress; (b) Viscosity	63

**List of Figures (Cont.)**

	<b>Page</b>
<b>Figures</b>	
4.15 FTIR of F1, F2, F3, F4 and BG.	65
4.16 DSC of LH, F1, F2, F3, and F4.	66
4.17 The comparison of TPA of the 4 formulations of Li HCl hydrogel (F1, F2, F3, and F4) That present in the table or graft for Hardness	67
4.18 Maximal force of detachment (Fmax) experiments at 37 °C using four formulation Li HCl hydrogels. The values represented are the mean $\pm$ SD (n = 3).	68
4.19 % Cumulative drug release profile of formulation F1, F2, F3, F4 and 5% LH solution.	70
4.20 Degradation of formulation F1, F2, F3 and F4 in artificial saliva at 37°C	72
4.21 Drug stability of F1, F2, F3 and F4 keep at 4°C, 30°C and 45°C	73
4.22 Box plots and summary showing the VAS(cm) during palatal injection to compare anesthetic efficacy of LTP (F3) hydrogel and topical Benzocaine gel.	74

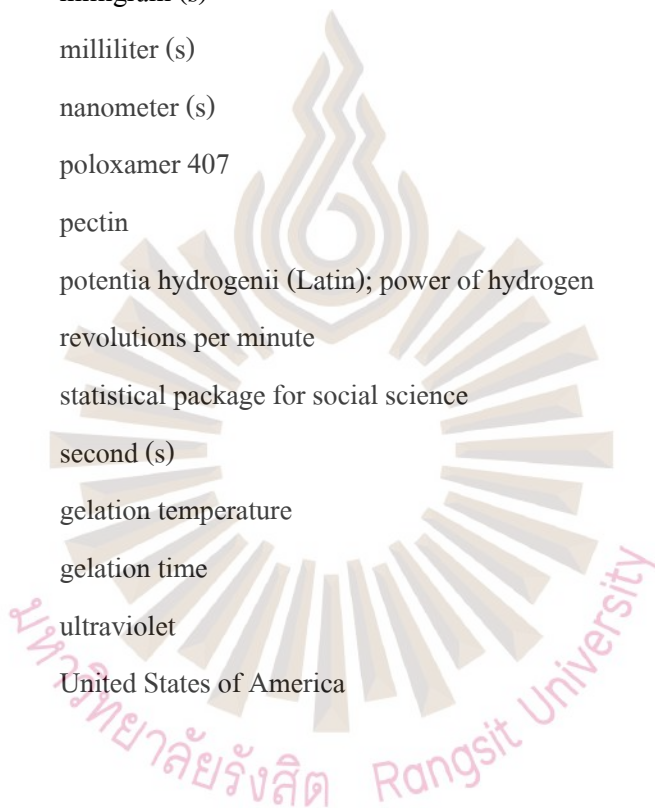
## Abbreviations

<b>Abbreviation</b>	<b>Meaning</b>
%	percentage(s)
%DL	percent drug loading capacity
% EE	percent of entrapment efficiency
%w/w	percent weight by weight
°C	degree Celsius
$r^2$	coefficient of determination
$\mu\text{g}$	microgram (s)
$\mu\text{L}$	microliter (s)
$\mu\text{m}$	micrometer (s)
n	viscosity
$\eta$	solvent release exponent value
AO	alveolar osteitis
CS	chitosan
cm	centimeter (s)
e.g. (Latin);	<i>et alia</i> (Latin abbreviation)
<i>et al.</i>	<i>et alia</i> (Latin abbreviation of “and others”, For references with more than two authors)
g	gram (s)
G (needle)	gauge
HA	hyaluronic acid
HPLC	high-performance liquid chromatography
hr	hour (s)
ICH	International Conference on Harmonization
LC	Lidocaine loaded into the chitosan–pectin–hyaluronic acid polyelectrolyte complex
LH	lidocaine hydrochloride



**Abbreviations (Cont.)**

<b>Abbreviation</b>	<b>Meaning</b>
LTP	lidocaine loaded in polyelectrolyte complex incorporate poloxamer for thermosetting gel
min	minute (s)
mg	milligram (s)
mL	milliliter (s)
nm	nanometer (s)
P407	poloxamer 407
PC	pectin
pH	potentia hydrogenii (Latin); power of hydrogen
rpm	revolutions per minute
SPSS	statistical package for social science
sec	second (s)
Tgel	gelation temperature
TimeG	gelation time
UV	ultraviolet
USA	United States of America



## Chapter 1

### Introduction

#### 1.1 Background

One of the most prevalent consequences following wisdom teeth extraction and surgical removal is dry socket (Tarakji, Saleh, Umair, Azzeghaiby, & Hanouneh, 2015). It is an extremely painful complication. Various words have been used to describe the dry socket, including alveolar osteitis (AO), and localized osteitis (Figure 1.1). The most recent definition is “postoperative pain in and around the extraction site, which increases in severity at any time between 1 and 3 days after the extraction accompanied by a partially or totally disintegrated blood clot within the alveolar socket with or without halitosis” (Blum, 2002).



Figure 1.1 Dry socket wound after right lower wisdom tooth surgical removal

Source: Mamoun, J., & Mamoun, J., 2018

The prevalence of dry sockets is documented in a variety of sources. The incidence of dry socket has been observed to be between 0.5% and 5%. Dry socket after extraction of mandibular third molars ranges from 1% to 45%.

According to the literature, the development of dry socket occurs 1-3 days following tooth extraction. Within a week, 95-100% of all instances of dry socket were recorded. The length of the dry socket is determined on the severity of the illness and typically ranges from 5 to 10 days.

There are many theories concerning the clear pathophysiology, however the true etiology is unknown. Birn (1973) proposed that enhanced local fibrinolysis causes a lysis clot by converting plasminogen to plasmin. As a primary cause in the pathogenesis of dry socket, clinical presence of denuded alveolar bare bone with intense pain from enhanced local fibrinolytic activity. The clot is destroyed by mediators released during inflammation by direct or indirect activation of plasminogen into the circulation (physiologic) and indirect (non-physiologic) from streptokinase and staphylokinase, all of which are generated by bacteria.

Many studies have found a variety of factors that contribute to dry socket development, for example, the role of trauma as a contributing factor in surgery. Trauma during extraction transfer to the jawbone around the roots and injury bone on the extraction socket surface might cause necrosis or apoptosis of osteoblasts within the extraction socket. Many studies have been published on the prevalence of dry sockets in smokers and users of oral contraceptives.

Because of the complex etiology, the treatment of dry sockets is different for each dentist. Exposed alveolar bone is a symptom of Alveolar osteitis caused by partial or complete blood clot lysis, which was treated by covering the exposed bone for many days to protect it from painful mechanical stimulation, food impaction, and bacterial infiltration. The most common symptom of this illness is pain, which is caused by the conversion of plasminogen to plasmin and the production of kinins. Kinins then stimulate the main afferent nerves, causing pain. Many etiologies and contributing factors of AO were shown but the main objective of treatment is a relief of the severe pain and to promote alveolar wound healing. The duration of AO varies

according on the severity of the condition, but it often runs from 5 to 10 days, which is frequently lost after returning to treatment with a dentist.

Lidocaine hydrochloride (LH) is one of the worldwide topical anesthesia. LH topical has a fast onset (1–2 minutes) and a high effectiveness within 5 minutes. (Lee, 2016) but short active duration (15 min).

Chitosan (CS), a cationic polymer with a positive charge due to primary amine functional groups, is widely utilized due to its biocompatibility and biodegradability (Wang et al., 2011).

Pectin (Pec) is well-known as a non-toxic, natural anionic polymer (Das, Chaudhury, & Ng, 2011). Weal polyanionic is easily generated from a stable polyelectrolyte combination with a positive charge biopolymer.

Chitosan and pectin interact with positive and negative charges to form complexes that, when combined with a medication of interest, can provide rapid and prolonged drug release. (Mitrevej, Sinchaipanid, Rungvejhavuttivittaya, & Kositchaiyong, 2001; Morris et al., 2016).

Hyaluronic acid (HA) is a glycosaminoglycan with a high molecular weight that is found in the extracellular matrix. HA is a biocompatible substance with anti-inflammatory, bacteriostatic, anti-edematous, and antioxidative effects. (Dahiya & Kamal, 2013). Hyaluronan, often known as HA, accelerates the healing of oral wounds by promoting cell proliferation, matrix cell migration into the granulation tissue matrix, and granulation tissue organization. (Asparuhova, Kiryak, Eliezer, Mihov, & Sculean, 2019).

Polyelectrolyte complexes (PECs) are self-assembling nanoparticles generated by electrostatic interactions between oppositely charged polyanions and polycations. (Abueva, Kim, Lee, & Nath, 2015; Limsitthichaikoon & Sinsuebpol, 2019) Electrostatic interactions between negatively charged macromolecules produce a variety of shapes and properties, such as spherical or wormlike micelles and hydrogels (Priftis et al., 2014). According to PEC features such as

controlled release, mucoadhesiveness, biocompatibility, and biodegradability, PEC has recently been used in studies for target medication delivery as well as medical devices for topical skin and mucosal applications. (Buriuli & Verma, 2017; Ishihara, Kishimoto, Nakamura, Sato, & Hattori, 2019; Potaś, Szymańska, & Winnicka, 2020)

Poloxamers are thermosetting polymers that are widely used in *in situ* gel systems in the world. Poloxamer 407 (P407) is a triblock copolymer comprising polyoxyethylene and polyoxypropylene. P407 is employed because of its excellent solubility, low toxicity, controlled drug release, and biocompatibility. P407 thermosetting hydrogels have been studied as useful mucosal drug delivery systems because they are non-irritating on the skin and mucosal membranes, control concentration for an extended period of time, and minimize efficacy dosage and side effects. The goal is to achieve a controlled release. aim of obtaining a controlled release.

The primary goal of this study was to look into a lidocaine hydrochloride-loaded chitosan-pectin-hyaluronic polyelectrolyte complex for fast onset and sustained release in the treatment of dry socket wounds. Particle size, polydispersion index, zeta potential, morphology, mucoadhesive, entrapment efficiency, loading capacity, percentage of medication released, cytotoxicity, and storage stability were all investigated, investigate a lidocaine hydrochloride-loaded ternary polyelectrolyte complex incorporated in P407 gel for physiochemical characteristic, factors affecting phase inversion from sol to gel of LH loaded in PEC thermosensitivity gel, rheology and viscosity, drug release, texture profile analyzer mucoadhesive effect, syringe injectability, biocompatibility, biodegradability and high anesthetic effective in animal and human.

## 1.2 Research Objectives

1.2.1 To develop and evaluate the physicochemical properties of lidocaine hydrochloride loaded in polyelectrolyte complex and poloxamer thermoresponsive hydrogel for dry socket treatment.

1.2.2 To evaluate the effective interaction of lidocaine hydrochloride loaded in polyelectrolyte complex and poloxamer thermoresponsive hydrogel for dry socket.

1.2.3 To evaluate the effectiveness of lidocaine hydrochloride loaded in polyelectrolyte complex and poloxamer thermoresponsive hydrogel for dry socket in humans.

### **1.3 Research hypothesis**

1.3.1 Design and optimization in lidocaine hydrochloride, Hyaluronic acid concentration could influence the physiochemical property of lidocaine hydrochloride and hyaluronic acid loaded chitosan pectin polyelectrolyte complex.

1.3.2 Design and optimization in lidocaine hydrochloride, Hyaluronic acid concentration could influence cytotoxicity of formulation and wound healing invitro study of lidocaine hydrochloride and hyaluronic acid loaded chitosan pectin polyelectrolyte.

1.3.3 Design and optimization in lidocaine hydrochloride, Hyaluronic acid concentration could influence the physiochemical property of lidocaine hydrochloride and hyaluronic acid loaded chitosan pectin polyelectrolyte complex incorporates poloxamer gel

1.3.4 Lidocaine hydrochloride and hyaluronic acid loaded chitosan pectin polyelectrolyte complex incorporates poloxamer gel can effective in anesthetic efficacy in clinical.



## 1.4 Research Framework

Table 1.1 Research Framework

Overall Objective	Specific Objective	Methodologies	Expected outcome
I. Development of lidocaine hydrochloride and hyaluronic acid loaded chitosan pectin polyelectrolyte complex carrier	I. Design and optimization in physicochemical property vary in: - lidocaine hydrochloride concentration - hyaluronic acid concentration	Formulation and preparation of lidocaine HCl and hyaluronic acid loaded chitosan pectin polyelectrolyte complex	Preparation of suitable formulations proper in: - Size, zeta - Drug release - %Entrapment efficiency - %Drug release (5min) - Mucoadhesive - Preliminary stability
	II. Determination of the morphology - Prove the larger morphology	SEM, TEM	Confirm morphology in structure and interaction
II. <i>In vitro</i> study of cytotoxicity and wound healing	I. <i>Safety formulations</i>	<i>In vitro</i> cytotoxicity test by MTT assay in human gingival fibroblast.	Appropriate safety formulation as a wound dressing
	II. Wound healing property ( <i>in vitro</i> cell culture)	Scratch wound assay - % wound closure	

Table 1.1 Research Framework (Cont.)

Overall Objective	Specific Objective	Methodologies	Expected outcome
III. Development and comparison of lidocaine hydrochloride loaded chitosan pectin polyelectrolyte complex thermoresponsive hydrogel	I. Determine sol to gel transition by varying poloxamer407 concentration.	Gelation temperature and time observation	Appropriate formulation in objectives: - Gelation temp in $37 \pm 2^\circ\text{C}$ - Gelation time in 3-5 min
	II. Morphology observation	FTIR analysis - Functional group bonding interaction	Polyelectrolyte complex hydrogel interaction
		DSC measurement - Thermal differential scanning.	
	IV. Physicochemical properties of lidocaine hydrochloride loaded chitosan pectin polyelectrolyte complex thermoresponsive hydrogel		1. Gel appearance, pH, phase separation, rheology (using Brook field viscometer in oscillatory mode), and viscosity (Brook field viscometer)
2. Texture Profile Analysis, syringeability, mucoadhesive test using a texture analyzer (TA.XT PlusC, Stable Micro Systems, USA)			- Physical property in hardness - Suitable formulation that is easy to injectable - Mucoadhesive force



Table 1.1 Research Framework (Cont.)

Overall Objective	Specific Objective	Methodologies	Expected outcome
III. Development and comparison of lidocaine hydrochloride loaded chitosan pectin polyelectrolyte complex thermoresponsive hydrogel (Cont.)	IV. Physicochemical properties of lidocaine hydrochloride loaded chitosan pectin polyelectrolyte complex thermoresponsive hydrogel (Cont.)	3. Drug content - Measurement by HPLC analysis	Amount of drug in the formulation
		4. % Drug releasing using Franz diffusion cell approach and determined the amount of lidocaine released by HPLC analysis	The appropriate formulation in drug release: - Fast-release activity - Sustained releasing
		5. Evaluate bacterial contaminated -Total plate count, Total Yeast and Mold, <i>Escherichia coli</i> , <i>Staphylococcus aureus</i>	- Drug safety
		6. Biodegradable property - <i>In Vitro</i> degradation test - Different gel weights in an initial and different time (1-5 days)	Biodegradable gel - erosion period in artificial saliva

Table 1.1 Research Framework (Cont.)

Overall Objective	Specific Objective	Methodologies	Expected outcome
III. Development and comparison of lidocaine hydrochloride loaded chitosan pectin polyelectrolyte complex thermoresponsive hydrogel (Cont.)	IV. Physicochemical properties of lidocaine hydrochloride loaded chitosan pectin polyelectrolyte complex thermoresponsive hydrogel	7. Stability - Accelerated stability test Follow ICH guideline - Evaluate physical property	The proper formulation in stability
IV. Clinical research in anesthetic efficacy	I. Safety	Safety test - Allergy - Drugs or products irritate	Allergy, irritated screening
	II. Onset and Effective time	Pinprick test - Time of pain when VAS score has an initial reduction. - Time of pain that VAS is Zero	The appropriate formulation in short onset with long-acting
	III. Comparing anesthetic efficacy	Pain score (VAS)	Comparing efficacy between LG and BG

## 1.5 Definition of Terms

**Gelation Temperature** “Temperature at which the biodegradable block copolymer undergoes reverse thermal gelation, i.e., the temperature below which the block copolymer is soluble in water and above which the block copolymer undergoes a phase transition to increase in viscosity or to form a semi-solid gel.”

**Gelation Time** “The gelation time is the amount of time it takes for the plastic encapsulant in the liquid form to transform into a gel.”

**Pinprick** “A test for cutaneous pain receptors. A small, clean, sharp object such as a pin or needle is gently applied to the skin or mucosa and the patient is asked to describe the sensation.”

**Polyelectrolyte Complexes** “the association complexes from between oppositely charged particles (e.g. polymer-polymer, polymer-drug and polymer-drug-polymer).”

**Split Mouth Method** “Split-mouth designs are frequently used in dental clinical research, where a mouth is divided into two or more experimental segments that are randomly assigned to different treatments. It has the distinct advantage of removing a lot of inter-subject variability from the estimated treatment effect.”

**Thermoresponsive Hydrogel** “subclass of the supramolecular hydrogels that gelate via hydrophobic interactions. Thermogels can undergo a sol-gel phase transition because they are constituted of amphiphilic polymers with both hydrophilic parts and hydrophobic parts.”

**Visual Analog Scale** “A tool used to help a person rate the intensity of certain sensations and feelings, such as pain. The visual analog scale for pain is a straight line with one end meaning no pain and the other end meaning the worst pain imaginable. A patient marks a point on the line

that matches the amount of pain he or she feels. It may be used to help choose the right dose of pain medicine. Also called VAS.”



## Chapter 2

### Literature Review

#### 2.1 Dry socket

Dry socket or Alveolar osteitis is the most common complication that occurs after tooth extraction and surgical removal of a wisdom tooth (Shevel, 2018; Tarakji et al., 2015). Many technical terms for dry socket, such as alveolar osteitis (AO), localized osteitis, several other terms have been used in referring to dry socket, such as alveolar osteitis (AO), localized osteitis, postoperative alveolitis, alveolalgia, alveolitis sicca dolorosa, septic socket, necrotic socket, localized osteomyelitis, and fibrinolytic alveolitis. The problem is severe pain that is causing the patient has many visits to return to the hospital and is characterized by persistent postoperative pain after the surgery and is not relieved by mild analgesics (Metin, Tek, & Sener, 2006).

##### 2.1.1 Incidence

Many studies have been reported about the incidence of the dry socket that reported about 1-5% overall. The incidence of dry socket after extraction of mandibular third molars varies from 1-45% (Blum, 2002b; Fridrich & Olson, 1990; Mamoun, J., & Mamoun, J., 2018). In literature, the onset of dry socket is considered to occur 2-4 days after tooth removal (Cardoso, Rodrigues, Ferreira, Garlet, & De Carvalho, 2010). The duration of dry socket depending on the severity of the disease usually ranges from 5-10 days (Gowda, Viswanath, & Kumar, 2013).

Alveolar osteitis is diagnosed based on clinical findings and subjective symptoms. Clinical findings included indications of one or more of the following: partial or complete absence of clot and exposed bone. Subjective symptoms included persisting or increased postoperative pain 2 or 3 days after surgery, as well as a throbbing pain at the surgical site (Metin et al., 2006).

Normal healing pain in the tooth socket began when the anesthetic agent's effect was removed, and pain increased to a higher level in around 10-24 hours. After that, the pain decreased until 2-3 days. The pain pattern of the dry socket differs in that it appears normal on the first day but increases and responds poorly to oral analgesics on the second or third day (Figure 2.1).

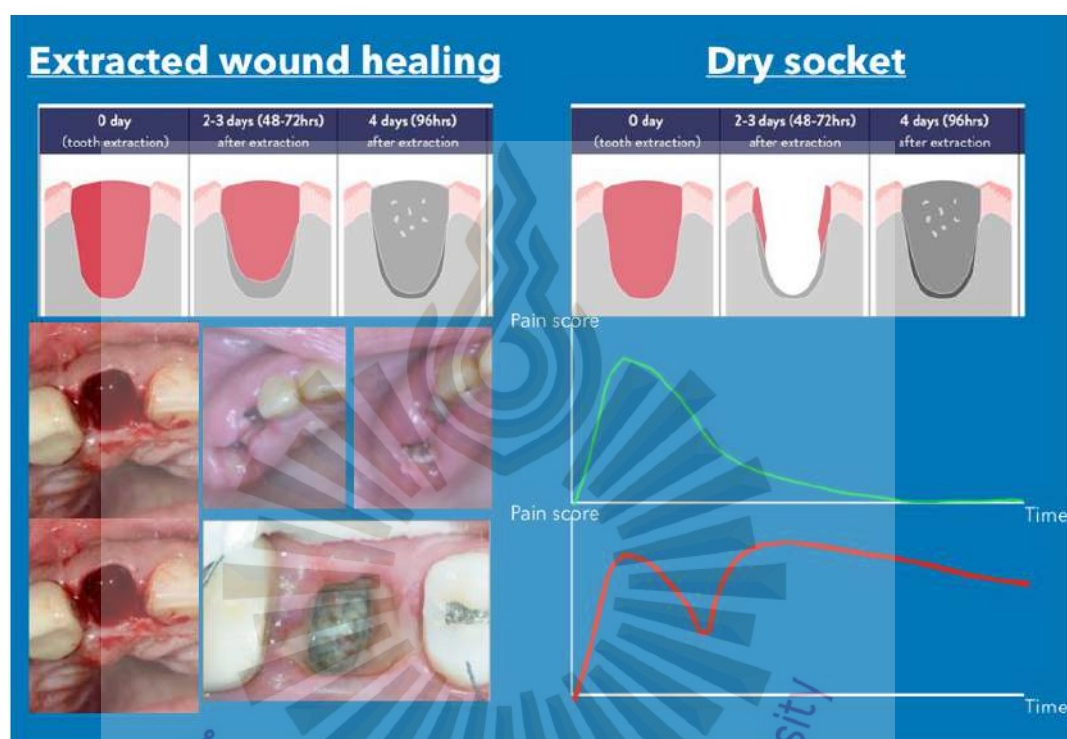


Figure 2.1 Pathophysiology of the tooth socket and dry socket and pain pattern

Source: Metin et al., 2006

### 2.1.2 Patho physiology

According to certain pathogenic theories, hyperfibrinolysis causes clot lysis by converting plasminogen to plasmin. The fibrinolysis is caused by the activation of the plasminogen pathway. The fibrinolysis pathway has two directions: direct or indirect activator chemicals. Following alveolar bone trauma, direct activators are released. Bacteria produce indirect activators (Figure 2.2). According to the literature, active plasmin is inactivated in the systemic circulation by antiplasmins (Lucas, Fretto, & Mckee, 1983). The plasminogen converts to plasmin and produces kinins, which stimulates the main afferent neurons to create pain (Figure 2.3), but the concept of dry socket etiology and healing

inflammation does not indicate that dry socket is the cause in all situations (Mamoun, J., & Mamoun, J., 2018).

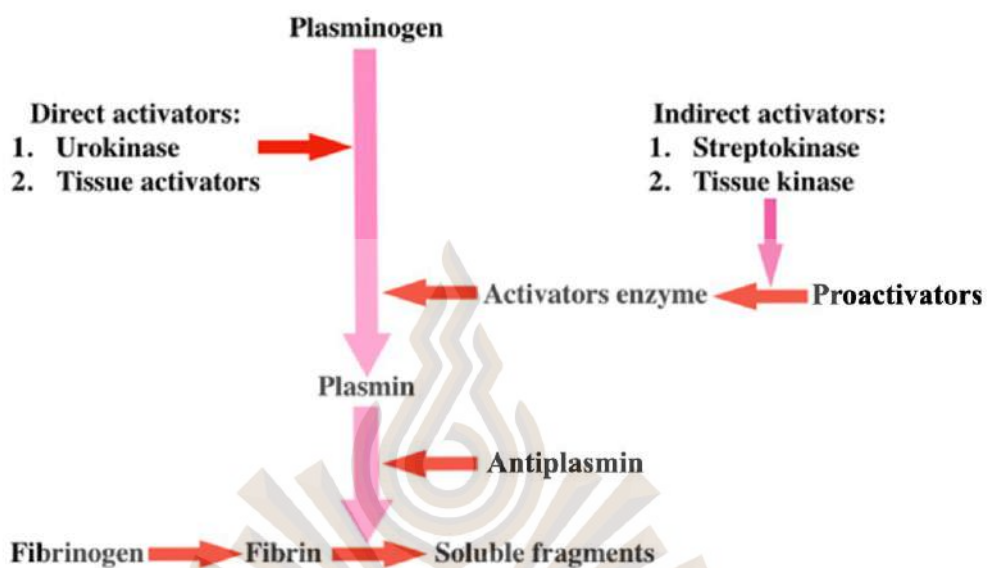


Figure 2.2 Pathway of dry socket

Source: Gowda et al., 2013

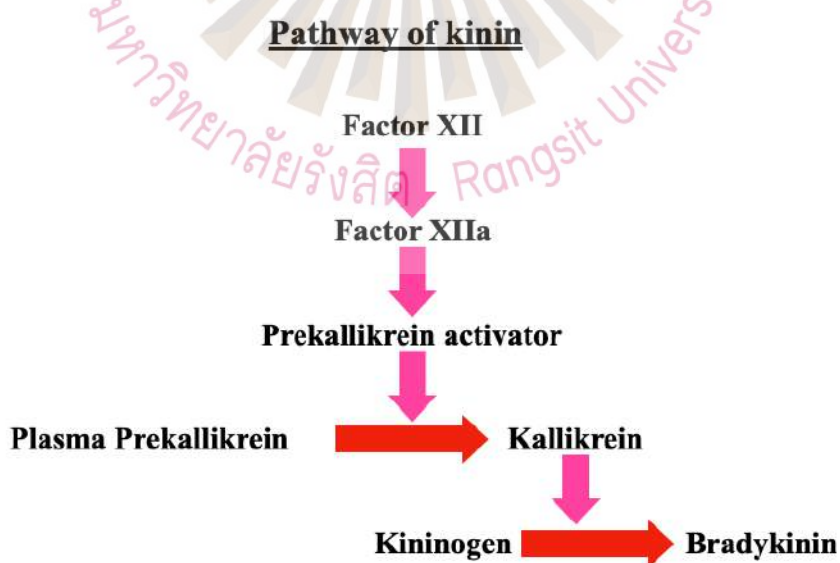


Figure 2.3 Kinin pathway modified from

Source: Isordia-Salas, Pixley, Sáinz, Martínez-Murillo, & Colman, 2005

On the other hand, investigations from the 1970s and afterward revealed several studies concerning the causes of dry sockets. A thorough examination of the etiology of dry socket revealed that the exact pathophysiology is unknown. Birn (1973) proposed that the etiology of dry socket enhanced fibrinolysis activity and occurred earlier in clot breakdown than usual. However, several factors, including smoking, surgical trauma, oral contraceptive drugs, and Menstrual Cycle, as well as excessive irrigation or curettage, have been linked to the genesis of dry socket (Tarakji et al., 2015), however, most theories remain controversial.

Because of the complicated etiology, the treatment of dry socket is due to each dentist. The misconception in bacteria is a cause of dry sockets, aseptic and antiseptic procedures that have been implemented based on this theory (Wald, 1932). Since then, a large number of antibiotics have been studied.

The condition cannot be treated until the underlying cause is determined, but exposed alveolar bone is a sign of dry socket from a partial or complete lysis blood clot that was treated by covering the exposed bone to protect the bone from activating the primary afferent nerves due to bone exposed to induce pain, and pain is the main symptom of this pathology. The management is the relief of the patient's pain, promotes alveolar wound healing and prevents bacterial infection during the healing stages until normal healing.

### **2.1.3 Review of treatments**

2.1.3.1 Dry socket treatment from review in many studies has been reported for 2 major techniques.

#### **(1) Non-dressing treatment**

Irrigate the socket with sterile normal saline for cleaning and prescription oral analgesic for relieving pain.

#### **(2) Dressing treatment.**



The pathology from hyperfibrinolysis and barebone with the free nerve exposed, from this idea of dressing to close bare bone and protect free afferent nerve exposed. The idea of close with wound dressing for protecting barebone was developed

The dressings technique can be classified as follows:

- (2.1) Antibacterial dressings such as clindamycin, metronidazole, and chlorhexidine.
- (2.2) Obtundent dressings such as Eugenol with strip gauze.
- (2.3) Topical anesthetic dressings such as Lidocaine, Oraqi gel<sup>®</sup>.
- (2.4) Promotes wound healing such as SaliCept Patch<sup>®</sup> (Acemannan Hydrogel), Honey, Platelet-rich fibrin.
- (2.5) Combinations technique. such as Alvogyl<sup>®</sup>.

The antibiotic dressing alone occurs from some hypothesis that belief about the bacterial cause of dry socket (Blum, 2002a). However, there is small evidence that antibiotics given after extraction reduce the incidence of dry socket (Lodi, Figini, Sardella, Carrassi, & Furness, 2012).

Only obtundent or topical anesthetic dressing is used for reducing pain but no accelerated effect for wound healing. The report in topical anesthetic gel produced a significantly greater reduction in pain in the dry socket than the eugenol over the next 48 hours, the pain level was nominally less with the thermosetting gel, but this difference was not statistically significant (Burgoyne, Giglio, Reese, Sima, & Laskin, 2010).

The combination group was done in many objectives such as obtundent or anesthetic agent with antimicrobial but a lot of dressings delay healing of the tooth extraction socket.

2.1.3.2 The common treatment in Thailand in dressing treatment has two groups.

- (1) Gauze or cotton pallet with medications.

Gauze strip or cotton soak with clove oil or surgical ointment pack in the socket (Figure 2.4.) and appointment the patient for change every 2-3 days and remove it when no pain and barebone was closed with granulation tissue. This technique is a low-cost medication but needs many times of appointments for treatment.



Figure 2.4 (a) gauze strip and cotton pallet, (b) clove oil, (c) gauze soak clove oil for dry socket wound dressing.

Source: Researcher

## (2) Alvogyl<sup>®</sup>

Alvogyl<sup>®</sup> is a commercial dry socket wound dressing that is the most favorite in Thailand (Figure 2.5) It contains eugenol, iodoform, butamben (mild anesthetic properties) and penqhwar.

Alvogyl<sup>®</sup> was used to pack in sockets that were diagnosed in the dry socket to cover bare bone and relieve pain. Supe (2018) showed the efficacy of Alvogyl<sup>®</sup> that is better for the management of dry socket with a short time for complete pain relief, fewer visits for dressing change, and faster clinical healing of the socket.



Figure 2.5 (a) Alveogyl<sup>®</sup>, (b) Pack Alveogyl<sup>®</sup> into the socket to treat dry socket

Source: Mamoun, J., & Mamoun, J., 2018

Faizel (2015) reported on retardation of healing when the tooth sockets were packed with Alveogyl<sup>®</sup> that present in exposed bone continue 7 days after treatment. The remaining wound dressing is a problem of healing in the dry socket that retards wound healing, the dentist has to make an appointment to remove it which is the cost to the patient. Revisit for clean or sometimes change the new one to prevent infection from dirty wound that impact in a gauze dressing and retard wound healing.

As a result, the objective of dry socket wound dressing should be fast relief of pain, biodegradability for a reduced period of removal dressing, not retard wound healing and promote healing to reduce the healing time of dry socket.

## 2.2 Lidocaine Hydrochloride (LH)

Lidocaine is an amide-based local oral topical anesthetic medication (Figure 2.6). Lidocaine is a white, odorless crystal with a bitter and numb taste. It is readily soluble in water, ethanol, and organic solvents such as water (50 mg/mL), chloroform, ethanol, and benzene but insoluble in ether. The onset of effect is roughly 1-2 minutes, and the duration of action is approximately 15 minutes.

Lidocaine is an efficient and dependable local anesthetic that has been frequently utilized in the dentistry procedure of early onset topical anesthesia. Lidocaine works on the peripheral nerves to reduce the sense of pain at the site of application, and it is used to manage local pain from various dental procedures (Lee, 2016).

Topical lidocaine inhibits voltage-gated sodium channels of peripheral nociceptor in A-delta and C fiber or neuropathic pain (Moore, Derry, & Mcquay, 2014), which was our goal in dry socket pain from the free nerve ending. Topical lidocaine is offered in 5% patches for post-therapeutic neuralgia therapy, which is a conventional treatment after tricyclic antidepressants, anticonvulsants, and opioids fail.

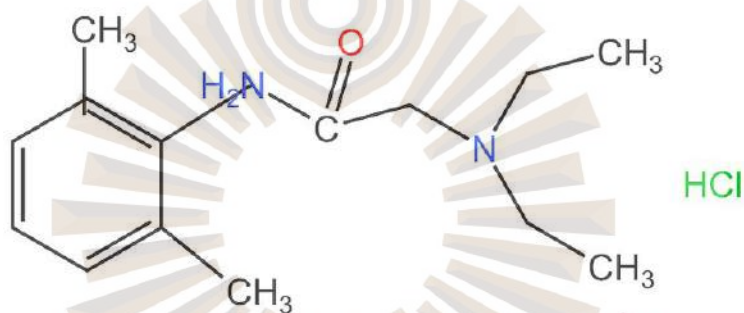


Figure 2.6 Structure of lidocaine hydrochloride retrieved from

Source: Omer & Ali, 2017

Compared with analgesic drugs, a local anesthetic was used to avoid adverse effects in a high dose of systemic NSAIDs, for example, less gastrointestinal effects and cardiovascular disease, especially in the patient with sensitivity to the oral route (Feres, Teles, Paulo, & Paulo, 2016). In addition, the high doses of acetaminophen cause liver damage and tramadol overdoses may cause brain damage. Long-term opioid use cause drug addiction.

Benzocaine is the most commonly used topical anesthetic in dentistry, with an onset time of 30 seconds and a duration of five to 10 minutes. Other contraindications for using benzocaine include ester allergies and methemoglobinemia.

Lidocaine has an advantage over benzocaine in methemoglobinemia as a cause of respiratory problems in infected patients exposed to topical anesthetics which is a mortal complication and many studies about benzocaine use may result in more cases of methemoglobinemia than lidocaine (Vallurupalli & Manchanda, 2011). The duration of lidocaine is longer than benzocaine and the ester type of benzocaine has an incidence of allergy more than amide.

### **2.3 Hyaluronic Acid (HA)**

Hyaluronic acid is a component of the extracellular matrix of high molecular weight glycosaminoglycan (Figure 2.7). HA was found in high concentrations in many tissues such as soft connective tissues, skin, umbilical cord, and synovial fluid. HA was shown in highly biocompatible and nonimmunogenic characteristics HA has led to its usage in a variety of therapeutic applications, including joint fluid in arthritis; as surgical assistance in eye surgery; and to promote bone repair and regeneration, surgical wounds, and wound healing. The anti-inflammation of HA was presented by removing prostaglandins, metalloproteinases, and other bioactive compounds, which may explain why HA has an anti-inflammatory effect. The bacteriostatic activity was demonstrated at high concentrations of medium and lower molecular weight. HA has the most potent bacteriostatic impact, notably on *Aggregatibacter actinomycetemcomitans*, *Prevotella oris*, and *Staphylococcus aureus* strains seen in oral gingival lesions. Anti-edematous of HA may also potentially be related to the osmotic activity. Because of its ability to accelerate tissue repair, it might be utilized as an adjuvant to mechanical treatment and antioxidant (Dahiya & Kamal, 2013).

The role of HA in healing oral wounds is as follows; Hyaluronan promotes cell proliferation, migration of matrix cells into granulation tissue matrix and granulation tissue organization. Eed (1997) demonstrated that low molecular weight HA has a marked angiogenic effect. In addition, autologous bone combined with an esterified low-molecular HA preparation showed accelerating new bone formation in the bone defects (Arau, 2007). Marouf and Rejab (2020) reported that HA can produce analgesic action in post-extraction sockets after surgical removal of impacted teeth. Therefore, it has the clinical benefit to reduce the usage of nonsteroidal anti-inflammatory drugs after dentoalveolar surgery.

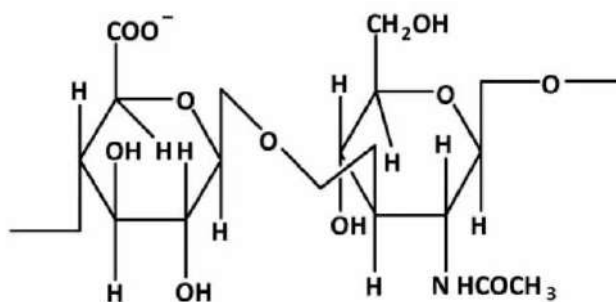


Figure 2.7 Structure of hyaluronic acid

Source: Sayed, 2008

## 2.4 Chitosan

Chitosan (Cheung, Ng, Wong, & Chan, 2015), is a linear polysaccharide composed of randomly distributed  $\beta$ -(1 $\rightarrow$ 4)-linked D-glucosamine (deacetylated unit) and N-acetyl-D-glucosamine (acetylated unit) (Figure 2.8). It is made by treating the chitin shells of shrimp and other crustaceans with an alkaline substance, like sodium hydroxide.

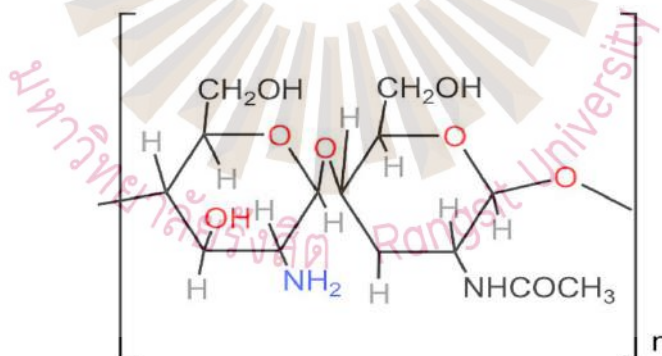


Figure 2.8 Structure of chitosan structure

Source: Kayan, G., &amp; Kayan, A., 2021

Chitosan is a polycation that has many beneficial properties for wound dressing for example nontoxicity, biodegradability, antibacterial, and biocompatibility (Kravanja & Primo, 2019). The positive density of chitosan can form complex with poly anionic.

Several studies demonstrated that chitosan had progress effects in wound healing product development.

The effect of chitosan as an accelerator of wound healing

1) Effect on Poly morphonuclear neutrophil (PMN) Chitosan can promote wound-healing by enhancing inflammatory cell functions such as macrophages, polymorphonuclear leukocytes and fibroblasts.

2) Effect on promotes granulation Chitosan promotes granulation tissue in the large open wounds of animals (Ueno, Mori, & Fujinaga, 2001; Ueno et al., 1999) The effects of chitin and derivatives of chitin on the proliferation of fibroblasts were showed *in vitro*. However, the inhibition of cell proliferation found in high concentrations of chitosan was not shown in cultures without Fetal calf serum (FCS) (Mori et al., 1997).

## 2.5 Pectin

Pectin is a structural acidic heteropolysaccharide contained in the primary cell walls of terrestrial plants. Its main component is galacturonic acid, a sugar acid derived from galactose (Figure 2.9). Pectin is a natural polyanion (Morris et al., 2017), a heterogeneous class of negatively charged polysaccharides derived from plant cell walls, pKa ~ 2.9 to 3.5, containing galacturonic acid which can be partially methyl esterified. Pectin has anti-inflammatory activity from galacturonic acid content (Markov, Popov, Nikitina, Ovodova, & Ovodov, 2011). The strong anti-inflammatory activity is due to Pectin's high level of esterified galacturonic acid residues which suppress Inducible nitric oxide synthase (iNOS) and COX-2, two of the most important enzymes in the inflammatory process. Pectin has recently been investigated for use in various biomedical applications including drug delivery, and chronic wound management.

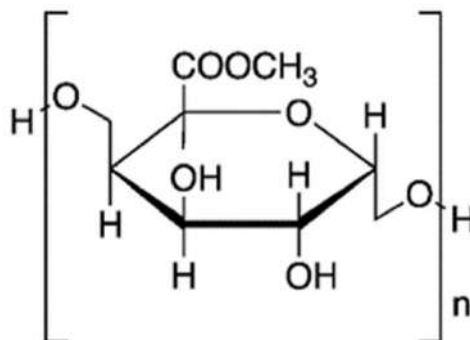


Figure 2.9 Pectin structure

Source: Kitir et al., 2018

## 2.6 Polyelectrolyte complexes

Polyelectrolyte complexes (PECs) are electrostatic interactions between the opposite charge of polyelectrolytes. The electrostatic interaction between the complementary ionic groups of polyelectrolytes is responsible for PEC formation. The properties of PECs are known to be influenced not only by the chemical composition of the polymers of PECs can be obtained by changing the chemical structure of component polymers, such as molecular weight, flexibility, functional group structure, charge density, hydrophilicity and hydrophobicity balance, stereoregularity and compatibility, as well as reaction conditions like pH, ionic strength, concentration, mixing ratio and temperature (Dakhara & Anajwala, 2010). Two structural models for polyelectrolyte complexes are discussed in the works of literature which are ladder-like structures and the scrambled egg model. These models have been extensively studied and it was concluded that most experimental structures lie between the two models, though probably closer to the scrambled egg than the ladder-type model (Figure 2.10). Polyelectrolyte complex has an emerging way for deliver the drug to target sites, controlling the rate of drug release by carriers and prolonging the therapeutic action (Jasmeet, Harikumar, & Amanpreet, 2012).



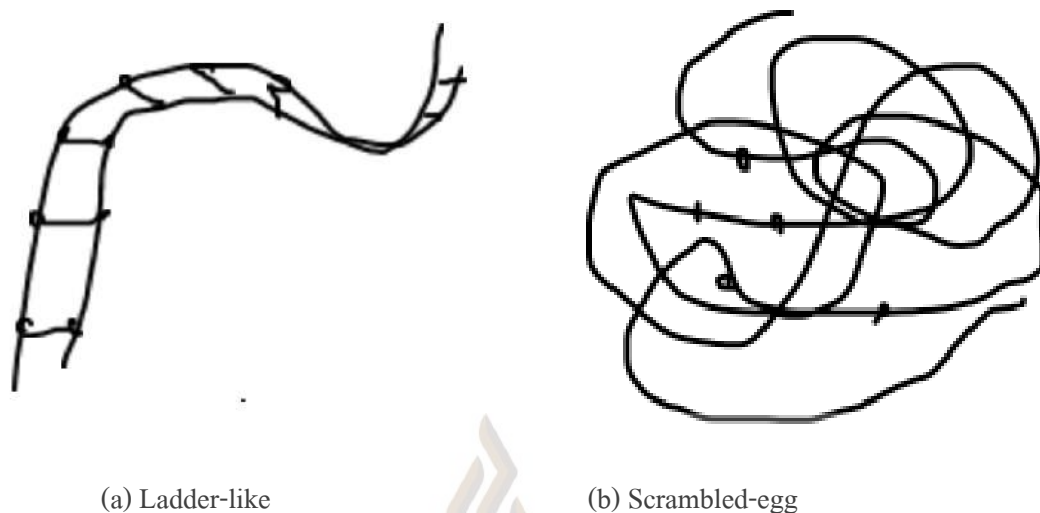


Figure 2.10 Model of polyelectrolyte complex structure, (a) Ladder-like, (b) Scrambled-egg

Source: Tauber, 2012

Many natural polysaccharides are excellent polyelectrolytes that controlled release carriers for making nanoparticle size and promote the efficacy of action. Chitosan and pectin are natural polysaccharides that show good potential in Nanoparticle delivery systems (Quiñones, Peniche, & Peniche, 2018).

## 2.7 *In situ* gel

*In situ* gel formation occurs due to factor stimuli like pH change, temperature modulation, and solvent exchange. Polymeric systems are presented in the delivery of the drugs that polymers undergo sol-gel transition. Various biodegradable polymers that are used for the formulation of *in situ* gels include gellan gum, alginic acid, xyloglucan, pectin, chitosan, poly (DL-lactic acid), poly(DL-lactide-co-glycolide) and poly-caprolactone (Nirmal, Bakliwal, Pawar, & College, 2010).

Temperature-sensitive hydrogels are the biomaterial that transit from sol-gel is triggered by the increase in temperature. Body temperature is required for trigger gelation that is used for critical temperature. (Jeong, Wan, & Han, 2002).

## 2.8 Poloxamer 407

Poloxamers are non-ionic polyoxyethylene–polyoxypropylene–polyoxyethylene (PEO<sub>*n*</sub>–PPO<sub>*n*</sub>–PEO<sub>*n*</sub>) tri-block copolymers with many pharmaceutical applications (Figure 2.11). Poloxamer 407, which has a molecular weight of 12,000 Daltons and a PEO/PPO ratio of 2:1 by weight, has been the most widely used of these copolymers. The release profiles of several drugs delivered with P407 gels have been reported: antibiotics, anesthetics, antipyretics, anti-inflammatory drugs, and peptides which have shown that release follows the Higuchi square root law. Poloxamer is biocompatible and the results support the possibility of using Poloxamer gel as a sustained release of lidocaine HCl injectable formulation on body temperature (Ricci, Bentley, Farah, Bretas, & Marchetti, 2002; Ricci, Lunardi, Nanclares, & Marchetti, 2005). Maintain prolonged duration, sol-gel easy to put gel in the wound in solid stage and turn to gel for maintaining dressing for cover bare bone.

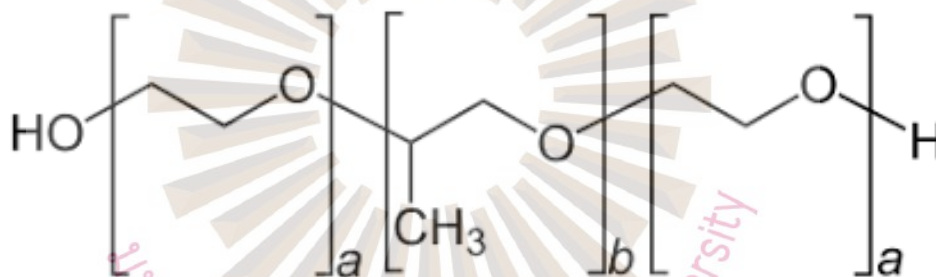


Figure 2.11 Structure of poloxamer 407

Source: Jiang, Zhang, & Li, 2020

## Chapter 3

### Research Methodology

#### 3.1 Materials

High methoxy pectin from citrus peels (PC, pKa = 3.5, lot no. SLBQ6929V, Sigma-Aldrich<sup>®</sup>, USA), hyaluronic acid (HA, MW = 1.8–2.2 MDa, SpecKare<sup>™</sup>, China), USA), lidocaine hydrochloride (LH, Sigma-Aldrich<sup>®</sup>, USA), low molecular weight chitosan (CS, MW = 50,000–190,000 Da, degree of deacetylation (DD) = 55–70%, pKa = 6.5, lot no. STBF8219V, Sigma-Aldrich<sup>®</sup>, USA), mucin type II from the porcine stomach (lot no. SLCC7713, Sigma-Aldrich<sup>®</sup>, USA), poloxamer 407 (P407, lot no. SIAL 16758, Sigma-Aldrich<sup>®</sup>, USA) and zinc sulfate (Zn, Fuka, Japan) were purchased from local suppliers and used as received.

#### 3.2 Product Development

##### 3.2.1 Development of lidocaine hydrochloride and hyaluronic acid loaded chitosan-pectin polyelectrolyte complex carrier (LC)

3.2.1.1 Formulations and preparation of lidocaine hydrochloride and hyaluronic acid-loaded chitosan-pectin polyelectrolyte complex carrier (LC) using factorial design.

###### (1) Design of experimental (DoE)

Following previous research, the CS-PC polyelectrolyte complex was formulated in fix ratio (3:1) with high stability (Birch & Schiffman, 2014). Our preliminary studies followed this ratio (3:1) and varied the ratios to 1:1, 1:3, and 3:3. The results showed that the ratio of 3:1 of CS-PC polyelectrolyte complex confirmed the suitable ratio of stable polyelectrolyte complex.

The LH and HA concentrations were studied at three levels of magnitude. A (+) sign represents a high level of sample concentration, (0) was a mid point between low and high levels and (-) represents a low level (Table 3.1). A 9-run design was obtained. The following responses were zeta potential, particle size, % entrapment efficiency, and %drug release at 5 min. The layout of  $2^3$  Full factorial Design is shown in Table 3.1, 3.2

Table 3.1 Factors and levels used in  $2^3$  Full factorial Designs of independent variables of LH and HA.

Factors	Range (Unit)	Levels		
		(-)	(0)	(+)
LH concentration	4-10 (%w/w)	4	7	10
HA concentration	0.5-1.5 (%w/w)	0.5	1.0	1.5

Table 3.2 Nine different formulations composed of chitosan (CS), pectin (PC), lidocaine hydrochloride (LH) and hyaluronic acid (HA) in various concentrations.

Formulation codes	Concentration (%w/w)			
	CS	PC	LH	HA
LC1	0.3	0.1	4	0.5
LC2	0.3	0.1	7	0.5
LC3	0.3	0.1	10	0.5
LC4	0.3	0.1	4	1.0
LC5	0.3	0.1	7	1.0
LC6	0.3	0.1	10	1.0
LC7	0.3	0.1	4	1.5
LC8	0.3	0.1	7	1.5
LC9	0.3	0.1	10	1.5

## (2) Method of preparation

Overnight, the CS was dissolved in 1% v/v acetic acid to generate a CS solution. Deionized water was used to dissolve PC. As stated in Table 2, LH was added to the PC

solution in varying concentrations of 4, 7, or 10% w/w. The PC-LH solution was added dropwise (4 seconds each drop) to 0.3% w/w of CS solution while homogenizing at 400 rpm and mixing was maintained for 5 minutes after dropping. Then 0.04% w/w zinc sulfate solution was added, followed by 5 minutes of continuous homogenization. The homogenizer was set to 10,000 rpm while adding HA at 0.5, 1, or 1.5% w/w and homogenized continuously for 10 minutes. To get LCs formulation, the PEC solution was sonicated for 10 minutes in an ultrasonication bath at a regulated temperature of 28-32°C.

### 3.2.2 Characterizations of LC formulations

#### 3.2.2.1 Particle size, poly dispersion index (PDI), and zeta potential

Dynamic light scattering (DLS) in a nanoparticle size and zeta potential analyzer (NanoPlus<sup>®</sup>, DLS Model NanoPlus-3 Serial no. 409314, USA) was used to assess particle size, PDI, and zeta potential. Before measuring, each LC formula was dispersed in distilled water with a dilution factor of 6.

#### 3.2.2.2 Viscosity and mucoadhesiveness

The viscosity ( $\eta$ , cps) of the nine formulations ( $n = 6$ ) was determined using a viscometer (Brookfield Model DV-II + viscometer; USA) at 100 rpm and room temperature. The bond strength between the formulation and the glycoproteins in mucus is measured by mucoadhesiveness. Graça (2018) was determined by inverting the tube five times without shaking after combining the mixture with type II mucin from a porcine stomach. The average viscosity of each formulation was calculated by mixing it with water instead of mucin. The viscosity of the formula-mucin mixtures was evaluated at 100 rpm for 0, 15, 30, and 60 minutes without shaking the sample. The percentage of mucoadhesive was calculated by the following Eq:

$$\% \text{Mucoadhesive} = \frac{\text{Average } \eta \text{ of the mixture} - \text{Average } \eta \text{ of formulation}}{\text{Average } \eta \text{ of formulation}} \times 100 \quad (3-1)$$

The average  $\eta$  of the formulation is the mean viscosity of the formulation

### 3.2.2.3 Entrapment efficiency (%EE) and drug loading capacity (%DL)

Centrifugal filter tubes containing 1 ml of each LC formula (Amicon® Ultra, MWCO of 3 K Da, Merck Millipore Ltd., Ireland) were centrifuged at 12,000 rpm for 30 minutes at room temperature. Using an ultraviolet (UV) spectrophotometer (Shimadzu UV1700; Japan) at 270 nm, the supernatant solution was utilized to assess drug concentration. Percent entrapment efficiency (% EE) and percent drug loading capacity (%DL) were calculated by the following Eqs:

$$\%EE = \frac{\text{Amount of total LH} - \text{Amount of free LH}}{\text{Amount of free LH}} \times 100 \quad (3-2)$$

$$\%DL = \frac{\text{Amount of total LH} - \text{Amount of free LH}}{\text{Amount of PEC}} \times 100 \quad (3-3)$$

### 3.2.2.4 *In vitro* drug release

formulation) were put in a dialysis bag (dialysis membrane standard RC Tubing MWCO 3.5 K Da, Spectra/ Por<sup>®</sup>, USA), avoiding the gas bubble and immersing the sample in an artificial saliva solution (pH = 7.4) receptor chamber. The receptor chamber was kept in a shaking water bath with magnetic clips at  $37 \pm 2^\circ\text{C}$  and agitated at 600 rpm during the experiment. 5 mL of receptor media was collected and replaced with new receptor medium at 5, 10, 15, 30, 60, 120, 240, 480, 720, and 1440 min. After that, each sample was taken from the receptor medium and tested for LH % at 270 nm. Each sample's cumulative total LH permeation was determined as a percentage of its donor's total LH content.

### 3.2.2.5 Stability study

To assess the stability of the LC formulae, they were kept in a desiccator at room temperature for three months. The physical parameters of the nine formulations were evaluated and their zeta potential was assessed after three months of storage.

### 3.2.2.6 Morphology of selected formulations

formulas that have been improved Due to the formulation's stability, the concentration of HA, and the variety in characteristics such as particle size, zeta potential, %EE, and% drug release, LC5 and LC8 were chosen to reflect each group's morphology.

The surface morphology and composition of LC samples were analyzed by scanning electron microscopy (SEM, FEI Quanta 450 Field Emission Scanning Electron Microscope, Austria). LC samples were pretreated by four-fold dilution with DI water sonicated for 5 mins., then mounted on a stub, gold-coated, and observed at 30,000 magnifications. The LC samples' morphological characteristics were observed by transmission electron microscopy (TEM, FEI Company, USA). TEM was observed at 10,000–20,000 magnification after a drop of each four-fold diluted sample was applied to a copper grid coated with carbon film and air-dried.

### 3.2.3 *In vitro* study of cytotoxicity and wound healing

#### 3.2.3.1 Cell viability

To investigate the effect of the LC formulations on cell viability, human gingival fibroblasts (HGF-1, ATCC®, CRL-2014TM, USA) were utilized. HGF-1 was cultured in high-glucose DMEM supplemented with 1% antibiotic-antimycotic (containing 100 U/mL penicillin, 100 g/mL streptomycin, and 25 g/mL amphotericin B; Invitrogen, USA) and 10% v/v fetal bovine serum (FBS) in a humidified incubator (Thermo Fisher Scientific TM, USA) at 5% CO<sub>2</sub> and 37°C. The cells were subsequently treated to LC3, LC6, LC9, and LH (concentrations ranging from 50 to 1000 g/mL) and incubated for 24 hours in a humidified incubator (5% CO<sub>2</sub>, 37 ± 1°C, 90% relative humidity). The percentage of cell viability was analyzed using the MTT method, which was calculated by the absorbance of the sample compared to the absorbance of the negative control (using DMEM solution and blank niosomes) in the same culture plate, following Eq.

$$\% \text{ Cell viability} = \frac{\text{Average absorbance of the sample}}{\text{Average absorbance of negative control}} \times 100 \quad (3-4)$$

#### 3.2.3.2 Scratch wound Assay (Wound healing property)

Human gingival fibroblasts (HGF-1, ATCC®, CRL-2014TM, USA) were employed in the cell migration investigation through the scratch assay. The cells were planted at a density of 50x10<sup>3</sup> cells/well in 12 well plates. After 24 hours of incubation, the culture medium was replaced. When the cells attained 90% confluency, a scratch was produced with a 100 L pipette tip. To eliminate dead cells, cells were washed with PBS. The wells were filled with the nine formulations and incubated for 24

hours. An Olympus (X53) microscope was used to capture time-dependent bright-field pictures. Experiments were carried out in triplicate. Equation was used to calculate wound distance to evaluate healing from images.

### 3.2.4 Development of LC incorporated in thermoresponsive polymeric hydrogel (LTP)

#### 3.2.4.1 Preliminary preparation of LTP formulation

Table 3.3 The composition of LTP by varying P407 concentration range 14-18 %w/w

Formulation codes	Concentration (%w/w)	
	LH	P407
LTP1	10	14
LTP2	10	16
LTP3	10	18

The LTP was made by changing the P407 concentration from 14 to 18%w/w. As indicated in Table 3.3, the most appropriate LC formula in adequate characterisation was chosen to include in the P407 gel-based. The gelation temperature and gelation duration of each formulation were measured during the transition from solution to gel.

P407 was prepared by the cold technique method. In brief, P407 was dispersed in 4-8°C DI water and then Before usage, the solution was stored in the refrigerator (4-8°C) overnight. Using a magnetic bar stirrer, the LC solution was mixed into the gel-based in a 1:1 (w/w) ratio. The gelation temperatures of the examined formulations of P407 were determined by the “Visual Tube Inversion Method”, as previously described (Ur-Rehman, Tavelin, & Gröbner, 2011) for preliminary inquiry In brief, each formulation was put in a centrifuge tube, tilted, and immersed in a slowly increasing bath temperature. The gelation temperature was determined by measuring the temperature at which the sample solution stopped flowing when tilted. A appropriate formulation would be chosen for future exploration.



### 3.2.4.2 Preparation and comparison of the effects of LH concentration loaded PEC and unloaded PEC hydrogel (F formulation)

P407 concentration of 16%w/w was selected for further investigation. LH was loaded in ternary polyelectrolyte complex formed from CS, PC and HA as in our previous study (topic 3.2.1). The comparisons of percentage of LH loaded in PEC thermoresponsive hydrogel were studied compared to free LH in the hydrogel. F3 was developed from LC9 incorporated in 16% w/w P407 that represented in LH in PEC group and F4 was formulated from 10% LH in P407 that represent in LH in P407 group. F1 and F2 was developed for compare in the combined effect in LH in PEC and LH in P407 by varies concentration LH but the total LH concentration in all of F formulations. The comparisons of percentage of LH loaded in PEC thermoresponsive hydrogel were studied compared to free LH in the hydrogel. The components of all 4 formulations were shown in Table 3.4 and 0.01% Benzalkonium chloride was used as antiseptic and preservative gel (Marple, Roland, & Benninger, 2004).

Table 3.4 Composition of concentration loaded PEC and unloaded PEC hydrogel

Formulation codes	Concentration (%w/w)			
	CS:PC:HA	P407	LH loaded PEC	LH unloaded PEC
F1	0.3:0.1:1.5	16	4	6
F2	0.3:0.1:1.5	16	7	3
F3	0.3:0.1:1.5	16	10	0
F4	0.3:0.1:1.5	16	0	10

### 3.2.4.3 Gelation temperature and gelation time

All formulations' phase transition from solution to gel was measured with a Brookfield viscometer (Brookfield Model DV-II+ viscometer; USA) at temperatures ranging from 4 to 42 °C. Gelation time was determined using tube inversion tests, which revealed that the sol-gel transitions of all four formulations occurred within 5 minutes at  $37 \pm 0.5$  °C. Interaction of LH loaded in PEC and P407 thermoresponsive hydrogel was investigated in this research.

#### 3.2.4.4 Morphology observation

##### (1) Fourier transform infrared spectroscopy (FTIR)

FTIR was used to determine functional groups and changes in the molecular fingerprints of the hydrogel compositions. FTIR spectrometer (PerkinElmer Inc., Spectrum One program, Waltham, MA, USA) was used to record the IR spectra in the region from 4000-400  $\text{cm}^{-1}$

##### (2) Differential scanning calorimetry (DSC)

Each sample formulation was placed in a pierced aluminum pan and heated at a scanning rate of 10°C per min from 25°C to 300°C using a nitrogen flush, at a rate of 20 mL/min. A blank aluminum pan was used as a reference. Thermographs were then obtained and analyzed using a differential scanning calorimeter (DSC) 8000 (PerkinElmer, MA, USA) to determine melting points and transition temperatures (exothermic or endothermic). A simultaneous thermal analyzer (STA) 6000 (PerkinElmer, USA) was used to determine physical changes in the materials by monitoring weight loss on heating.

#### 3.2.4.5 Physicochemical properties of the formulations (F).

##### (1) Determination of viscosity and elastic property

###### Rheology

Using a Kinexus pro rheometer, Malvern, UK, the oscillatory rheological trials improved the hydrogel formulations (F). PL20 SR1575 SS Probe (Parallel plate: diameter 20 mm). Time sweeps at a constant temperature of 37°C with a frequency of 1 Hz were used to calculate the gelation time, which was then studied at 25°C. The gel's rheology was investigated at shear rates ranging from 1-400<sup>-1</sup>. After a set length of 5 minutes, constant measures of viscosity were collected and recorded in centipoises.

###### Viscosity

The viscosity of the F hydrogel formulations was determined at 25°C using a Brookfield Viscometer (Brookfield Engineering Laboratories, Inc. Middleboro, MA, USA) with an S16 spindle at 2 rpm.

## (2) Texture Profile Analyzer

Texture Analyzer TA.XT Plus was used to measure hardness (Stable Micro Systems Ltd., Surrey, UK). A standard beaker (50 mL) was filled with approximately 30 mL of the F hydrogels formulations, avoiding the introduction of air into the sample and ensuring the generation of a smooth upper surface. The disk was compressed into the gel and redrawn with a 40-mm diameter. The technique settings, including speed rate and distance (depth of insertion), were selected based on the kind of hydrogel. For each formulation, three replicate analyses were performed at 37°C.

## (3) Mucoadhesive

Mucoadhesive testing of the F hydrogels formulations was conducted using a TA.XT Plus Texture Analyzer. The mucin disc was attached to the lower end of the cylinder probe (P 0.5 Perspex: 12.5 mm) with double-sided adhesive tape and attached mucin disc was at the opposite position on the Petri disc. Apply formulation on lower mucin disc and move prob with mucin disc was moved down to contact to mucin disc for 30 sec in 37°C. The highest force necessary to dislodge the mucin disc from the surface of each formulation was used to determine mucoadhesive force. (ex. maximum detachment force; Fmax).

Discs of 200-mg mucin sample were prepared by direct compression using a single punch hydraulic press (Model 15011, Specac, USA). The discs were compressed at the pressure of 2 tons for 30 seconds and kept in a desiccator until used.

## (4) Injectability

The force required to inject sample formulations is used to test syringeability. The injection force was measured at room temperature using a TA.XT Plus texture analyzer (Stable Micro Systems, Surrey, UK) in compression mode. A 3-mL syringe with the freshly produced sample (1 mL) was positioned at the holder using vertical additional stability. The samples were then passed through an 18-gauge needle using a cylindrical probe (P 0.5) pushed onto the plunger end of the syringe with a crosshead test speed of 1 mm/s for 10 mm. A texture analysis profile was used to measure the maximum injection force. All tests were carried out in triplicate.

#### 3.2.4.6 Percentage of drug content

The hydrogels “F” formulations were determined percentage of LH content by the HPLC analysis system (SHIMADZU LC10) equipped with an auto sample, UV detector, and an Inertsil ODS-3 (4.6 x 250 mm, 5 $\mu$ m I.D.) column. An isocratic mode of elution with a mobile phase consisting of 5% acetic acid in water and methanol at a flow rate of 1.0 mL/min was employed to quantify the drug at a wavelength of 254 nm.

#### 3.2.4.7 *In vitro* release study of thermoresponsive hydrogel

The diffusion of the hydrogels “F” formulations was evaluated by using the Franz diffusion cell system. The *in situ* hydrogel was placed in the donor compartment of a Franz diffusion cell system and the temperature was adjusted to 37°C. The diffusional sectional area was 1 cm<sup>2</sup> and the receptor phase volume was 2.5 mL. A dialysis membrane (Sigma®, USA) with a 12,000 Da pore size was used as the diffusion membrane between the donor and receptor phase. The receptor phase containing artificial saliva (pH 7.0-7.4) was stirred by magnetic bars at 37°C. Samples were taken periodically from the receptor phase. The received samples were determined HPLC system (SHIMADZU LC10) equipped with an auto sample, UV detector, and an Inertsil ODS-3 (4.6 x 250 mm, 5  $\mu$ m I.D.) column. An isocratic mode of elution with a mobile phase consisting of 5% acetic acid in water and methanol at a flow rate of 1.0 mL/min was employed to quantify the drug at a wavelength of 254 nm. for CT.

#### 3.2.4.8 Drug safety

The drug safety and contamination of the F hydrogels formulations were determined following the USP40 guideline. After being prepared, all 4 formulations were kept under 37°C for 14 days. The microbial tests were carried out on bacterial and mold culture in Total template count, Total Yeast, and Mold, *Escherichia coli*, and *Staphylococcus aureus*.

#### 3.2.4.9 The *in vitro* degradation tests

The biodegradation of the F hydrogels formulations was observed in the rate of hydrogel erosion in the oral environment. The socket models were molded with a tooth that imprints to dental impression material. The F hydrogels formulations were injected into a 15 mL

tooth socket model and then artificial saliva (200 mL, pH 7.0) The model was incubated at 37°C and sampled in order at 0, 6, 12, 24, 36, and 48 hr. The weight remaining of the hydrogel was calculated by the following equation:

$$\text{Weight remaining (\%)} = \frac{W_t}{W_0} \times 100 \quad (3-5)$$

$W_0$  is Weight at an initial time

$W_t$  is Weight at the time

#### 3.2.4.10 Stability

An accelerated stability test was performed by following the ICH guideline. A protocol of stability study developed in four (F) hydrogel formulations were stored in tightly sealed amber vials (15 mL) at different temperatures (4±1°C, 25±1°C, and 40±1°C) 75% relative humidity (RH) ±5% for 3 months.

### 3.3 Clinical research in anesthetic efficacy

#### 3.3.1 Inclusion and exclusion criteria

Thirty healthy volunteers were dental students recruited from the college of dental medicine, Rangsit University. All volunteers are healthy with no history of systemic disease allergy to lidocaine hydrochloride and benzocaine. The exclusion criteria were loss of study. The sample size was determined based on a similar study (Priprem et al., 2014).

After explaining the study procedure, a written consent form was obtained from all participants before the commencement of the trial. The Committee of the RSU ethics review board approved all the aspects and approved No. RSUERB2022-038.

According to the performance of the thermoresponsive hydrogel formula 3 (F3) which provided significant physicochemical properties, percentage of drug release, drug content, and biodegradation, it was selected for the clinical trial evaluation.

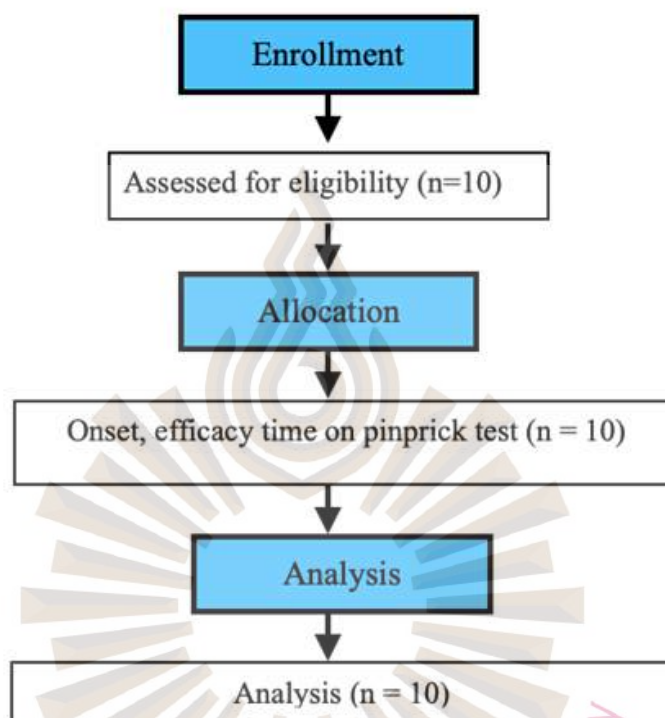


Figure 3.1 Flow consort diagram of the irritating and allergy test

### 3.3.2 Irritating and allergy tests

Before processing the anesthetic assay, irritating and allergy tests of the F3 hydrogel were performed by monitoring any immediate irritation signs (erythema, itching, pain, or soreness) after applying 0.5 g of the gel to the inner lips for 30 minutes. The flow consort diagram of irritating and allergy tests was shown in Figure 3.1

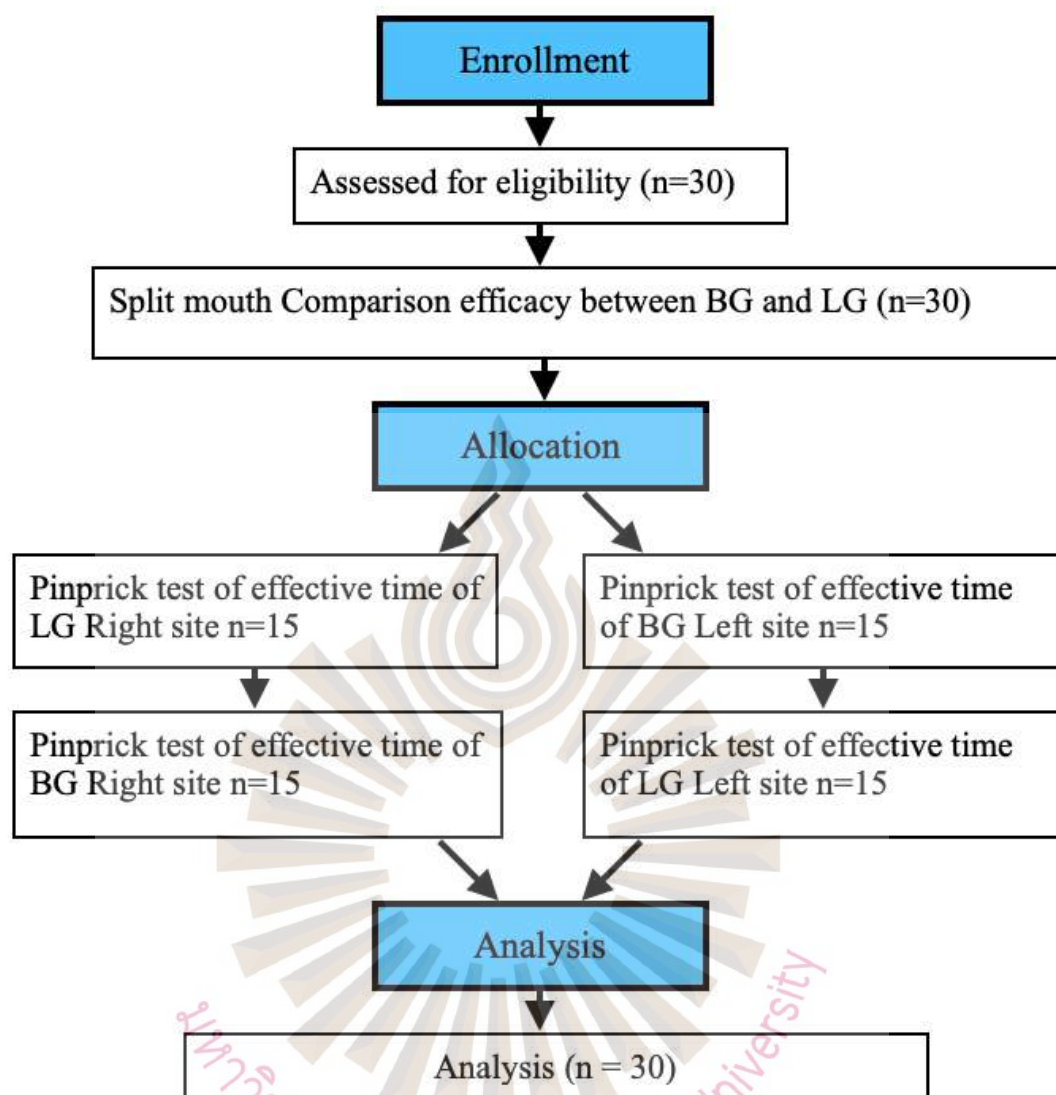


Figure 3.2 Flow consort diagram of the anesthetic human trials; (a) Onset of anesthesia ( $T_{on}$ ) the effective time ( $T_{eff}$ ) of LCT; (b) Comparison efficacy of this split-mouth randomized trial between LG and BG

### 3.3.3 Onset and Effective time

A pinprick test at the palatal mucosa was performed on the healthy volunteers (Figure 3.2). The palatal mucosa around the roots of the upper cuspids was used as a test site (number 13 or number 23). Light-cured gingival protection material used in tooth whitening operations was employed to label the area (Figure 3.3). For each pinprick, sixteen tiny boxes were carefully

allotted inside the area such that the stimulus was administered evenly throughout the defined area). As a pricking tool, a modified WHO periodontal probe with the tip replaced by the tip was utilized. The pain baseline VAS (visual analog scale) was recorded on the pinprick just outside the test area at the beginning of the test without any anesthesia. Inside the test area, F3 LH hydrogel (LG) was administered to the mucosa. For 4 minutes, the region was pricked every 15 seconds, starting with pixels 1, 2, 3, 4, and so on. The ten participants were asked to rate their pain after each pinprick. The initial time point in each patient was used to determine the onset of anesthesia (Ton) (15, 30, 45 s, etc.) The VAS was reduced by over 0.5 cm. The first time the VAS reached its lowest values (the effective time, Teff) was used to calculate the time the anesthetic attained maximum power (the effective time, Teff). The average time duration spent by all ten participants was computed. The subjects were asked to evaluate their pain after each pinprick.

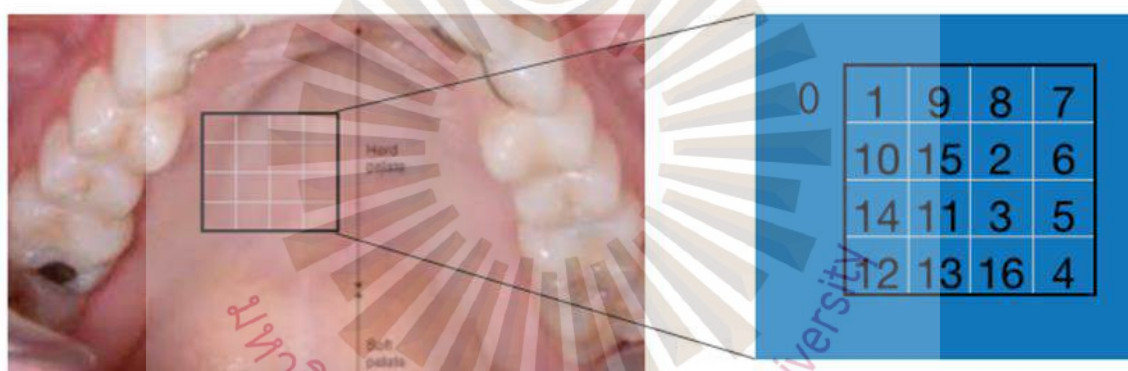


Figure 3.3 Box table of pinprick test at the palate and random table

- 1) The onset of anesthesia was determined by the first time point VAS was decreased more than 0.5 cm.
- 2) The time the anesthetic reached its full strength (the effective time) was derived from the first time point at which the VAS reached its minimum value.

### 3.3.4 Anesthetic efficacy

The split-mouth comparison design trial included thirty healthy volunteers. The participants were seated in a dental chair in a supine position. The palatal mucosa around the root of the cuspid was



treated with one of the topical anesthetics (either LG or BG), and the types of anesthetics were chosen at random. The anesthetic (either LG or BG) was applied slightly longer than the mean effective time of LG obtained in the pinprick test to ensure maximum efficacy. The test area was injected with needle gauge 27. The dentist who applied the topical anesthetics was different from the one who gave the injections, and the side of the first injection was randomized. Subjects were asked to rate how much pain they felt just after each injection. Next week, test the other side with a different local anesthetic agent.

### 3.4 Data Analysis

The data were presented as means and standard deviations (SD), and the normality of the distribution was verified. Using SPSS 13 software, the student t-test and analysis of variance (ANOVA) were used to analyze for differences between or among experimental groups (SPSS Inc, Chicago, IL, USA). Design-Expert! v.11.0.3 was used to design the 3<sup>2</sup> full factorial experiment (Stat-Ease, Inc., Minneapolis, MN, USA). A Paired t-test or ANOVA were used to analyze the average values for explanations for statistical significance ( $p < 0.05$ ).



## Chapter 4

### Research Results

#### 4.1 Development of lidocaine hydrochloride and hyaluronic acid loaded chitosan pectin polyelectrolyte complex carrier (LC)

##### 4.1.1 Formulation development

PEC was investigated the complex forming through the interaction between positive charges of CS and negative charges of PC. The effect of polymer mass ratio will increase particle sizes and decrease the zeta potential of the PEC system (PotaŚ et al., 2020; H. Wang, 2017). The polyelectrolyte complex of CS-PC-HA was developed using a CS:PC ratio of 3:1 (Figure 4.1).

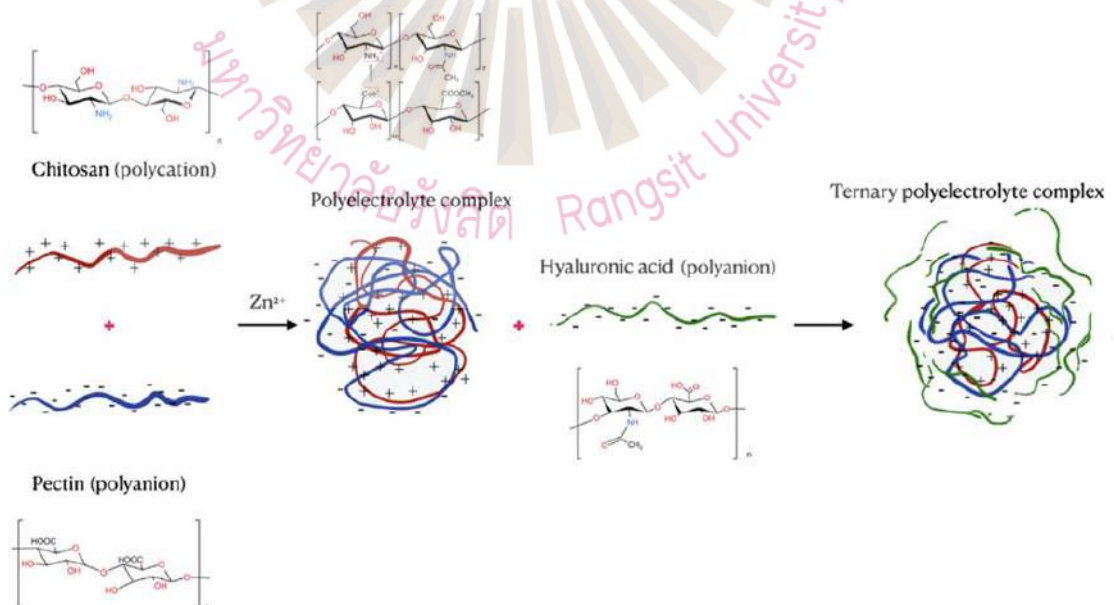


Figure 4.1 The development of polyelectrolyte complexes and the three different polymeric structures Chitosan, pectin, hyaluronic acid, and polyelectrolyte complex chemical structures.

Nine formulations of PEC composed of the positively charged chitosan and the negatively charged pectin with HA and LH were analyzed by a  $3^2$  full factorial design. The LH varied from 4-10% w/w and HA from 0.5-1.5% w/w according to the range of lidocaine and hyaluronic dose concentration (Table 4.1).

Table 4.1 Full factorial design 2 factors 3 levels for optimization of lidocaine hydrochloride (LH) and hyaluronic acid (HA) loaded in chitosan pectin polyelectrolyte complex

Formulation	LH (X1)	HA (X2)	Viscosity (100 rpm)	Size ( $\mu\text{m}$ ) (Y1)	PDI	Zeta (mV) (Y2)	% EE (Y3)	% Drug released within 5 min (Y4)
LC1	-1	-1	5.4 $\pm$ 0.9	2.7 $\pm$ 0.9	0.544 $\pm$ 0.086	-7.2 $\pm$ 0.5	46.0 $\pm$ 0.3	41.9 $\pm$ 0.4
LC2	0	-1	8.8 $\pm$ 0.9	3.8 $\pm$ 2.0	0.519 $\pm$ 0.430	-10.0 $\pm$ 1.9	45.9 $\pm$ 0.7	20.8 $\pm$ 0.8
LC3	1	-1	14.4 $\pm$ 2.1	3.9 $\pm$ 0.6	0.337 $\pm$ 0.249	-13.2 $\pm$ 4.3	40.5 $\pm$ 0.4	12.6 $\pm$ 0.5
LC4	-1	0	26.8 $\pm$ 2.3	3.4 $\pm$ 1.2	0.004 $\pm$ 0.001	-22.8 $\pm$ 0.5	73.0 $\pm$ 0.1	43.1 $\pm$ 0.1
LC5	0	0	32.0 $\pm$ 1.7	5.7 $\pm$ 3.2	0.139 $\pm$ 0.211	-22.3 $\pm$ 9.3	74.7 $\pm$ 0.0	21.4 $\pm$ 0.2
LC6	1	0	57.0 $\pm$ 4.4	5.7 $\pm$ 0.7	0.122 $\pm$ 0.107	-25.0 $\pm$ 5.1	74.2 $\pm$ 0.2	15.0 $\pm$ 0.1
LC7	-1	1	177.2 $\pm$ 0.2	5.8 $\pm$ 0.9	0.127 $\pm$ 0.155	-27.7 $\pm$ 0.8	76.3 $\pm$ 0.4	52.2 $\pm$ 0.2
LC8	0	1	273.4 $\pm$ 2.3	6.2 $\pm$ 1.1	0.006 $\pm$ 0.011	-21.1 $\pm$ 0.1	86.7 $\pm$ 0.0	24.0 $\pm$ 0.1
LC9	1	1	210.8 $\pm$ 0.3	6.3 $\pm$ 0.5	0.004 $\pm$ 0.003	-22.6 $\pm$ 1.0	92.3 $\pm$ 0.1	15.8 $\pm$ 0.2

#### 4.1.2 Physicochemical characterization

##### 4.1.2.1 Particle size, poly dispersion index (PDI), and zeta potential

The LC particle sizes were in the range of 2.7–6.3  $\mu\text{m}$  (Table 4.1), in which a high concentration of HA groups (LCs 7–9) provided the largest sizes. The ternary complexes composed of chitosan, pectin, and hyaluronic acid were formed by the interaction of opposing charges and the electrostatic force of the amino ionic groups of chitosan ( $\text{NH}_3^+$ ), the carboxyl groups ( $\text{COO}^-$ ) of (Archana, Dutta, & Dutta, 2013; Borges, Maciel, Yoshida, & Teixeira, 2015; Hong, Jeong, & Nah, 2018) and the hydroxyl group ( $\text{OH}^-$ ) of hyaluronic (Nath et al., 2015). The anionic-cationic charge ratio of chitosan: pectin: hyaluronic results from the formation of a macromolecules polyelectrolyte complex (Limsitthichaikoon & Sinsuebpol, 2019; Priftis et al., 2014). Compared to the CS-PC

binary polyelectrolyte complex, the present of HA significantly increased the particle sizes from nanosize range (400–600 nm) to micron scales (2–7  $\mu\text{m}$ ). The larger size of LCs 7, 8, and 9 might result from ternary PEC preparation, which influences the strength of electrostatic interaction (Hong, Jeong, & Nah, 2018; Wang, 2017). Moreover, the PDI increased disproportionately with increasing particle size, demonstrating the particle size uniformity (Figure 4.2a).

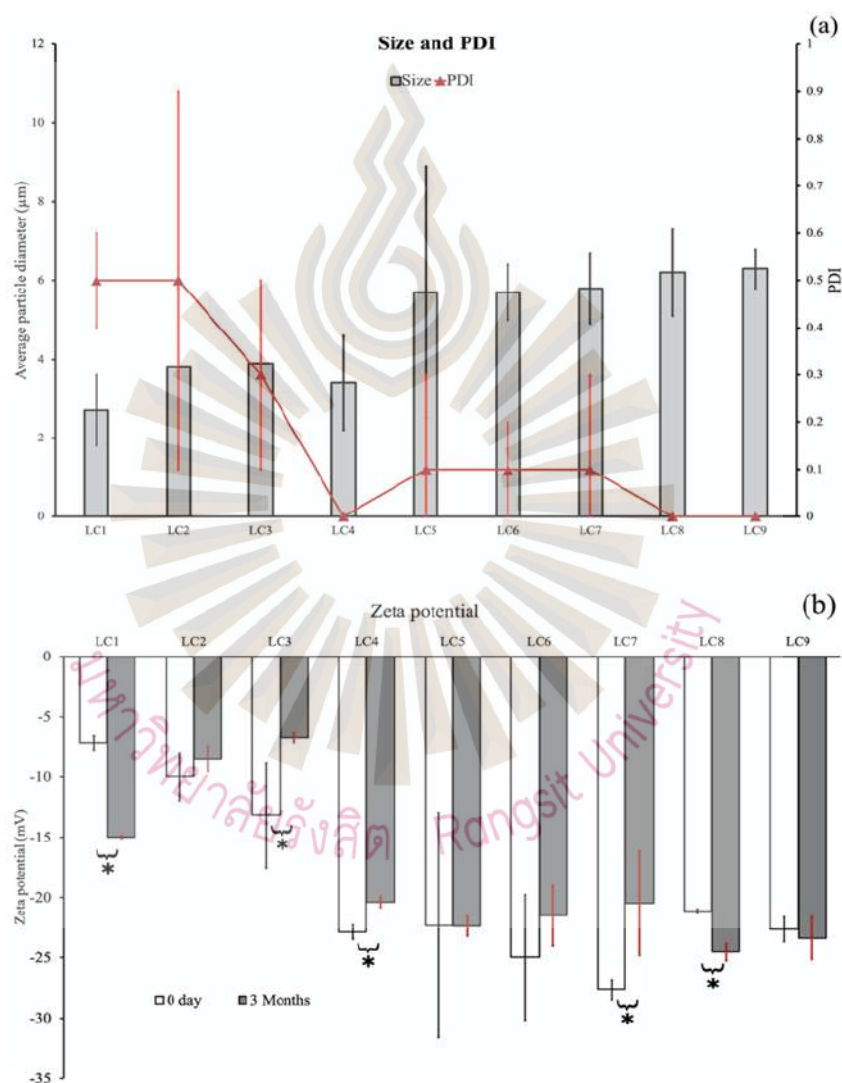


Figure 4.2 The comparison of particle size (gray columns) and polydispersity index (PDI) (red dot) (a) and zeta potential of LC formulations varied using a 32factorial design (b), with white columns representing the zeta potential of freshly prepared LC (day 0) and grey columns representing zeta potential values after 3 months of LC storage at room temperature.

The error bars represent standard deviations ( $n = 6$ ); the symbols indicate significant changes at  $p < 0.05$ : \*when compared to freshly prepared and (3 months) stored LCs, using Student's *t*-test.

All formulations had a negative zeta potential value due to the amounts of LH, HA, and pectin. As demonstrated in Figure 4.2b, the zeta potentials of nine formulations ranged from -7.2 to -27.7 mV. The lowest HA concentration produced the lowest zeta potential value, with an absolute charge of 13.2 mV. The formulation LC4-LC9 has zeta potentials ranging from -21.1 to -27.7 mV. The zeta potential value of negative or positive charge that is 15 mV represents the beginnings of particle agglomeration and leads to less area of interaction with incoming substances or particles, whereas the value above 16-30 mV is a delicate dispersion threshold and leads to prompt interaction with incoming substances or particles. (Mohamed, 2016). The LC4-LC9 could reflect the approximate stability of the dispersion if the absolute value of zeta potential was more than -20 mV (Figure 4.2b). Despite the fact that all LC formulations had zeta potentials less than -30 mV, LC8 had a substantially higher zeta potential after three months of room temperature storage ( $p < 0.01$ ). The zeta potential of LC9 did not alter substantially between preserved and fresh samples ( $p > 0.05$ ). (Figure 4.2b). As the levels of LH and HA increased, so did the particle size and zeta potential. Because of its negative charge, HA had a bigger influence on particle size than LH (Table 4.1), allowing it to establish cross-links and maybe coat the particle.

#### 4.1.2.2 Viscosity and mucoadhesion

The formulation LC9 exhibited the highest viscosity and mucoadhesiveness, as well as the highest LH and HA contents (Table 4.1). (Figure 4.3). As seen in the findings of LC3, LC6, and LC9 formulations, the HA content had a bigger influence than the LH concentration: viscosity rose four-fold from LC3 to LC6 and from LC6 to LC9. The concentration of HA is the most important factor influencing LC viscosity. This could be explained by the molecule's nature, which acts as a reservoir to entrap specific factors in an extracellular matrix. The interaction of formula and mucin affected mucoadhesiveness by %. (Figure 4.3). The percentage mucoadhesiveness was highest at 15 minutes and decreased after 30 and 60 minutes of bonding. The formula-mucin bond was weak, which

could be attributed to hydrogen bonding between the hydroxyl and carboxyl. The ionic bond of the formula-mucin complex can be active, but the negative charges of the formula and mucin allow for a weak bond that may weaken over time. (Graça, Gonçalves, Raposo, Ribeiro, & Marto, 2018) Furthermore, we discovered that external forces (or stimuli) such as vibration boosted the formula-mucin interaction. This result is most likely impactful in formula application.

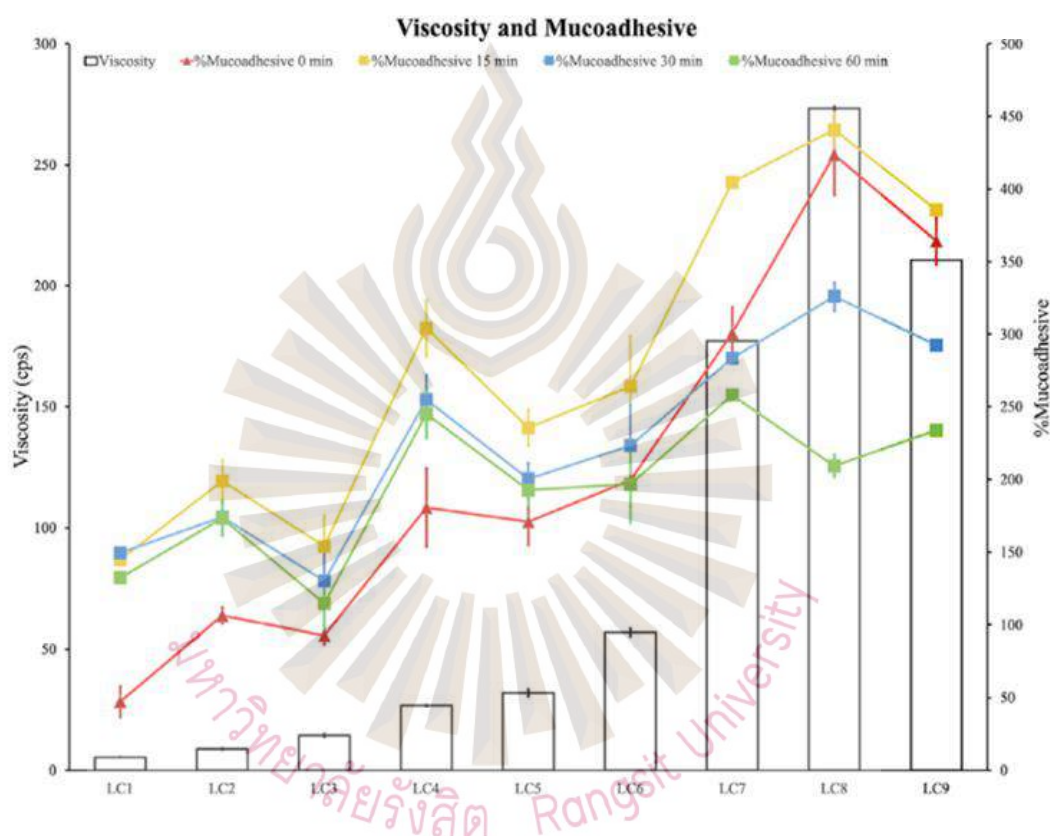


Figure 4.3 Comparison in viscosity of the formulation (white columns) and % mucoadhesiveness at 0 (red line), 15 (yellow line), 30 (blue line) and 60 min (green line). Error bars represent standard deviations (SD) (n = 6).

#### 4.1.2.3 Entrapment efficiency and drug loading capacity

The entrapment efficiency and drug loading capacity were also affected by the LH/HA ratio. When the concentration of HA remains constant while the concentration of LH increases, entrapment increases in all formulations. Likewise, increasing LH concentration while decreasing HA concentration improves entrapment efficiency. (Figure 4.4). As opposed to

viscosity, the increase in viscosity could be attributed to LH entrapment within the PEC, which led to a formulation with a high% EE and% DL. (Da Silva, Ferreira, Reis, Cook, & Bruschi, 2018; Graça et al., 2018).

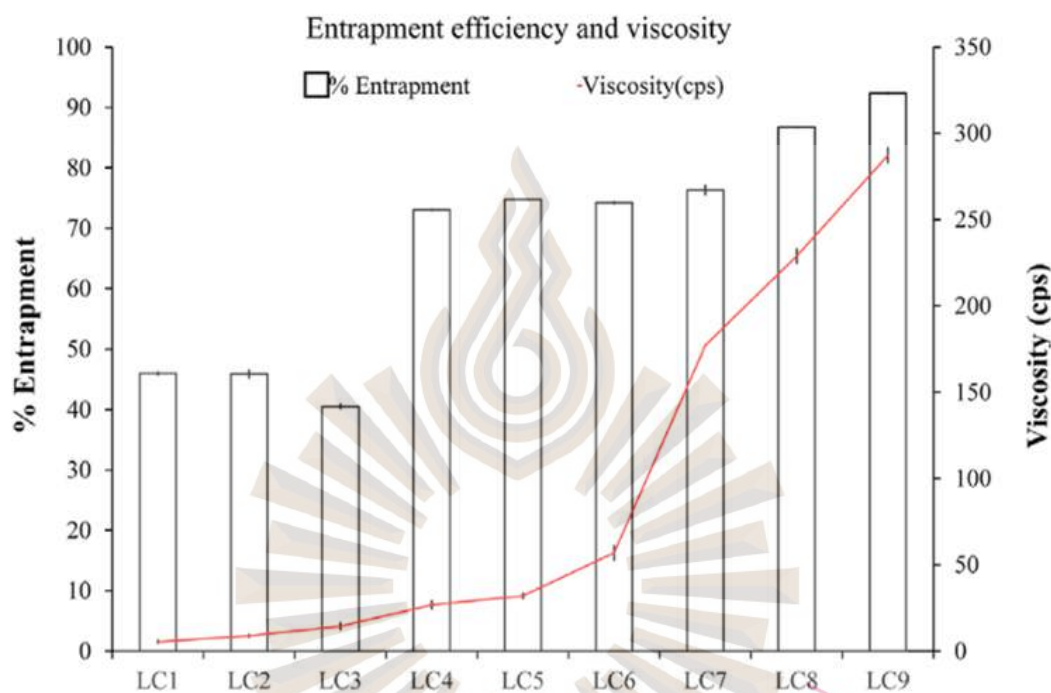


Figure 4.4 Comparison of percentage of entrapment efficiency (white column) and viscosity of freshly prepared LC formulations (red line). Error bars represent standard deviations (SD) (n = 6).

#### 4.1.2.4 *In vitro* drug release of LH from LC carrier

*In vitro* research on the cumulative release of LH from LC over periods of 5 min, 2 hr, and 24 hr was conducted. Our objective for dry socket treatment is to provide initial drug release in 5 minutes using an LH burst effect. (Table 4.1) demonstrated that the increased viscosity of the higher HA concentrations retard drug release when comparing formulations with the same HA concentrations (low HA group LC1, LC2, and LC3; medium HA group LC4, LC5, and LC6; and high HA group LC7, LC8, and LC9).

From table 4.2, in the 2 hr. of LH release were examined using multiple kinetic models, zero-order is a model that plotted as cumulative amount of drug released and time (9), first-order is a model that plotted as log cumulative amount of drug released and time (10), and Higuchi is a model that plotted as cumulative amount of drug released and square root of time (11):

$$Q = k_0 t \quad (4-1)$$

$$\ln Q = \ln Q_0 - k_1 t \quad (4-2)$$

$$Q = k_H t^{1/2} \quad (4-3)$$

where  $Q$  is the amount of drug released at the time.

$Q_0$  is the initial drug concentration.

$k_0$  is the rate constant corresponding to zero-order model.

$k_1$  is the rate constant corresponding to first-order model.

$k_H$  is the rate constant corresponding to Higuchi order model.

$t$  is time in hour.

$t^{1/2}$  is the square root of time.

The drug release within 2 hr. was analyzed by linear regression (Table 4.2), and each formula was fitted into zero-order, first-order, and Higuchi kinetic models (De Oliveira, Hudebine, Guillaume, & Verstraete, 2016). As the  $r^2$  approached 1, the LC release was best matched to the zero-order kinetic, indicating that the LC formulations provided controlled delivery (Laracuenta, Yu, & McHugh, 2020).

Two to three days after the tooth is extracted, the most painful dry socket symptom appears. Therefore, it is necessary to quickly relieve pain and manage it until granulation heals and covers the exposed bone in the socket. The typical duration of an AO is between 5 and 10 days. For all formulations, the cumulative LH controlled release percentage at 4 hours and at 24 hours is displayed (Figure 4.5).



Table 4.2 Drug release for 2 hr. which the coefficient of correlation ( $r^2$ ) demonstrated in zero-order, first-order, and Higuchi release model.

Formulation	Zero-order			First-order			Higuchi		
	$r^2$	slope	Intercept	$r^2$	slope	Intercept	$r^2$	slope	Intercept
LD1	0.9982	35.488	39.973	0.9706	0.2154	1.6337	0.9781	60.892	19.808
LD2	0.9615	37.605	23.129	0.8593	0.3171	1.4112	0.9976	66.396	0.4129
LD3	0.9814	40.157	23.129	0.8726	0.4102	1.32238	0.9934	69.856	10.769
LD4	0.993	35.585	43.15	0.9533	0.2082	1.6618	0.9888	61.55	22.575
LD5	0.9781	39.648	19.924	0.8976	0.3396	1.3714	0.9901	69.146	3.4092
LD6	0.9889	43.803	15.815	0.8688	0.3878	1.3057	0.9869	75.853	9.575
LD7	0.993	33.373	49.871	0.9684	0.1816	1.7184	0.9803	57.477	30.753
LD8	0.9951	39.021	20.637	0.9427	0.3208	1.238	0.9766	67.005	1.5733
LD9	0.9961	36.218	13.028	0.9355	0.375	1.238	0.9765	62.159	7.5636

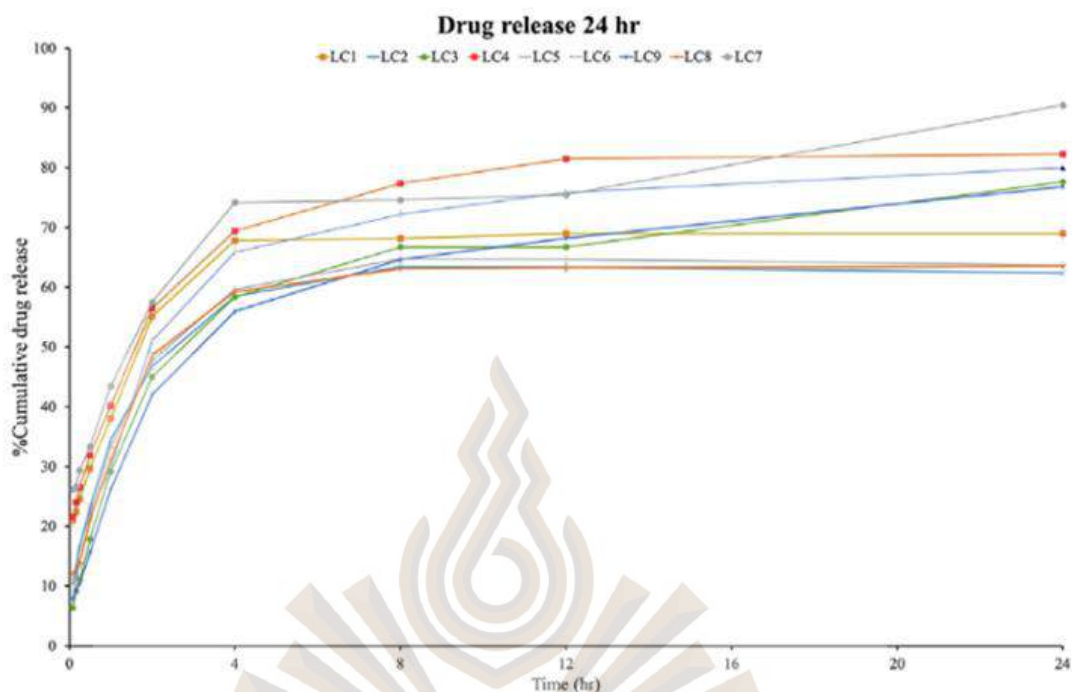


Figure 4.5 Comparison of percentage of cumulative drug-release of 9 formulations of LC varied in 3<sup>2</sup> factorial designs at 24 hr, which data are average % cumulative amount  $\pm$  SD (n = 6).

Error bars represent standard deviations (SD) (n = 6).

#### 4.1.2.5 Stability analysis

Zeta potentials of LC formulations stored for three months were compared to zeta potentials of formulations that had just been prepared (Figure 4.6). The results demonstrate that 10 minutes after preparation, the low HA concentration formulations (LCs 1-3) started to separate, and they were completely separated by 30 minutes (Figure 20b). The divided formulations show unstable formulations. Zeta potential of close to 30 mV improves stability. Formulations with a zeta potential of about -20 mV or lower were more stable (Figure 4.6 and Table 4.1), aggregating more quickly than other groups. Zeta potential of 10 to 30 mV is optimal. behavior with signs of instability (Kong, Sun, & Bao, 2017).

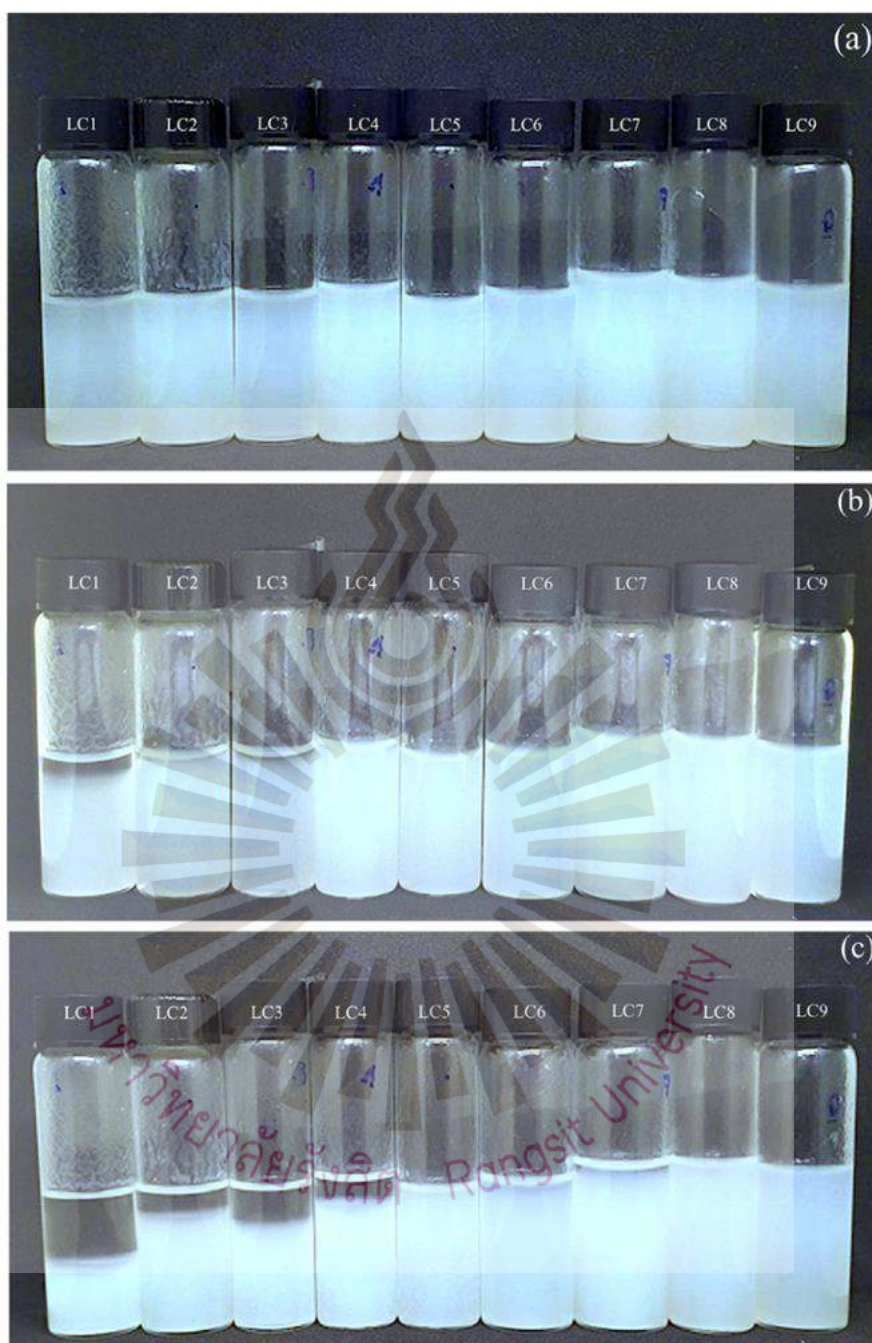


Figure 4.6 At room temperature, the stability of LC1 to LC9 formulations was tested (a) immediately after preparation, (b) 15 minutes later, and (c) three months later. When compared to freshly prepared, LC1–LC3 particles began to separate quickly within 15 minutes, but LC4–LC7 took three months to fully separate. These PEC formulations were stable, as evidenced by the homogeneous solutions of LC8 and LC9.

After three months, LCs 4 through 7 showed co-aggregation and separation, whereas LCs 8 and 9 were homogeneous (Figure 4.6c). The stored LC 4-7 formulations' zeta potentials were lower than those of the freshly prepared samples, suggesting that these formulas are unstable. The formulation stability was also influenced by viscosity, and LCs 1 through 7 had lower viscosities than LCs 8 and 9. (Figure 4.4). The influence of the colloidal forces on the viscosity may have an impact on the repulsion energy. This phenomenon may be caused by electrostatic repulsion and Van der Waals attraction, which slow the colloidal system's Brownian movement and provide precipitate protection. (López-Esparza, Balderas Altamirano, Pérez, & Gama Goicochea, 2015).

### 4.1.3 Morphology observation

#### 4.1.3.1 SEM, TEM

Figure 4.7a and 4.7b, which are SEM images of all formulations, display nanoparticles (red arrowhead) dispersed on a polymeric micelle background (white arrowhead). Similar to this, TEM images of LCs show them to be sphere-like vesicles with nanometer-sized particles (Figure 4.7c and 4.7d). The morphology was identical in both the LC5 and LC8 photos. The results of the DLS particle size analyses showed that these polymeric micelles surrounded the LC molecule and reflected the light, giving the impression that it was larger than the particles, in contrast to the SEM and TEM-based size estimates. Polymeric micelles might not be accurately modeled by the DLS method. Images from optical microscopy and SEM or TEM at high magnifications may better describe particle morphology and micelle structure.

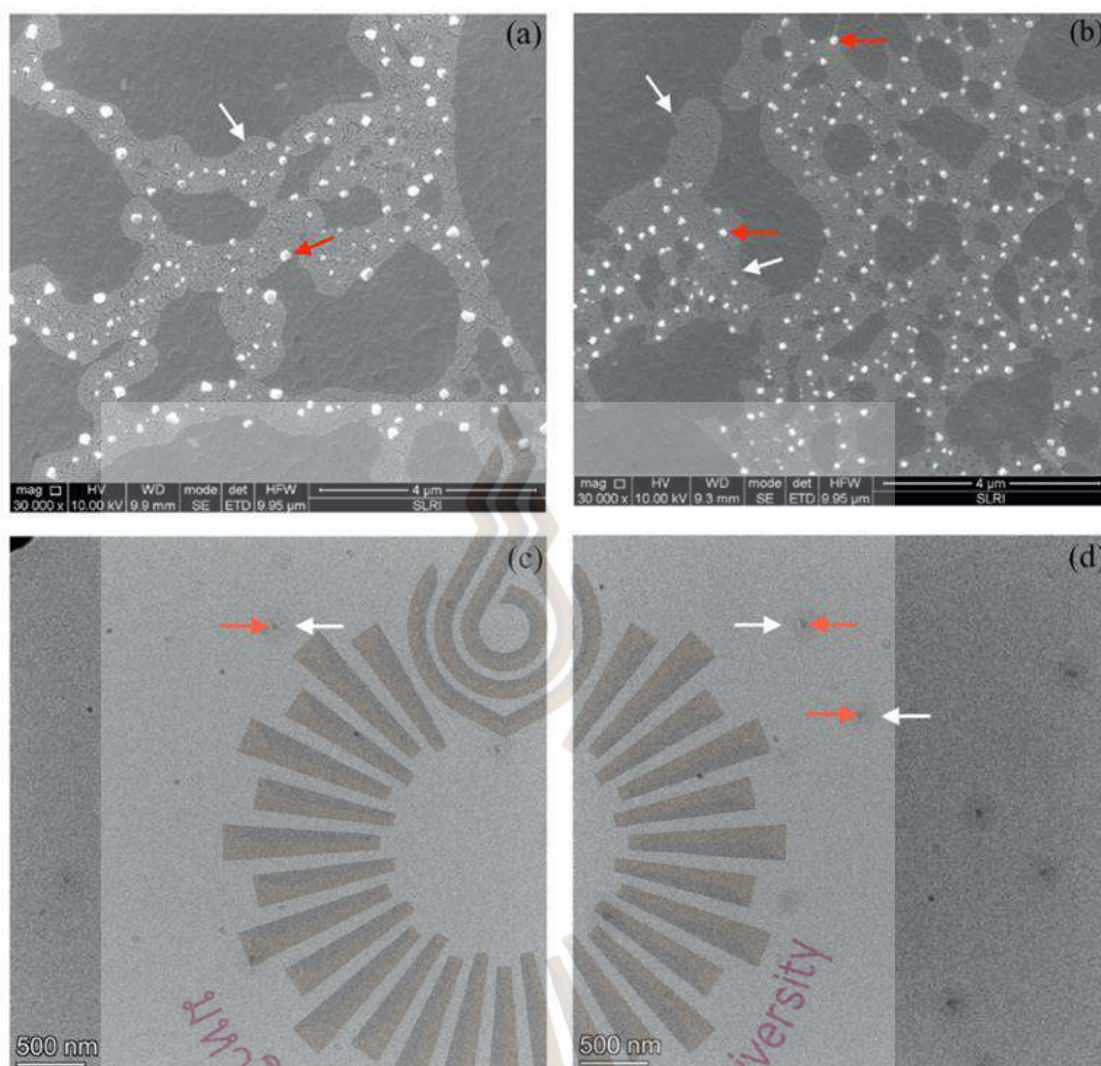


Figure 4.7 SEM images of LC5 (a), LC8 (b), and transmission electron microscopy (TEM) images of LC5 (c) and LC8 (d), all at 25,000 magnification, show molecular dispersions of LH in PEC form between 50 and 100 nm. PEC particles are indicated by the red arrows, while polymeric micelles are indicated by the white arrows.

#### 4.1.4 Optimization: Factorial analysis and validation

The dependent factors were A was the concentration of lidocaine hydrochloride and B was the concentration of hyaluronic acid. The independent factors (response parameters) were particle size, zeta potential, % entrapment efficiency, and % drug release within 5 min.

$$\text{Size} = 678.1A + 1312.11B + 4812.23 \quad (4-4)$$

$$(R^2 = 0.8668)$$

$$\text{Zeta} = 6.42B^2 - 1.94A^2 + 2.75AB - 6.84B - 0.51A - 22.07 \quad (4-5)$$

$$(R^2 = 0.9855)$$

$$\text{Entrapment efficiency} = -2.06A^2 - 9.4B^2 + 5.37AB + 1.96A + 20.49B + 75.41 \quad (4-6)$$

$$(R^2 = 0.9978)$$

Drug release at 5 min resulting from  $3^2$  full factorial design

$$\text{Drug release} = 8.24A^2 - 1.1B^2 - 1.76AB - 15.48A + 2.8B + 21.36 \quad (4-7)$$

$$(R^2 = 0.9929)$$

Particle size, zeta potential, % EE, and drug release within 5 minutes were all significantly affected by LH and HA concentrations ( $p < 0.05$ ). Multiple regression analyses revealed a linear relationship between LH and HA concentrations and particle size, % EE, and drug release, while concentration and zeta potential had a quadratic relationship. Equations (7), (8), (9), and (10), respectively, show the equations for particle size, zeta potential, % EE, and drug release. Figure 4.8a, b, c, and show the 3D response surface and contour plots demonstrating the effect of variables. These effects are most likely due to two factors. First, the concentration of HA raises the viscosity. The final ingredient, HA, is a hydrophilic polymer that can expand to envelop the other components. It increased particle size and % EE while prolonging drug release. Second, the addition of HA, an anionic polymer, may result in a high negative zeta potential. (Gennari et al., 2019; Graça, Miguel, Cabral, & Correia, 2020). As a result, increasing the HA concentration directly raises the zeta potential.

The optimization of minimized size, minimize zeta, maximize %EE and maximize %release 5 min which values were close to LC4 and LC7. However, these conditions did not provide good stability. As a result, LC9 was selected for development in this study.

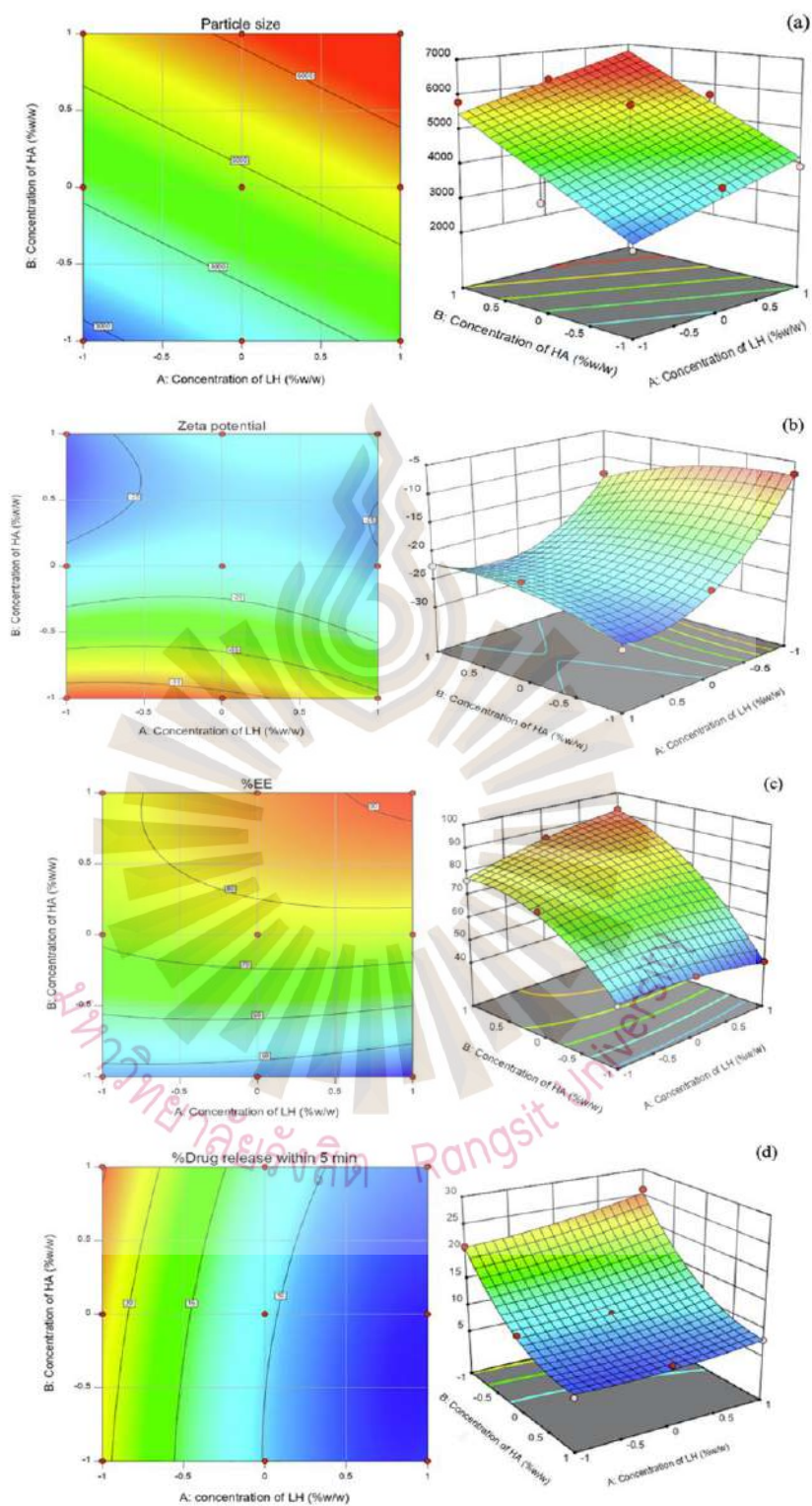


Figure 4.8 Response surface plot and contour plot of independent variables LH (lidocaine hydrochloride) and HA (hyaluronic acid) on (a) particle size, (b) zeta potential, (c) entrapment efficiency, and (d) drug release at 5 min.

The factorial design is an excellent method for studying the influence of variables in small sample sizes at a low cost and in a short period of time. A three-level complete factorial design study is being carried out to evaluate the quadratic relationship between the response and each variable and of the polyelectrolyte complex, optimized  $3^2$  full factorial designs of CS-PC polyelectrolyte complex for colon target drug delivery, and demonstrated success in drug releasing to the colon. (Pandey et al., 2013). Unusually, their CS:PC ratio design was 3:1.1, which was identical to our study, and their findings revealed that this ratio could provide the highest percentage swelling and percentage drug release at 12 hours. Although our design tested the interaction of LH and HA in a fixed ratio of CS:PC at 3:1, this intervention had no effect on percent release; rather, LH and HA were responsible for the main effect of percent swelling and percent drug release.

## **4.2 *In vitro* study of cytotoxicity and wound healing**

### **4.2.1 Cell viability**

Cell proliferation, as implied by cell viability, was measured in formulations containing high LH and varying HA concentrations. The effects of PEC loaded with 50-1000 g/mL of LH (formulations LC3, LC6, and LC9) and different HA concentrations on cell viability were investigated. HGF-1 cells were also used to assess the viability of blank PEC, HA, and Zn cells. The findings (Figure 4.9a) revealed that all other PECs except LC3, LC6, and LC9 had no effect on cell viability. The LC3, LC6, LC9 formulations, and the LH solution all had a dose-dependent effect on HGF-1 after 24 hours of exposure when compared to unloaded LH (Figure 4.9b). Cell viability was reduced by approximately 20% at 250-1000 g/mL LCs compared to the negative control, but LCs were not cytotoxic at lower concentrations (50-100 g/mL). Rather, these concentrations increased cell proliferation (Figure 4.9b). In comparison to the negative control, 500-1000 g/mL LH significantly reduced HGF-1 viability below 50% ( $p < 0.05$ ). Cell viability greater than 70%, according to ISO standards, indicates that the compound is non-toxic or non-cytotoxic (Srivastava et al., 2018). As a result, LC3, LC6, LC9, and LH at concentrations less than 100g/mL were found to be non-cytotoxic to HGF-1 cells.



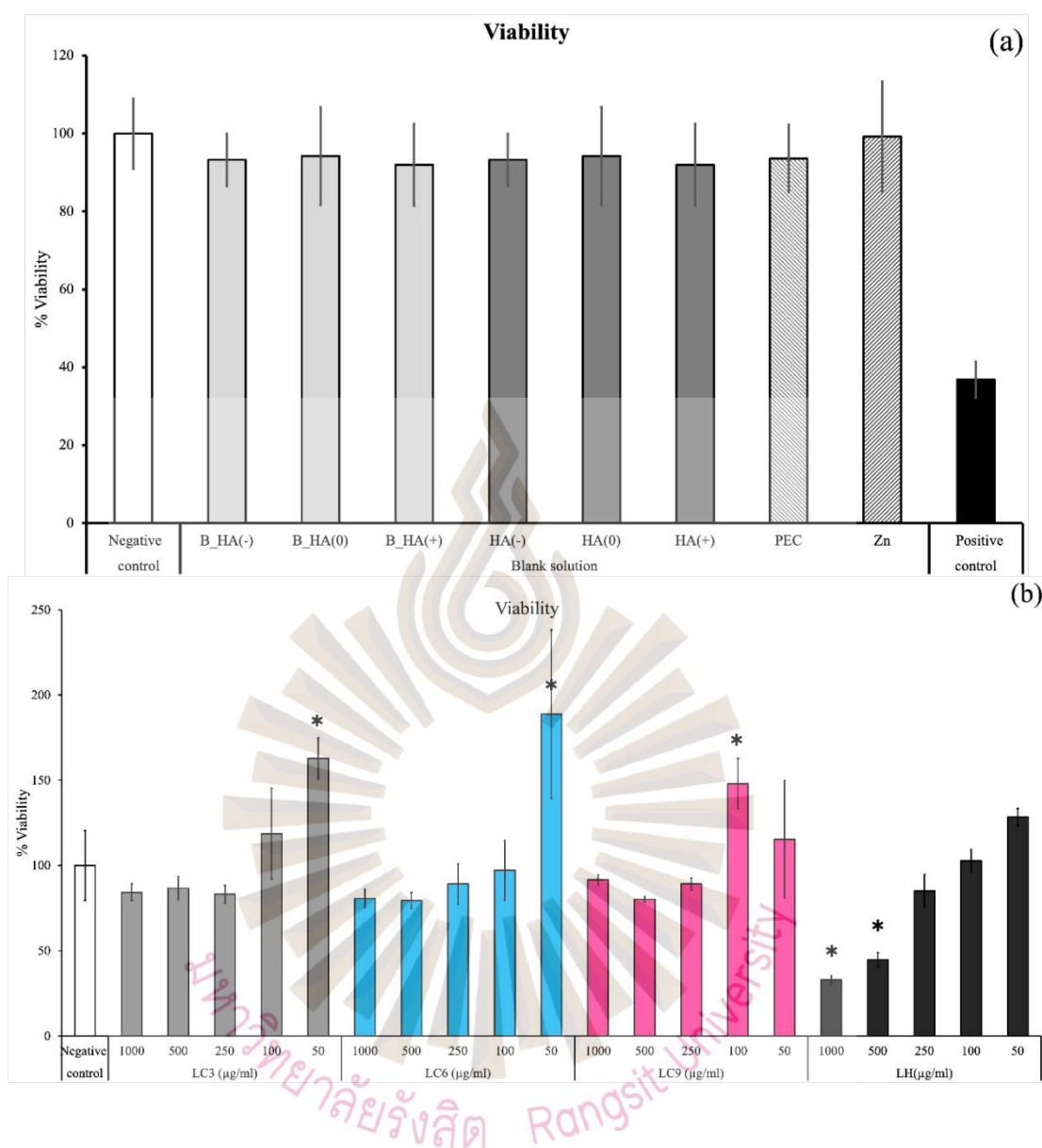


Figure 4.9 Percentage of cell viability by MTT assay (n = 8) at 24 hr. of control in blank DMEM as a negative control, HA (-), HA (0), HA (+), DMEM with FBS as a positive control, chitosan-pectin-hyaluronic polyelectrolyte complex (PEC), and Zinc phosphate (Zn) (a) in comparison with cells viability of formulation LS. Symbols indicate significant differences at  $p < 0.05$ : \* compared to the negative controls (DMEM), and # compared between LS and LC at the same concentration, using the student t-test.

The most important aspect of developing the lidocaine hydrochloride-loaded chitosan-pectin-hyaluronic acid polyelectrolyte complex formulation is determining which ingredient provides the most stable formulation, appropriate physicochemical properties, and rapid and steady-state, controlled

release with no toxicity. Despite having the highest particle size, zeta potential, and % EE, the 1.5% HA formulations (LC7, LC8, LC9) demonstrated adequate physicochemical stability. Furthermore, the high HA concentration resulted in rapid release within 5 minutes and prolonged release over 24 hours, showed no cytotoxicity to gingival fibroblasts and remained homogeneous after three months of storage. Particle size, %EE, %drug release, and cytotoxicity are all variables that can help determine pharmaceutical effects and drug uptake. More research on biocompatibility and therapeutic efficacy is needed.

First, our main goal is to design a topical pain killer formulation to treat dry socket wounds as we proposed a quality by designing lidocaine hydrochloride loaded in chitosan-pectin-hyaluronic acid polyelectrolyte complex that has a fast onset of action within 5 minutes and a continuous sustained release of lidocaine for 24 hours to suppress the pain from dry socket. The formation of kinins in the alveolar bone has been linked to the pathology of the dry socket, which includes early blood clot loss, bearing bone, and pain induced by characteristic dry socket pain. Kinins stimulate the primary afferent nerve endings. (Blum, 2002; Cardoso et al., 2010) Dry socket treatment in direct techniques involves applying a wound dressing containing medication to the exposed bone to protect it from pain stimulation and to release medication to relieve pain. According to the pathogenesis of a dry socket, the pain comes from the nerve at the bone exposure area in a couple of minutes, so our primary goal is to relieve such acute pain and aim to sustain release of our formation for a longer duration until the healing process is over the exposed bone. Our findings are in accordance with the nature of dry socket pathogenesis because we present a quality by design of lidocaine hydrochloride loaded in chitosan-pectin-hyaluronic acid polyelectrolyte complex that has a rapid onset within 5 minutes and continues sustained release of lidocaine for 24 hours to control dry socket pain. Furthermore, we discovered that our formulations had no cytotoxicity to gingival fibroblasts and remained homogeneous after 3 months of storage. These findings could be the primary outcome and could be investigated further in order to develop a more effective formulation.

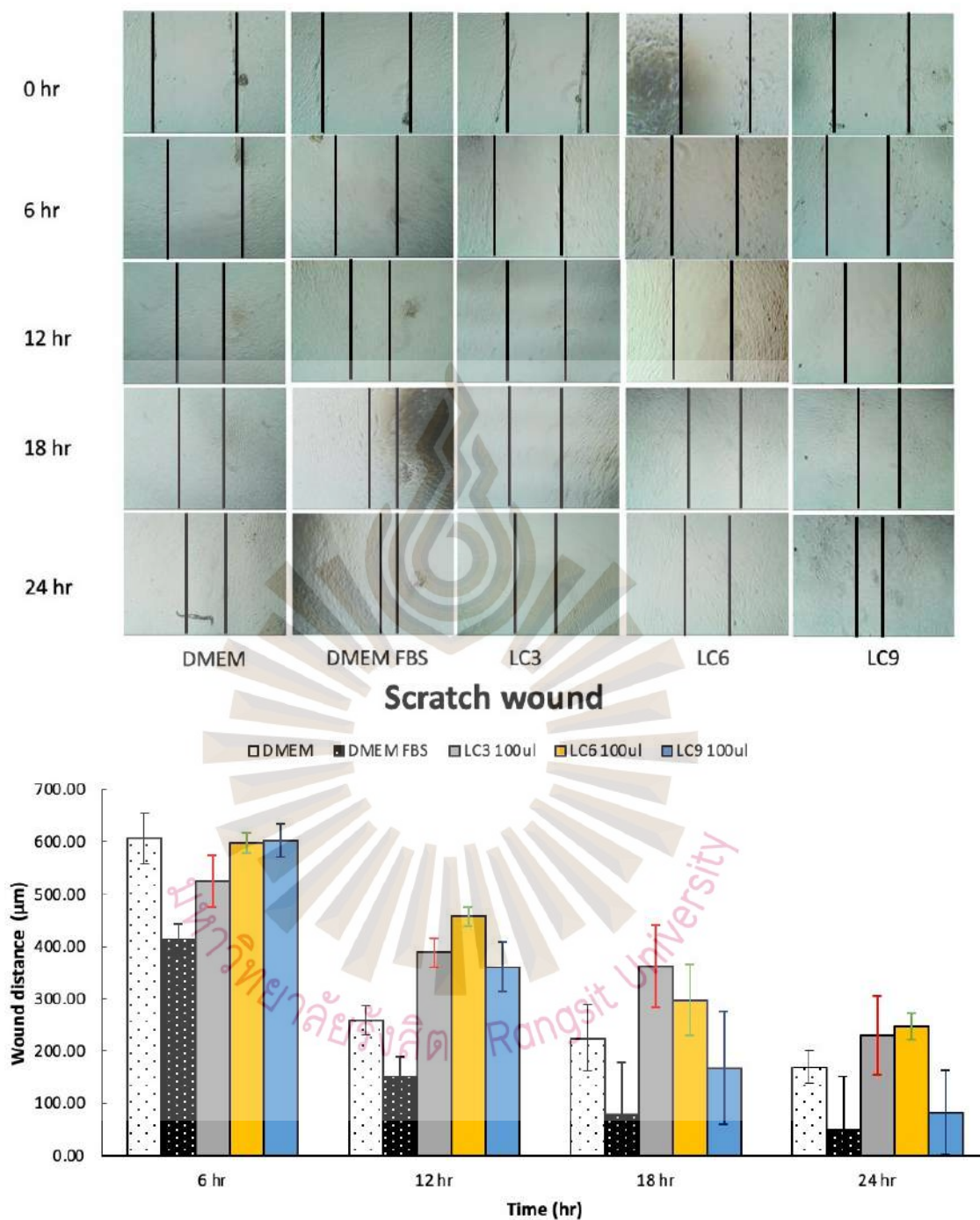


Figure 4.10 (a) The images from *in vitro* scratch wound healing assays show that cell migration into the gap is accelerated in LC3, LC6, and LC9 when compared to DMEM controls and accelerated healing conditions (DMEM FBS). (b) Wound distance summary bar graph at time period of the scratch.

#### 4.2.2 Scratch wound assay

The scratch wound assay was measured compared with DMEM (control condition), DMEM+FBS (accelerated healing condition), and LC3, LC6, and LC9 as shown in Figure 4.10. In the early observation of 6-12 hr. of the treatment, DMEM+FBS increased the highest cellular movement and wound gap closer. However, after 18-24 hr. of the treatment, LC9 which contained the highest HA concentration demonstrated the wound gap decreased significantly higher than the other LC formulation and DMEM treatment. Thus, the higher concentration of HA, the greater accelerated wound healing.

The conclusion of optimization in PEC and safety in cytotoxicity and scratch wound assay proved that LC9 showed less toxicity and potency of cell proliferation. HA was added in PEC to create a ternary polyelectrolyte complex from CS-PC-HA is a complex structure that showed increased zeta potential, increase stability and cell proliferation. High potency to promote healing and rapid in cover bone exposed can increase in potency in treated and decrease pain duration of the dry socket that confirm in LC9 for development to the hydrogel.

### 4.3 Development of lidocaine hydrochloride loaded polyelectrolyte complex incorporated in the thermoresponsive hydrogel.

#### 4.3.1 Formulation development

From previous research, the complex formed by the interaction of the positive charges of CS and the negative charges of PC was studied by the LH-loaded PEC carrier. The ternary polyelectrolyte complex of CS-PC-HA was created using a CS:PC ratio of 3:1. LC9 of ratio 0.3:0.1:1.5 was chosen according to the proper size, high stability, high mucoadhesive, fast LH release within 5 minutes and presented sustained release of drug which as long as the pain-reduction period is completed.

Further investigation was on the development of LC9 incorporated in thermoresponsive polymeric hydrogel (LTP).

4.3.1.1 Determine the temperature and the time of the transition stage between the sol stage and gel stage by varying poloxamer407 concentrations.

Table 4.3 Preliminary study of gelation temperature and gelation time of LC9 incorporated in poloxamer 407 by varying the poloxamer concentration.

Formulation codes	P407 (%w/w)	Gelation temperature (°C)	Gelation time (sec)
LTP1	14	42	-
LTP2	16	37	60
LTP3	18	32	45

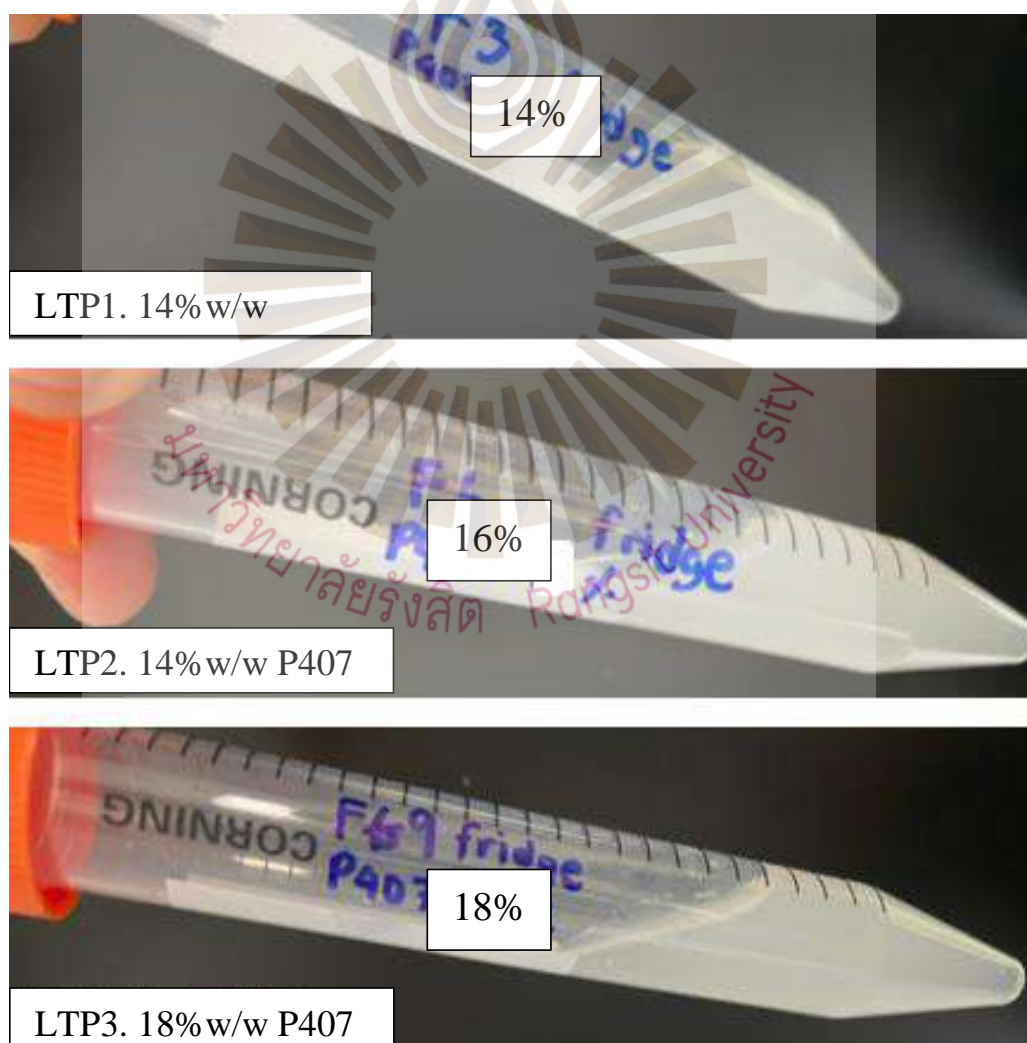


Figure 4.11 LTPs at 4°C were presented in the solution phase.

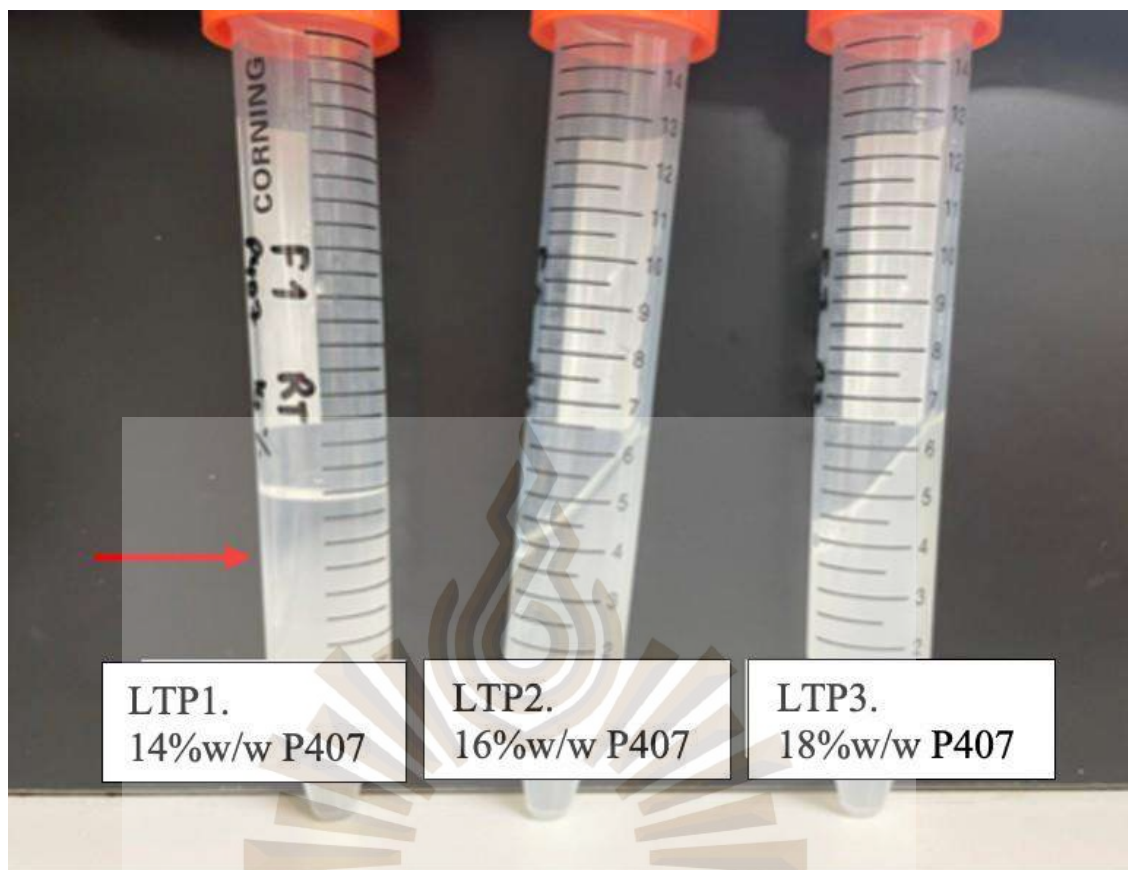


Figure 4.12 LTPs at 37°C temperature, LTP1 was presented in solution phase and LTP2 and 3 in gel phase.

The LC9 was incorporated in P407 gel in various concentrations in a ratio of 1:1 to provide 3 different LTP formulations (Table 4.3). All LPT formulations appeared to be the turbid white solution at 4°C (Figure 4.11). A tube inverting experiment was carried by using a tilted tube in a water bath. The tube inverting test was performed by increasing the temperature in the water bath from 4°C-50°C. Gelation temperatures were shown in the range of 32-42°C. P407 concentration was presented inverse variable to gelation temperature. Gelation time of LTP2 was present at 45 sec and LPT3 at 60 sec but LTP1 could not form the gel at 37°C (Table 4.3, Figure 4.12).

4.3.1.2 Determine temperature and time of the transition stage between the sol stage and gel stage vary LH in PEC and P407.

The gelation temperature ( $T_{gel}$ ) of various LTP (F1, F2, F3, and F4) in LH was studied in this work. The hydrogel formulations' gelation temperature ranged between  $26.17 \pm 0.70$  and  $28.03 \pm 0.87^\circ\text{C}$ , as reported in Table 4.4, and they produced gels at body temperature (Figure 4.13). All formulations' gelation temperatures are appropriate for oral administration. At  $37^\circ\text{C}$ , gelation time ( $Time_G$ ) ranges between  $1.30 \pm 1.25$  and  $2.35 \pm 0.21$ , with 3 minutes of gelation time acceptable for working time in the oral cavity.

Table 4.4 Gelation temperature, gelation time, drug content and stability

Formulation	Gelation temp	Gelation time	Viscosity	Drug content
F1	$26.17 \pm 0.70$	$2.15 \pm 0.21$	$9597.95 \pm 1.11$	$103.65 \pm 2.49$
F2	$27.30 \pm 0.72$	$2.10 \pm 0.14$	$7678.36 \pm 1.48$	$106.1 \pm 1.12$
F3	$28.03 \pm 0.87$	$2.35 \pm 0.21$	$6838.54 \pm 1.70$	$105.66 \pm 1.92$
F4	$27.57 \pm 0.55$	$1.30 \pm 1.25$	$4798.98 \pm 1.36$	$100.28 \pm 0.63$

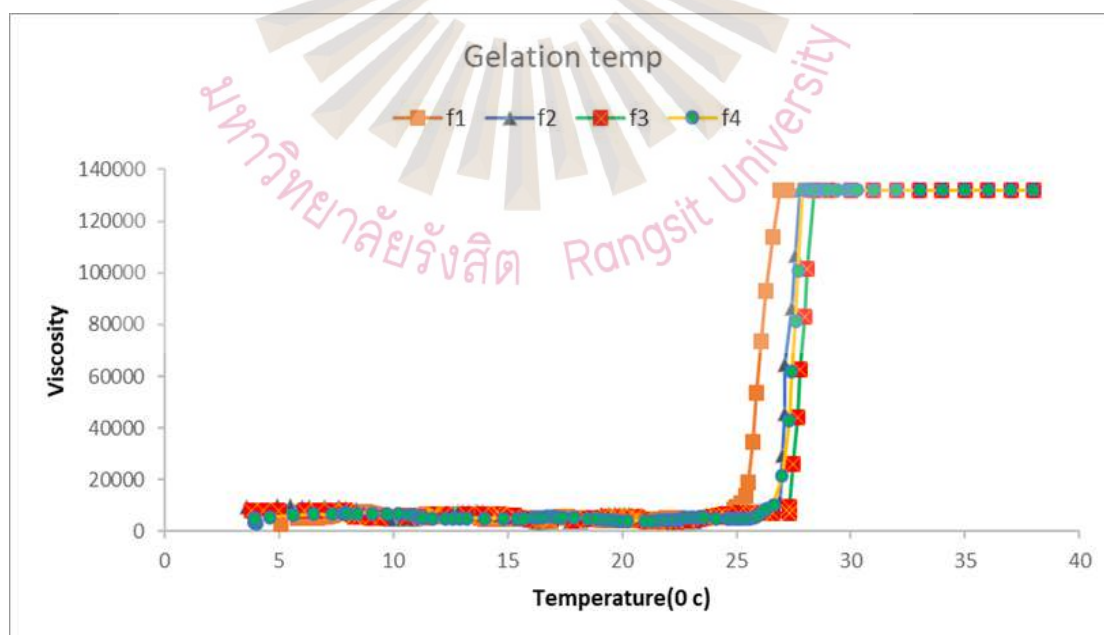


Figure 4.13 Gelation temperature and gelation time of LTP (F1, F2, F3 and F4)

The micelle's center is made of PPO, and the shell's surround is made of hydrophilic PEO. Hydrophobic drugs can be incorporated into the hydrophobic component of poloxamer. (Zarrintaj et al., 2020). LH is a weak base. Because charged molecules are unable to permeate the hydrophobic cores of micelles, Lidocaine did not affect to gelation temperature (Ricci et al., 2002, 2005). As a result, LH in PEC (F3) and LH in P407 (F4) gelation temperatures were similar.

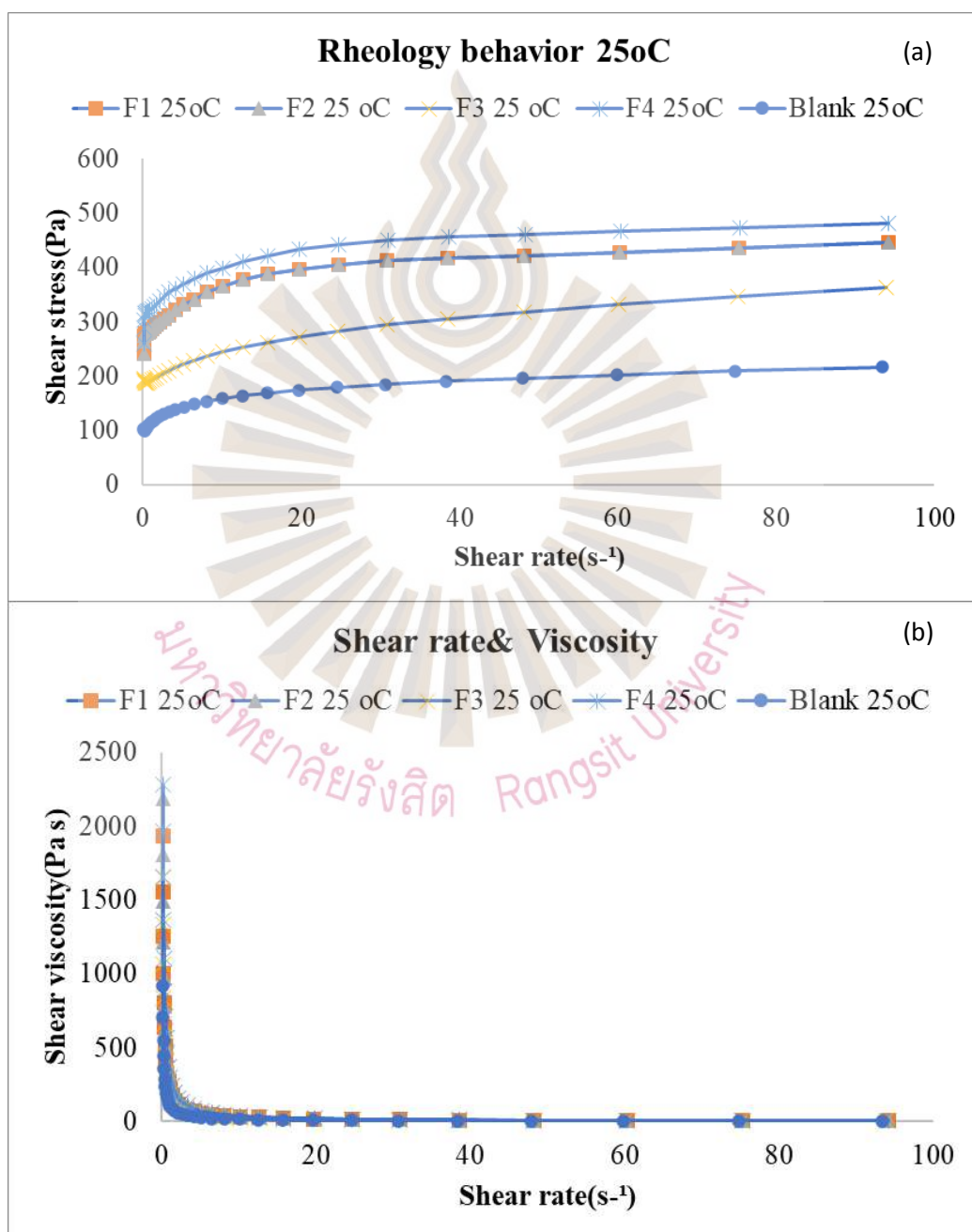


Figure. 4.14 Rheology of four formulations and blank. (a) Shear stress; (b) Viscosity



#### 4.3.1.3 Determined rheology viscosity and elastic property

Shear stress increases as the shear rate increases. The decreasing slope of the curve as the shear rate increases indicates that the hydrogel has pseudoplastic rheologic behavior.

At 25°C, shear rate viscosity was measured. Figure 4.14 demonstrates the gel viscosity curves, while Table 4.4 demonstrates the viscosity measurements. The gels' viscosity decreased as shear rate increased; they were pseudoplastic. In other words, as shear rate increased, they became less viscosity. (Figure 4.14).

### 4.3.2 The interaction of thermoresponsive gel formation

#### 4.3.2.1 Fourier transform infrared spectroscopy (FTIR)

Molecular interactions between components in the hydrogel “F” formulations were characterized by FTIR spectra. FTIR was also used to determine the functional groups present on the surface of the nanoparticle (Figure 4.15).

LH showed two sharp bands appeared at the range 1450–1550  $\text{cm}^{-1}$  due to C-N stretching whereas the one with higher energy was due to the bond with a higher inductive effect (O-C-N). However, there was only one broad peak in the same range revealing the equivalency of the two C-N bonds in lidocaine base. where a broad peak appeared at the range 1650–1715  $\text{cm}^{-1}$  due to summation of the two carbonyl groups stretching of the polymer and the drug. Wave number about a plane O-H bend 1,340  $\text{cm}^{-1}$  in F1, F2, F3 and BG, Wave number shifted to 1,280  $\text{cm}^{-1}$  in F4, Wave number about a  $\text{CH}_2$  bend and  $\text{CH}_3$  bend 1,440  $\text{cm}^{-1}$  in F1, F2, F3 and BG, Wave number shifted to 1,380  $\text{cm}^{-1}$  in F4, Wave number about a  $\text{CH}_2$  bend and  $\text{CH}_3$  bend 1,620  $\text{cm}^{-1}$  in F1, F2, F3 and BG, Wave number shifted to 1,600  $\text{cm}^{-1}$  in F4 indicated LH in P407 without interaction.

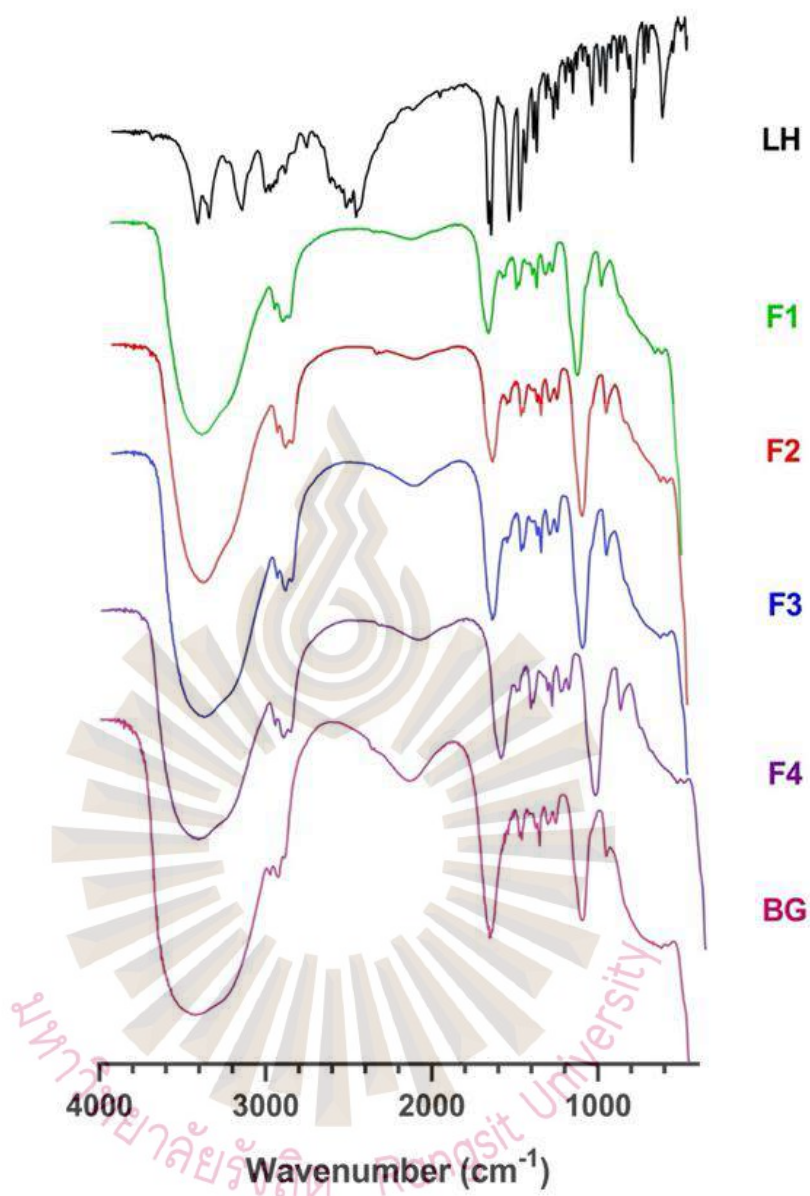


Figure 4.15 FTIR spectrum of F1, F2, F3, F4 and BG.

#### 4.3.2.2 Differential scanning calorimetry (DSC)

LH showed an endothermic peak at 77.9°C followed by a boiling and volatilization peak starting from 188°C. The endothermic peak of lidocaine hydrochloride was not present in the formulation. This is presumably explained by the fact that lidocaine hydrochloride is being solubilized in the formulation (Figure 4.16).

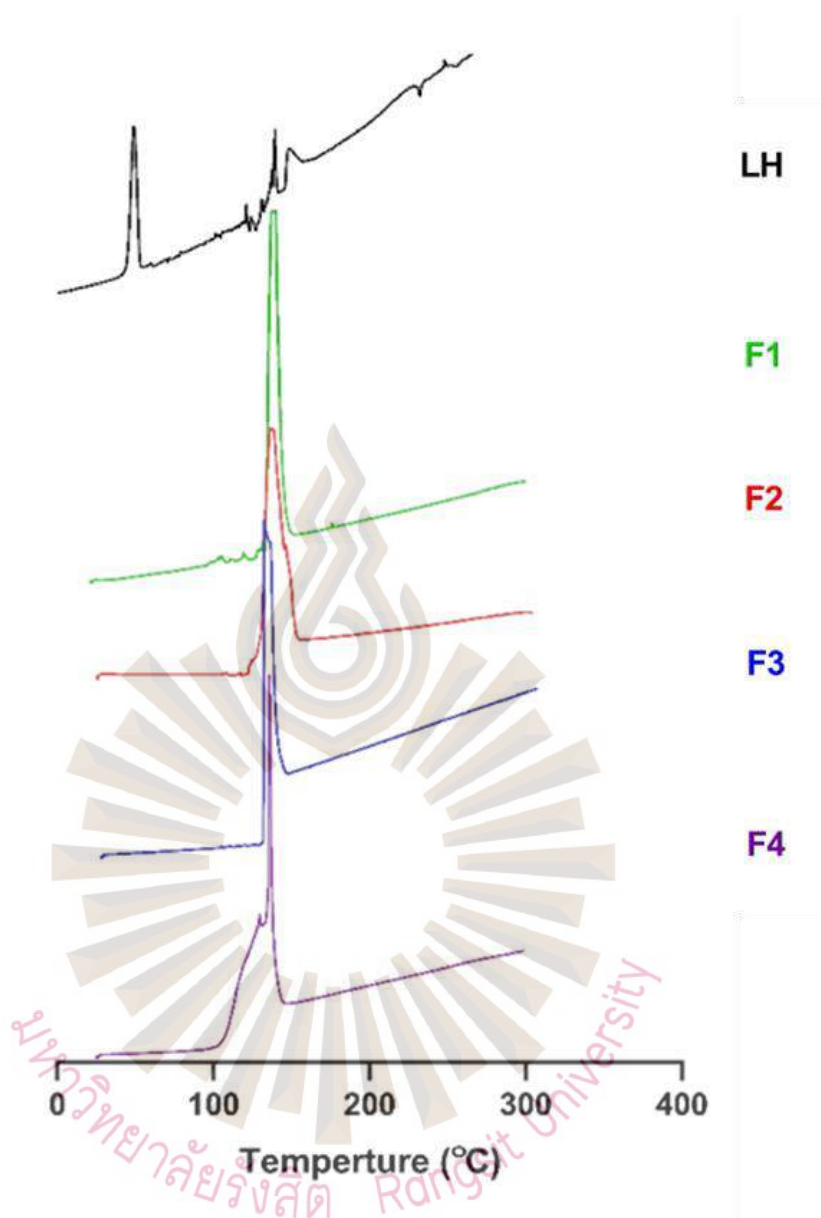


Figure 4.16 DSC of LH, F1, F2, F3, and F4.

### 4.3.3 Effects of lidocaine hydrochloride loaded thermoresponsive gel formation on texture profile analysis

#### 4.3.3.1 Hardness, syringeability and mucoadhesive

The comparison of TPA of the 4 formulations of thermoresponsive gel formation (F1, F2, F3, and F4) that are present in the table or graft for hardness, mucoadhesive and syringeability. The hardness test was performed to measure the force required to produce the deformation of gels. The

hardness ranked in the order of  $F3 > F2 > F1$  and when compare between  $F3$  with  $F4$ , this test was present of LH in polyelectrolyte complex has hardness more than LH in P407 may be LH from PEC with anion charge polymer (Nurkeeva, Mun, Khutoryanskiy, Bitekenova, & Dzhusupbekova, 2002). The syringeability was showed ranked in the order of  $F3 > F2 > F1$  (Table 4.5). and when comparing between  $F3$  and  $F4$  LH in polyelectrolyte complex has syringeability force more than LH in P407 maybe from complex but the most syringeability in  $F3$  ( $122.291 \pm 59.74$ ) is injectable when push like a normal injection. In Figure 4.17, syringeability varies directly from the hardness that this study presents when to increase hardness, syringeability will increase.

The mucoadhesive was implied in maximum detachment force. The mucoadhesive rank in the order of  $F3 > F2 > F1$  and  $F3$  compared to  $F4$  mucoadhesive of LH in polyelectrolyte complex higher than LH in P407. Because mucoadhesive does not affect LH concentration, all formulations demonstrated mucoadhesive, with no statistically significant difference ( $p > 0.05$ ) (Figure 4.18).

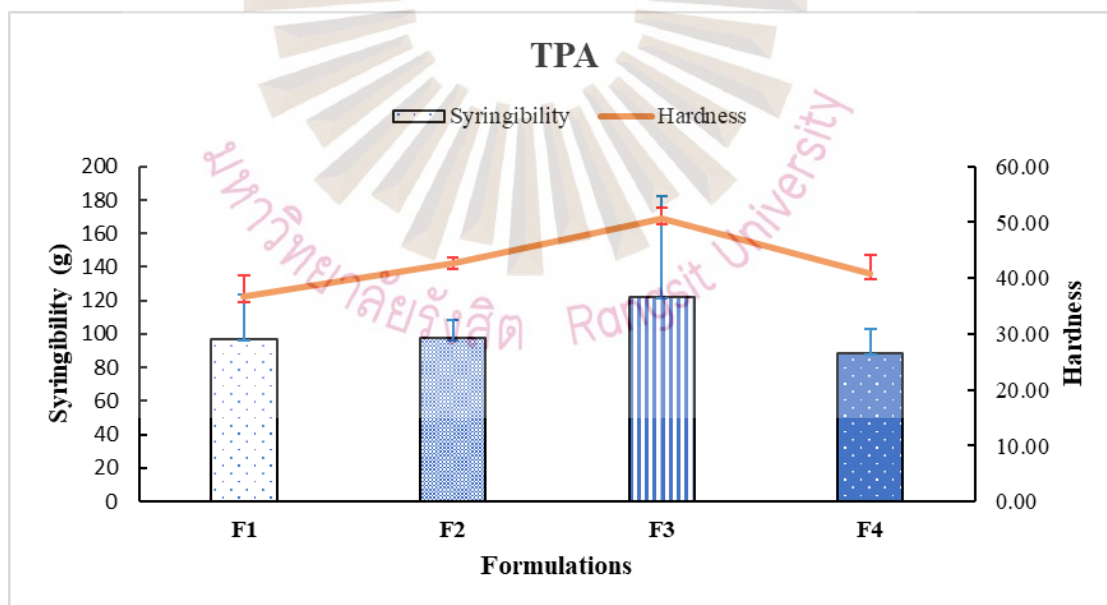


Figure 4.17 The comparison of TPA of the four formulations of Li HCl hydrogel (F1, F2, F3, and F4) That present in the table or graft for Hardness

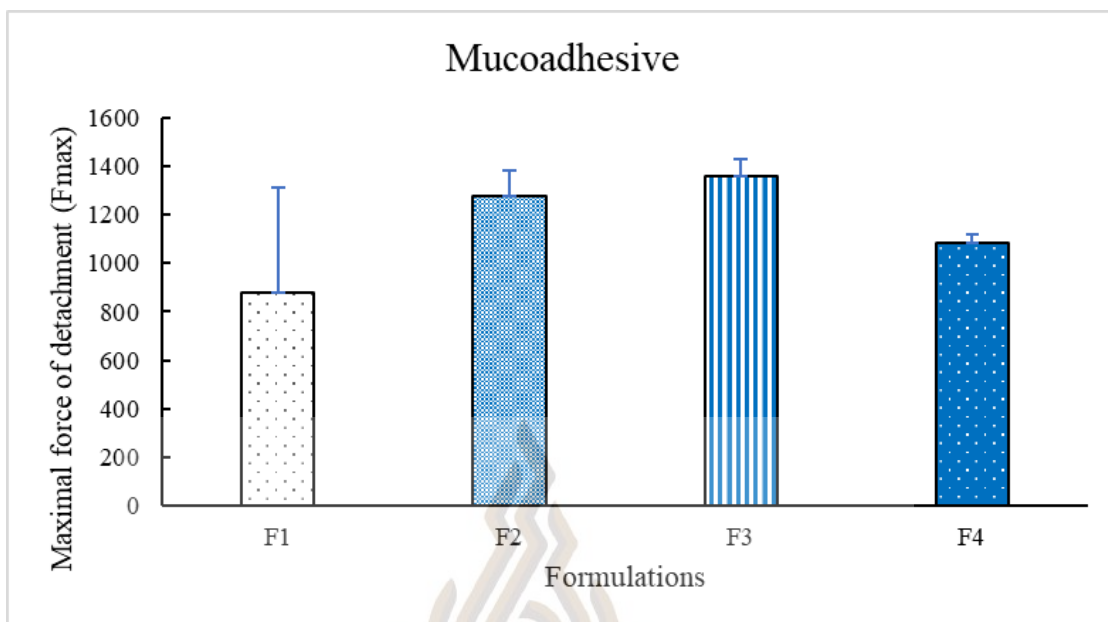


Figure 4.18 Maximal force of detachment (Fmax) experiments at 37 °C using four formulations of LH hydrogels. The values represented are the mean  $\pm$  SD (n = 3)

Table 4.5 TPA of the four formulations That are present in Hardness, and Syringibility

Formulation	Hardness (G)	Syringeability (G)	Mucoadhesive Fmax (G)
F1	36.761 $\pm$ 3.64	96.783 $\pm$ 27.01	881.441 $\pm$ 428.10
F2	42.681 $\pm$ 1.10	97.466 $\pm$ 10.77	1278.194 $\pm$ 105.09
F3	50.602 $\pm$ 1.91	122.291 $\pm$ 59.74	1360.688 $\pm$ 65.92
F4	40.856 $\pm$ 3.24	88.418 $\pm$ 14.87	1083.355 $\pm$ 36.92

#### 4.3.4 Drug content

As previously described, LTP containing 5% LH w/w was successfully prepared. For each formula, the drug content of the prepared in-situ gels ranged from 100.28 to 106.1%. (Table 4.4).

#### 4.3.5 *In vitro* drug release

The kinetic models zero-order, first-order, and the Higuchi model were used to investigate LH release and permeation (Tables 4.6). As shown in equation (16), zero-order kinetic models were plotted as the cumulative amount of drug released over time. The logarithmic cumulative amount of drug released over time was plotted in first-order kinetic models (as shown in equation (17)). Higuchi models were plotted as the cumulative amount of drug released over time (as shown in equation (18)). The Korsmeyer-peppas model was plotted as a log cumulative percentage of drug released versus log time (as shown in equation (19)).

$$Q = k_0 t \quad (4-8)$$

$$\ln Q = \ln Q_0 - k_1 t \quad (4-9)$$

$$Q = k_H t^{1/2} \quad (4-10)$$

$$D_t / D_{\infty} = K_{KP} t^n \quad (4-11)$$

Where:

$k_0$  = rate constant for zero-order kinetics.

$k_1$  = rate constant for first-order kinetics.

$K_H$  = rate constant for Higuchi-model kinetics.

$Q_t$  = percentage of the released drug after time  $t$ .

$Q_0$  = initial percentage of the released drug (Usually 0).

$k_{KP}$  = constant of nanoparticles incorporating geometric characteristic structures.

$n$  = release exponent (related to the drug release mechanism).

$t^{1/2}$  = the square root of the time

$t$  = the time in hours

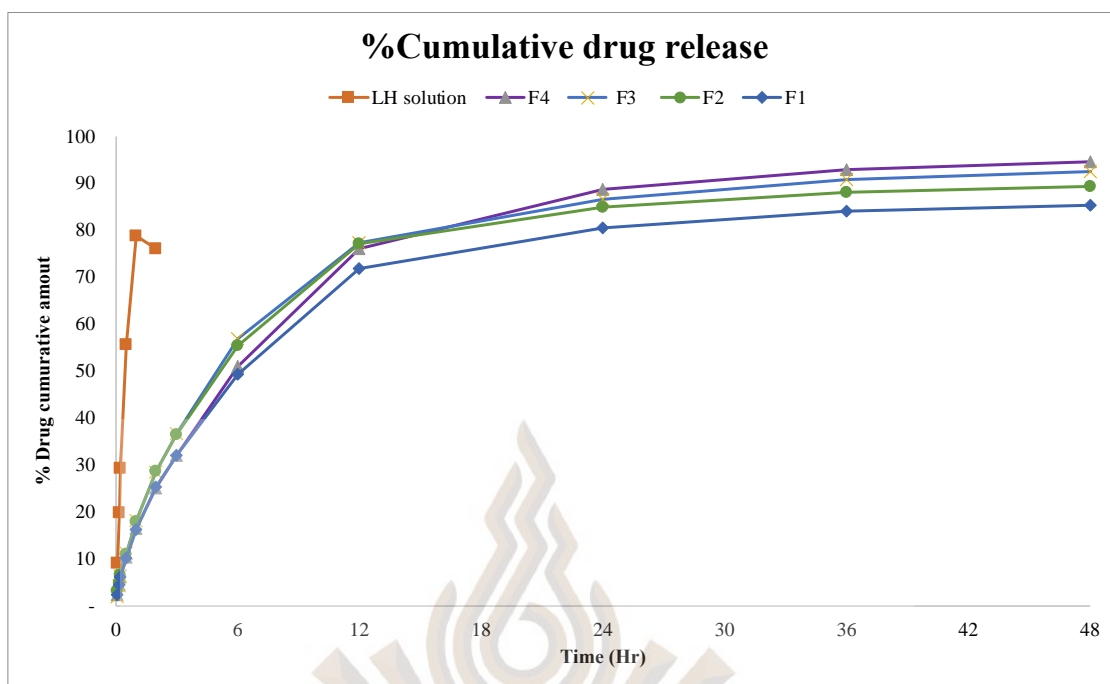


Figure 4.19 % Cumulative drug release profile of formulation F1, F2, F3, F4, and 5% LH solution.

LH drug release in P407 (F3) was comparable to LH drug release in polyelectrolyte complex (F4). Drug releases of F4 and F3 were similar and showed prolonged release but the LH in the polyelectrolyte. The release of Korsmeyer Peppas is most likely the main cause why all of the formulations had a different release value.

Kinetic treatment of the release was also performed. Release kinetics analysis of F1-F4 is best fit to the prolonged drug release behavior of gel formulations after diffusion and erosion is indicated by the Korsmeyer-Peppas exponent value, and F5 is fit in the first order. The n value is used to analyze the release mechanism., the n value = 0.5 in Fickian diffusion, the  $0.45 < n = 0.89$  in non-Fickian transport, the n value is 0.89 in Case II transport and super case II transport when the n value higher than 0.89 (Baishya, 2017). The n value of F1- F4 is 0.583-0.732 which presented the drug release mechanism of non-Fickian transport in this research (Table 4.6).

Table 4.6 Drug release over 8 hours according to zero-order, first-order, and Higuchi release models, including the coefficient of correlation ( $r^2$ ), slope (k), and intercept.

Kinetic models	Zero-order		First-order		Higuchi		Korsmeyer -Peppas		
	$K_0$	$r^2$	$K_1$	$r^2$	$K_H$	$r^2$	$K_{KP}$	n	$r^2$
F1	0.1140	0.8622	0.1117	0.5966	2.5300	0.9803	1.379	0.603	0.9986
F2	0.1240	0.8350	0.1102	0.9346	2.7820	0.9830	1.704	0.583	0.9959
F3	0.1250	0.8360	0.1120	0.5380	2.8020	0.9790	1.677	0.587	0.9929
F4	0.1190	0.8857	0.1115	0.5633	2.6270	0.9737	1.251	0.626	0.9991
F5	1.458	0.9055	0.0250	0.9923	9.2550	0.8944	4.063	0.732	0.9778

#### 4.3.6 Drug safety

The result of Total template count is lower than 10 CFU/mL, Total Yeast and Mold is lower than 10 CFU/g, *Escherichia coli* is not detected and *Staphylococcus aureus* is not detected. The results showed about the safety of bacterial contamination was proved.

#### 4.3.7 In vitro degradation

As shown in Figure 4.19, four LTP formulations (F1-F4) on the 48 hr., the amount of weight loss is present in degradation. Degradation in 24 hr. of F1 to F4 was 95.721±7.75%, 88.104±13.92%, 71.327±3.11% and 69.265±13.48 % in order, degradation in 48 hr. of F1 to F4 was 59.770±6.26%, 52.10±10.05%, 35.430±8.72%, and 47.265±25.73%. As a result, all of the formulations have a faster rate of biodegradation, which assists in biocompatibility. F3 demonstrates that the least biodegradable formulation may be one of the causes of prolonged release.



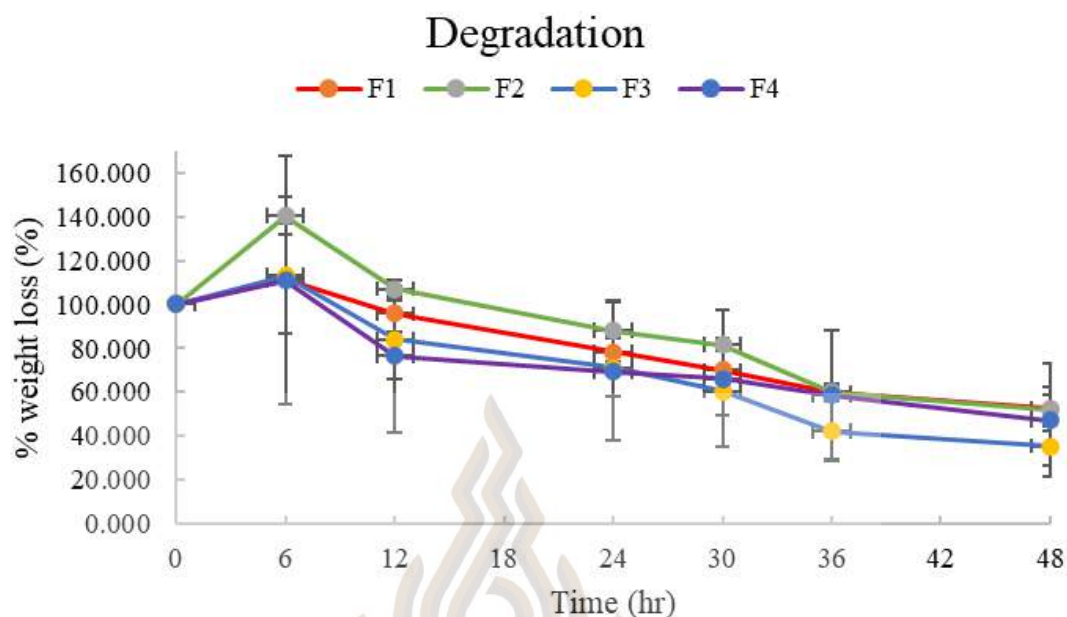


Figure. 4.20 Degradation of formulation F1, F2, F3 and F4 in artificial saliva at 37°C

#### 4.3.8 Stability

After keep formulation in 4°C (refrigerator), 30°C (Thailand room temperature), 45°C (Accelerate condition) (Figure 4.21). The separated formulation was discovered after 1 month. At 4°C, drug content presented in 80.1% in F4, 84.18% in F2, 97.75% in F3 and 100.84% in F4. At 2 months, all formulations had been separated and showed low drug content (F1 = 80.99%, F2 = 87.82%, F3 = 93.47% and F4 = 89.34%). The formulations which keep at 30°C showed a slight decrease in drug content in the gel situation. At 2 months, 30°C drug content of formulation showed higher than 94.78% accepted F2 (74.35%). The accelerated condition (45°C) drug content of formulation had a trend to decrease, F3 at 45°C is the lowest formulation that drug degrade (2 mo. F3 45°C = 92.70%).

The result of this study recommended keeping formulation at 30°C and F3 is the best formulation in all situations. Maybe F3 has a strong crosslink and high hardness that protects drug degradation from the environment.

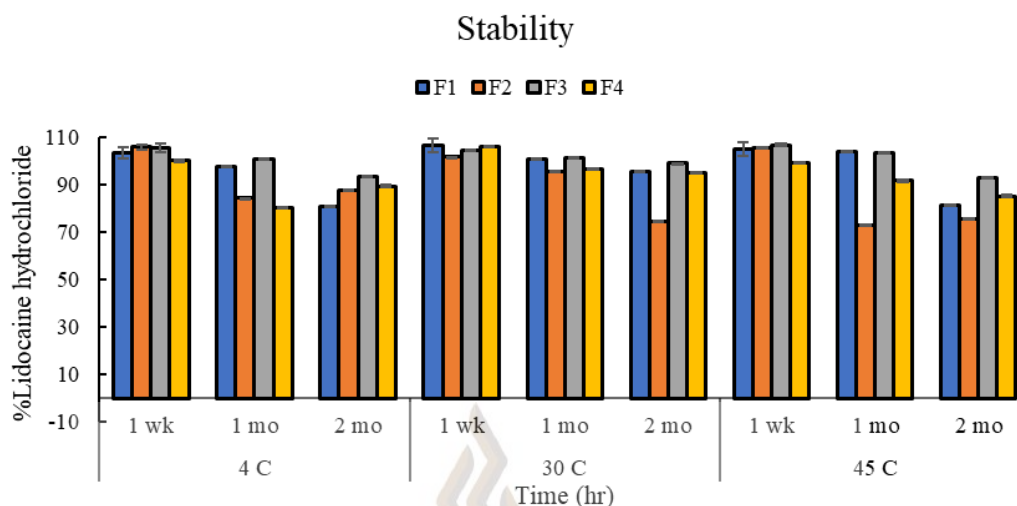


Figure 4.21 Drug stability of F1, F2, F3 and F4 keep at 4°C, 30°C and 45°C

#### 4.4 Clinical research in anesthetic efficacy

##### 4.4.1 Irritating and allergy tests

There was no allergy or irritation found in all participants. Thus, the product was used for further study.

##### 4.4.2 Onset and efficacy time

A pinprick test on the palatal mucosa was performed on the ten healthy volunteers. the onset of anesthesia ( $T_{on}$ ) was measured is  $46.5 \pm 22.5$  sec and the effective time ( $T_{eff}$ ) is  $202.5 \pm 41.0$  sec and the rank is 120-240 sec.

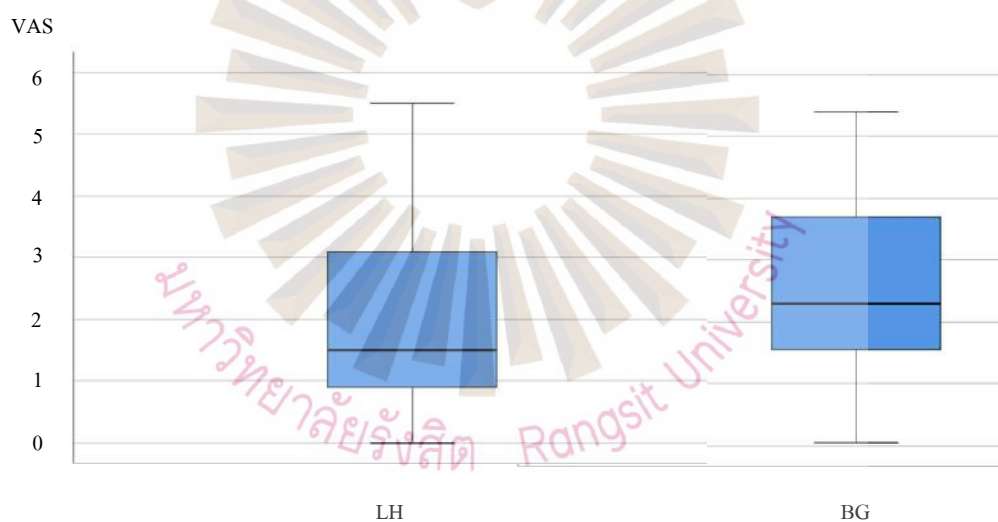
##### 4.4.3 Comparison of anesthetic efficacy

Thirty volunteers Their average age was 24.85 years, with a range of 23 to 28 years. Sixteen patients were female, and fourteen were male. Since the data from the split-mouth in anesthetic efficacy comparison were not normally distributed (Shapiro-Wilk test).

After the application of BG, the mean VAS of the injection was  $2.59 \pm 1.46$  cm, which was significantly higher than the mean VAS of the injection after the application of LN, which was mean =  $1.94 \pm 1.43$  cm, ( $p < 0.05$ ) (Figure 4.22). The result of VAS of palatal injection in LH groups showed less than BG groups from 21 in 30 participants (70%) and After topical BG application, VAS during palatal injection was significantly higher than after topical LG application ( $p = 0.043$ ).

In an inferior alveolar nerve block, 2% lignocaine and 20% benzocaine were used to relieve needle insertion pain. In terms of reducing needle insertion pain, 2% lignocaine performed better than 20% benzocaine. (Manisha Nair, 2019)

When compared to benzocaine gel, the preparation may improve the anesthetic efficacy of lidocaine and reduce palatal injection pain.



	LH	BG	Difference
Min	0	0.05	0.005
Max	5.5	5.4	0.1
Mean	1.94	2.59	0.65
Median	1.5	2.3	0.8
Range	5.5	5.35	0.15

Figure 4.22 Box plots and a summary showing the VAS (cm) during palatal injection to compare the anesthetic efficacy of LTP (F3) hydrogel and topical Benzocaine gel

## Chapter 5

### Conclusion

#### 5.1 Conclusion

This study verified the formulations of LH and HA-loaded PEC in nine formulations in a full factorial design (2 factors 3 levels). 10%LH and 1.5%HA-loaded PEC (LC9) showed proper physiochemical properties in the proper size, mucoadhesive property, easy onset in 5 mins, sustained release, and good biocompatibility in MTT assay which could accelerate wound healing when compared to control (*in vitro*). The LC9 presented high stability in 3 months therefore LC9 was chosen to further develop into in situ gel.

After incorporating LH-loaded PEC into P407 hydrogel, the drug interaction of LH in PEC and LH in P407 was determined. All formulations turn to gel at 37°C within 3 minutes. The interaction of LH in all formulations was not changed in gelation temperature. The texture analyzer showed 10%LH loaded in PEC incorporated hydrogel (F4) showed high hardness and easy to inject in syringe model 1 ml. with needle gauze no. 18. Mucoadhesive does not affect LH concentration, all formulations demonstrated mucoadhesive, with no statistically significant difference. All formulations presented in sustain release and fit in Korsmeyer-Peppas. F3 tended to be longer release than LH in P407. In the degradation study, % weight loss was shown in 69.26-95.72% and 35.43-59.77% at 24 and 48 hr, respectively. The fast biodegradability for safety in the wound was shown in all formulations and imply to no removal in drug use, F3 demonstrates that the least biodegradable formulation may be one of the causes of prolonged release.

The onset of anesthesia ( $T_{on}$ ) was measured as  $46.5 \pm 22.5$  sec. and the effective time ( $T_{eff}$ ) is  $202.5 \pm 41.0$  sec and the rank is 120-240 sec. The mean comparison between F3 and BG in anesthetic effect presented mean injection pain VAS after the application of BG was  $2.59 \pm 1.46$

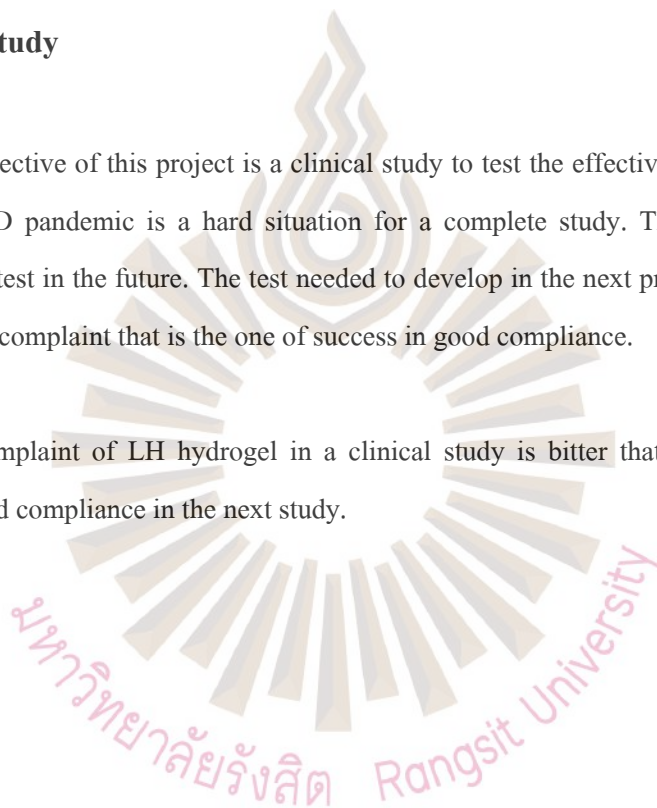
cm, significantly different than that after the application of LH that was a mean of  $1.94 \pm 1.43$  cm, ( $p < 0.05$ ) result showed high anesthetic efficacy of F3 than BG.

These results confirmed the property of polymeric hydrogel containing Lidocaine loaded polyelectrolyte complex is one choice that is good in fast onset, prolonged release, safety, and good compliance by easy to use syringe injection, safe time to see the dentist to remove.

## 5.2 Further Study

The objective of this project is a clinical study to test the effectiveness of the dry sockets but in a COVID pandemic is a hard situation for a complete study. The study on dry socket patients should test in the future. The test needed to develop in the next project because the test is the most one of complaint that is the one of success in good compliance.

The complaint of LH hydrogel in a clinical study is bitter that needs to improve and develop for good compliance in the next study.



## References

- Abueva, C., Kim, B., Lee, B. T., & Nath, S. D. (2015). Chitosan-hyaluronic acid polyelectrolyte complex scaffold crosslinked with genipin for immobilization and controlled release of BMP-2. *Carbohydrate Polymers*, *115*(1), 207–214. <https://doi.org/10.1016/j.carbpol.2014.08.077>
- Arau, M. D. (2007). *Peri-implant maintenance of immediate function implants : a pilot study comparing hyaluronic acid and chlorhexidine*. *Int J Dent Hygiene*, *5*(1), 87–94.
- Archana, D., Dutta, J., & Dutta, P. K. (2013). Evaluation of chitosan nano dressing for wound healing: Characterization, in vitro and in vivo studies. *International Journal of Biological Macromolecules*, *57*(1), 193–203. <https://doi.org/10.1016/j.ijbiomac.2013.03.002>
- Asparuhova, M. B., Kiryak, D., Eliezer, M., Mihov, D., & Sculean, A. (2019). Activity of two hyaluronan preparations on primary human oral fibroblasts. *Journal of Periodontal Research*, *54*(1), 33–45. <https://doi.org/10.1111/jre.12602>
- Baishya, H. (2017). Application of Mathematical Models in Drug Release Kinetics of Carbidopa and Levodopa ER Tablets. *Journal of Developing Drugs*, *06*(02). <https://doi.org/10.4172/2329-6631.1000171>
- Birch, N. P., & Schiffman, J. D. (2014). Characterization of self-Assembled polyelectrolyte complex nanoparticles formed from chitosan and pectin. *Langmuir*, *30*(12), 3441–3447. <https://doi.org/10.1021/la500491c>
- Birn, H. (1973). Etiology and pathogenesis of fibrinolytic alveolitis ('dry socket'). *International Journal of Oral*, *2*(5), 211–263.
- Blum, I. R. (2002). Contemporary views on dry socket (alveolar osteitis): A clinical appraisal of standardization, aetiopathogenesis and management: A critical review. *International Journal of Oral and Maxillofacial Surgery*, *31*(3), 309–317. <https://doi.org/10.1054/ijom.2002.0263>
- Borges, V., Maciel, V., Yoshida, C. M. P., & Teixeira, T. (2015). Chitosan / pectin polyelectrolyte complex as a pH indicator. *Carbohydrate Polymers*, *132*(1), 537–545. <https://doi.org/10.1016/j.carbpol.2015.06.047>

### References (Cont.)

- Burgoyne, C. C., Giglio, J. A., Reese, S. E., Sima, A. P., & Laskin, D. M. (2010). The Efficacy of a Topical Anesthetic Gel in the Relief of Pain Associated With Localized Alveolar Osteitis. *Journal of Oral and Maxillofacial Surgery*, *68*(1), 144–148.  
<https://doi.org/10.1016/j.joms.2009.06.033>
- Buriuli, M., & Verma, D. (2017). *Advances in Biomaterials for Biomedical Applications*, *66*(1).  
<https://doi.org/10.1007/978-981-10-3328-5>
- Cardoso, C. L., Rodrigues, M. T. V., Ferreira, O., Garlet, G. P., & De Carvalho, P. S. P. (2010). Clinical concepts of dry socket. *Journal of Oral and Maxillofacial Surgery*, *68*(8), 1922–1932. <https://doi.org/10.1016/j.joms.2009.09.085>
- Cheung, R. C. F., Ng, T. B., Wong, J. H., & Chan, W. Y. (2015). Chitosan: An update on potential biomedical and pharmaceutical applications. *Mar. Drugs* *2015*, *13*(8), 5156–5186.  
<https://doi.org/10.3390/md13085156>
- Da Silva, J. B., Ferreira, S. B. de S., Reis, A. V., Cook, M. T., & Bruschi, M. L. (2018). Assessing mucoadhesion in polymer gels: The effect of method type and instrument variables. *Polymers*, *10*(3), 1–19. <https://doi.org/10.3390/polym10030254>
- Dahiya, P., & Kamal, R. (2013). Hyaluronic acid: A boon in periodontal therapy. *North American Journal of Medical Sciences*, *5*(1), 309–315. <https://doi.org/10.4103/1947-2714.112473>
- Dakhara, S., & Anajwala, C. (2010). Polyelectrolyte complex: A pharmaceutical review. *Systematic Reviews in Pharmacy*, *1*(2), 121. <https://doi.org/10.4103/0975-8453.75046>
- Das, S., Chaudhury, A., & Ng, K. Y. (2011). Preparation and evaluation of zinc-pectin-chitosan composite particles for drug delivery to the colon: Role of chitosan in modifying in vitro and in vivo drug release. *International Journal of Pharmaceutics*, *406*(1–2), 11–20.  
<https://doi.org/10.1016/j.ijpharm.2010.12.015>
- De Oliveira, L. P., Hudebine, D., Guillaume, D., & Verstraete, J. J. (2016). A Review of Kinetic Modeling Methodologies for Complex Processes. *Oil and Gas Science and Technology*, *71*(3), 1–49. <https://doi.org/10.2516/ogst/2016011>
- Faizel, M., & Awad, A. (2015). *Four Dimensional Supersymmetric Theories in Presence of a Boundary*. Retrieved from <https://arxiv.org/pdf/1502.07717.pdf>

### References (Cont.)

- Feres, M., Teles, F., Teles, R., Figueiredo, L. C., & Faveri, M. (2016). The Subgingival Periodontal Microbiota in the Aging Mouth. *Periodontology 2000*, 72(1), 30-53. <http://dx.doi.org/10.1111/prd.12136>
- Fridrich, K. L., & Olson, R. A. J. (1990). Alveolar osteitis following surgical removal of mandibular third molars. *Anesthesia Progress*, 37(1), 32–41. [https://doi.org/10.1016/0278-2391\(91\)90238-h](https://doi.org/10.1016/0278-2391(91)90238-h)
- Gennari, A., de la Rosa, J. M. R., Hohn, E., Pelliccia, M., Lallana, E., Donno, R., . . . Tirelli, N. (2019). The different ways to chitosan/hyaluronic acid nanoparticles: Templated vs direct complexation. Influence of particle preparation on morphology, cell uptake and silencing efficiency. *Beilstein Journal of Nanotechnology*, 10(1), 2594–2608. <https://doi.org/10.3762/bjnano.10.250>
- Gowda, G., Viswanath, D., & Kumar, M. (2013). Dry Socket (Alveolar Osteitis): Incidence, Pathogenesis, Prevention and Management. *Journal of Indian Academy of Oral Medicine and Radiology*, 25(3), 196-199. Retrieved from [http://www.jaypeejournals.com/eJournals/ShowText.aspx?ID=6534&Type=FREE&TYP=TOP&IN=\\_eJournals/images/JPLOGO.gif&IID=493&isPDF=YES](http://www.jaypeejournals.com/eJournals/ShowText.aspx?ID=6534&Type=FREE&TYP=TOP&IN=_eJournals/images/JPLOGO.gif&IID=493&isPDF=YES)
- Graça, A., Gonçalves, L. M., Raposo, S., Ribeiro, H. M., & Marto, J. (2018). Useful in vitro techniques to evaluate the mucoadhesive properties of hyaluronic acid-based ocular delivery systems. *Pharmaceutics*, 10(3), 110. <https://doi.org/10.3390/pharmaceutics10030110>
- Graça, M. F. P., Miguel, S. P., Cabral, C. S. D., & Correia, I. J. (2020). Hyaluronic acid—Based wound dressings: A review. *Carbohydrate Polymers*, 241(April), 116364. <https://doi.org/10.1016/j.carbpol.2020.116364>
- Hong, W. G., Jeong, G. W., & Nah, J. W. (2018). Evaluation of hyaluronic acid-combined ternary complexes for serum-resistant and targeted gene delivery system. *International Journal of Biological Macromolecules*, 115(1), 459–468. <https://doi.org/10.1016/j.ijbiomac.2018.04.053>
- Ishihara, M., Kishimoto, S., Nakamura, S., Sato, Y., & Hattori, H. (2019). Polyelectrolyte complexes of natural polymers and their biomedical applications. *Polymers*, 11(4), 1–12. <https://doi.org/10.3390/polym11040672>



### References (Cont.)

- Isordia-Salas, I., Pixley, R. A., Sáinz, I. M., Martínez-Murillo, C., & Colman, R. W. (2005). The role of plasma high molecular weight kininogen in experimental intestinal and systemic inflammation. *Archives of Medical Research*, 36(1), 87–95. <https://doi.org/10.1016/j.arcmed.2005.02.001>
- Jasmeet, K., Harikumar, S. L., & Amanpreet, K. (2012). Interpolyelectrolyte complexes as prospective carriers for controlled drug delivery. *International Research Journal of Pharmacy*, 3(4), 58–62. <https://doi.org/10.1242/jcs.071001>
- Jeong, B., Wan, S., & Han, Y. (2002). Thermosensitive sol – gel reversible hydrogels. *Advanced Drug Delivery Reviews*, 54(1), 37–51. <https://doi.org/10.1016/j.addr.2012.09.012>
- Jiang, Q., Zhang, P., & Li, J. (2020). Elucidation of Colloid Performances of Thermosensitive In Situ-Forming Ophthalmic Gel Formed by Poloxamer 407 for Loading Drugs. *Journal of Pharmaceutical Sciences*, 109(5), 1703–1713. <https://doi.org/10.1016/j.xphs.2020.01.021>
- Jorge, L. L., Feres, C. C., & Teles, V. E. (2010). Topical preparations for pain relief: efficacy and patient adherence. *Journal of pain research*, 4(1), 11–24. <https://doi.org/10.2147/JPR.S9492>
- Kayan, G. Ö., & Kayan, A. (2021). Composite of Natural Polymers and Their Adsorbent Properties on the Dyes and Heavy Metal Ions. *Journal of Polymers and the Environment*, 29(11), 3477–3496. <https://doi.org/10.1007/s10924-021-02154-x>
- Kitir, N., Yildirim, E., Şahin, Ü., Turan, M., Ekinci, M., Ors, S., . . . Ünlü, H. (2018). *Peat Use in Horticulture*. Retrieved from [https://www.researchgate.net/profile/Ertan-Yildirim-2/publication/327894825\\_Peat\\_Use\\_in\\_Horticulture/links/5bb5c28ba6fdccd3cb852f96/Peat-Use-in-Horticulture.pdf](https://www.researchgate.net/profile/Ertan-Yildirim-2/publication/327894825_Peat_Use_in_Horticulture/links/5bb5c28ba6fdccd3cb852f96/Peat-Use-in-Horticulture.pdf)
- Kong, L., Sun, J., & Bao, Y. (2017). Preparation, characterization and tribological mechanism of nanofluids. *RSC Advances*, 7(21), 12599–12609. <https://doi.org/10.1039/c6ra28243a>
- Kravanja, G., & Primo, M. (2019). *Chitosan-Based (Nano)Materials for Novel Biomedical Applications*. Retrieved from [https://pdfs.semanticscholar.org/a56d/78c43088b2ac7a56289637da29bfb46321ab.pdf?\\_ga=2.122754443.1235858644.1660478953-2016616799.1650989445](https://pdfs.semanticscholar.org/a56d/78c43088b2ac7a56289637da29bfb46321ab.pdf?_ga=2.122754443.1235858644.1660478953-2016616799.1650989445)

### References (Cont.)

- Laracuate, M. L., Yu, M. H., & McHugh, K. J. (2020). Zero-order drug delivery: State of the art and future prospects. *Journal of Controlled Release*, 327(September), 834–856. <https://doi.org/10.1016/j.jconrel.2020.09.020>
- Lee, H.-S. (2016). Recent advances in topical anesthesia. *Journal of Dental Anesthesia and Pain Medicine*, 16(4), 237. <https://doi.org/10.17245/jdapm.2016.16.4.237>
- Limsitthichaikoon, S., & Sinsuebpol, C. (2019). Electrostatic effects of metronidazole loaded in chitosan-pectin polyelectrolyte complexes. *Key Engineering Materials*, 819 KEM, 27–32. <https://doi.org/10.4028/www.scientific.net/KEM.819.27>
- Lodi, G., Figini, L., Sardella, A., Carrassi, A., M, D. F., & Furness, S. (2012). *Antibiotics to prevent complications following tooth extractions (Review)*. Retrieved from [https://exodontia.info/wp-content/uploads/2021/07/Cochrane\\_Review\\_2012\\_Review\\_Antibiotics\\_to\\_prevent\\_complications\\_following\\_tooth\\_extractions.pdf](https://exodontia.info/wp-content/uploads/2021/07/Cochrane_Review_2012_Review_Antibiotics_to_prevent_complications_following_tooth_extractions.pdf)
- López-Esparza, R., Balderas Altamirano, M. A., Pérez, E., & Gama Goicochea, A. (2015). Importance of molecular interactions in colloidal dispersions. *Advances in Condensed Matter Physics*, 2015(689716), 1-8. <https://doi.org/10.1155/2015/683716>
- Lucas, M. A., Fretto, L. J., & Mckee, A. (1983). The Binding of Human Plasminogen to Fibrin and Fibrinogen. *National Library of Medicine*, 258(7), 4249-56.
- Mamoun, J., & Mamoun, J. (2018). Dry Socket Etiology , Diagnosis , and Clinical Treatment Techniques. *Journal of The Korean Association of Oral and Maxillofacial Surgeons*, 44(2), 52–58. <https://doi.org/10.5125/jkaoms.2018.44.2.52>
- Manisha Nair, D. G. D. (2019). Original Article Comparative evaluation of the efficacy of two anesthetic gels (2% lignocaine and 20% benzocaine) in reducing pain during administration of local anesthesia – A randomized controlled trial. *Journal of Anaesthesiology Clinical Pharmacology*, 34(3), 46–50. <https://doi.org/10.4103/joacp.JOACP>
- Markov, P. A., Popov, S. V., Nikitina, I. R., Ovodova, R. G., & Ovodov, Y. S. (2011). Anti-inflammatory activity of pectins and their galacturonan backbone. *Russian Journal of Bioorganic Chemistry*, 37(7), 817–821. <https://doi.org/10.1134/S1068162011070132>

### References (Cont.)

- Marouf, I., & Rejab, A. (2020). Effects of Local Application of Hyaluronic Acid on Postoperative Sequelae after Surgical Removal of Impacted Lower Third Molars. *Al-Rafidain Dental Journal*, 20(2), 154–164. <https://doi.org/10.33899/rden.2020.126803.1026>
- Marple, B., Roland, P., & Benninger, M. (2004). Safety review of benzalkonium chloride used as a preservative in intranasal solutions: An overview of conflicting data and opinions. *Otolaryngology - Head and Neck Surgery*, 130(1), 131–141. <https://doi.org/10.1016/j.otohns.2003.07.005>
- Metin, M., Tek, M., & Sener, I. (2006). Comparison of Two Chlorhexidine Rinse Protocols on the Incidence of Alveolar Osteitis following the. *Journal of Contemporary Dental Practice*, 7(2), 1–5.
- Mitrevej, A., Sinchaipanid, N., Rungvejhavuttivittaya, Y., & Kositchaiyong, V. (2001). Multiunit controlled-release diclofenac sodium capsules using complex of chitosan with sodium alginate or pectin. *Pharmaceutical Development and Technology*, 6(3), 385–392. <https://doi.org/10.1081/PDT-100002247>
- Mohamed, A. R. (2016). Dimethyl formamide as Dispersing Agent for Electrophoretically Deposited of Multi-Walled Carbon Nanotubes. *International Journal of Petrochemical Science & Engineering*, 1(1), 13–16. <https://doi.org/10.15406/ipcse.2016.01.00004>
- Moore, R. A., Derry, S., & Mcquay, H. J. (2014). *Topical analgesics for acute and chronic pain in adults*. Retrieved from <https://www.ncbi.nlm.nih.gov/pmc/articles/PMC4234085/pdf/emss-58353.pdf>
- Mori, T., Okumura, M., Matsuura, M., Ueno, K., Tokura, S., Okamoto, Y., . . . Fujinaga, T. (1997). Effects of chitin and its derivatives on the proliferation and cytokine production of fibroblasts in vitro. *Biomaterials*, 18(13), 947–951. [https://doi.org/10.1016/S0142-9612\(97\)00017-3](https://doi.org/10.1016/S0142-9612(97)00017-3)
- Morris, G. A., Kök, S. M., Harding, S. E., Adams, G. G., Alba, K., Kontogiorgos, V., . . . McClements, D. J. (2017). Comparison of emulsifying properties of food-grade polysaccharides in oil-in-water emulsions: Gum arabic, beet pectin, and corn fiber gum. *Food Hydrocolloids*, 68(1), 144–153. <https://doi.org/10.1016/j.foodhyd.2016.12.019>

### References (Cont.)

- Morris, G. A., Kök, S. M., Harding, S. E., Adams, G. G., Morris, G. A., Kök, S. M., . . . Harding, E. (2016). Polysaccharide drug delivery systems based on pectin and chitosan Polysaccharide delivery systems systems Polysaccharide drug drug delivery based on pectin and chitosan based on pectin and chitosan. *Biotechnology and Genetic Engineering Reviews*, 27(1), 257-284. <https://doi.org/10.1080/02648725.2010.10648153>
- Nirmal, H. B., Bakliwal, S. R., Pawar, S. P., & College, P. S. G. V. P. M. (2010). *In-Situ gel : New trends in Controlled and Sustained Drug Delivery System*, 2(2), 1398–1408.
- Nurkeeva, Z. S., Mun, G. A., Khutoryanskiy, V. V., Bitekenova, A. B., & Dzhusupbekova, A. B. (2002). Polymeric complexes of lidocaine hydrochloride with poly(acrylic acid) and poly(2-hydroxyethyl vinyl ether). *Journal of Biomaterials Science, Polymer Edition*, 13(7), 759–768. <https://doi.org/10.1163/156856202760197393>
- Omer, L. S., & Ali, R. J. (2017). Extraction-Spectrophotometric Determination of Lidocaine Hydrochloride in Pharmaceuticals. *International Journal of Chemistry*, 9(4), 49. <https://doi.org/10.5539/ijc.v9n4p49>
- Pandey, S., Mishra, A., Raval, P., Patel, H., Gupta, A., & Shah, D. (2013). Chitosan-pectin polyelectrolyte complex as a carrier for colon targeted drug delivery. *Journal of Young Pharmacists*, 5(4), 160–166. <https://doi.org/10.1016/j.jyp.2013.11.002>
- Potaś, J., Szymańska, E., & Winnicka, K. (2020). Challenges in developing of chitosan – Based polyelectrolyte complexes as a platform for mucosal and skin drug delivery. *European Polymer Journal*, 140(September). <https://doi.org/10.1016/j.eurpolymj.2020.110020>
- Priftis, D., Xia, X., Margossian, K. O., Perry, S. L., Leon, L., Qin, J., . . . Tirrell, M. (2014). Ternary, tunable polyelectrolyte complex fluids driven by complex coacervation. *Macromolecules*, 47(9), 3076–3085. <https://doi.org/10.1021/ma500245j>
- Priprem, A., Paphangkorakit, J., Limsitthichaikoon, S., Sermswatsri, S. R., Pitiphat, W., Thaiprasong, P., & Patchadee, P. (2014). Efficacy comparison of on-site preparation of 5%lidocaine niosome dispersion and benzocaine/tetracaine gel. *Advanced Materials Research*, 853(1), 237–242. <https://doi.org/10.4028/www.scientific.net/AMR.853.237>

### References (Cont.)

- Quiñones, J. P., Peniche, H., & Peniche, C. (2018). Chitosan based self-assembled nanoparticles in drug delivery. *Polymers*, *10*(3), 1–32. <https://doi.org/10.3390/polym10030235>
- Ricci, E. J., Bentley, M. V. L. B., Farah, M., Bretas, R. E. S., & Marchetti, J. M. (2002). Rheological characterization of Poloxamer 407 lidocaine hydrochloride gels. *European Journal of Pharmaceutical Sciences*, *17*(3), 161–167. [https://doi.org/10.1016/S0928-0987\(02\)00166-5](https://doi.org/10.1016/S0928-0987(02)00166-5)
- Ricci, E. J., Lunardi, L. O., Nanclares, D. M. A., & Marchetti, J. M. (2005). Sustained release of lidocaine from Poloxamer 407 gels. *Int J Pharm*, *288*(2), 235–244. <https://doi.org/10.1016/j.ijpharm.2004.09.028>
- Sayed, A. M. (2008). Intra-Articular Drug Delivery: A Fast Growing Approach. *Recent Patents on Drug Delivery & Formulation*, *2*(3), 231–237. <https://doi.org/10.2174/187221108786241651>
- Shevel, E. (2018). Painful dry socket: an alternative perspective. *South African Dental Journal*, *73*(7), 456–458. <https://doi.org/10.17159/2519-0105/2018/v73no7a5>
- Srivastava, G. K., Alonso-Alonso, M. L., Fernandez-Bueno, I., Garcia-Gutierrez, M. T., Rull, F., Medina, J., . . . Pastor, J. C. (2018). Comparison between direct contact and extract exposure methods for PFO cytotoxicity evaluation. *Scientific Reports*, *8*(1), 1–9. <https://doi.org/10.1038/s41598-018-19428-5>
- Supe, N. B., Choudhary, S. H., Yamyar, S. M., Patil, K. S., Choudhary, A. K., & Kadam, V. D. (2018). Efficacy of alvogyl (Combination of Iodoform + Butylparaminobenzoate) and zinc oxide eugenol for dry socket. *Annals of Maxillofacial Surgery*, *8*(2), 193–199. [https://doi.org/10.4103/ams.ams\\_167\\_18](https://doi.org/10.4103/ams.ams_167_18)
- Tarakji, B., Saleh, L. A., Umair, A., Azzeghaiby, S. N., & Hanounch, S. (2015). Systemic Review of Dry Socket: Aetiology, Treatment, and Prevention. *Journal of Clinical and Diagnostic Research*, *9*(4), ZE10–ZE13. <https://doi.org/10.7860/JCDR/2015/12422.5840>
- Tauber, E. (2012). Review article. *Romani Studies*, *22*(2), 175–182. <https://doi.org/10.3828/rs.2012.10>
- Ueno, H., Mori, T., & Fujinaga, T. (2001). Topical formulations and wound healing applications of chitosan. *Advanced Drug Delivery Reviews*, *52*(2), 105–115. [https://doi.org/10.1016/S0169-409X\(01\)00189-2](https://doi.org/10.1016/S0169-409X(01)00189-2)

### References (Cont.)

- Ueno, H., Yamada, H., Tanaka, I., Kaba, N., Matsuura, M., Okumura, M., . . . Fujinaga, T. (1999). Accelerating effects of chitosan for healing at early phase of experimental open wound in dogs. *Biomaterials*, *20*(15), 1407–1414. [https://doi.org/10.1016/S0142-9612\(99\)00046-0](https://doi.org/10.1016/S0142-9612(99)00046-0)
- Ur-Rehman, T., Tavelin, S., & Gröbner, G. (2011). Chitosan in situ gelation for improved drug loading and retention in poloxamer 407 gels. *International Journal of Pharmaceutics*, *409*(1–2), 19–29. <https://doi.org/10.1016/j.ijpharm.2011.02.017>
- Vallurupalli, S., & Manchanda, S. (2011). Risk of acquired methemoglobinemia with different topical anesthetics during endoscopic procedures. *Local and Regional Anesthesia*, *4*(1), 25–28. <https://doi.org/10.2147/LRA.S22711>
- Wang, H. (2017). Pectin-Chitosan Polyelectrolyte Complex Nanoparticles for Encapsulation and Controlled Release of Nisin. *American Journal of Polymer Science and Technology*, *3*(5), 82. <https://doi.org/10.11648/j.ajpst.20170305.11>
- Wald, A. (1932). Postoperative complications in exodontia: their treatment and prevention. *Dent Cosmos*, *74*(1), 72-77.
- Wang, J. J., Zeng, Z. W., Xiao, R. Z., Xie, T., Zhou, G. L., Zhan, X. R., & Wang, S. L. (2011). Recent advances of chitosan nanoparticles as drug carriers. *International Journal of Nanomedicine*, *6*(1), 765–774. <https://doi.org/10.2147/ijn.s17296>
- Zarrintaj, P., Ramsey, J. D., Samadi, A., Atoufi, Z., Yazdi, M. K., Ganjali, M. R., . . . Thomas, S. (2020). Poloxamer: A versatile tri-block copolymer for biomedical applications. *Acta Biomaterialia*, *110*(1), 37–67. <https://doi.org/10.1016/j.actbio.2020.04.028>

**Appendices**



The logo of Rangsit University is a circular emblem. At the top is a stylized flame or sunburst. Below it is a central circle containing a Thai character. The bottom half of the emblem consists of a semi-circle of radiating lines. The text 'มหาวิทยาลัยรังสิต' is written in Thai script along the bottom arc, and 'Rangsit University' is written in English along the bottom arc.

**Appendix A**

**Validation of Lidocaine Hydrochloride by HPLC**

มหาวิทยาลัยรังสิต Rangsit University



## HPLC condition and validation of lidocaine hydrochloride

Validation data of lidocaine hydrochloride

<b>Machine</b>	SHIMADZU LC10
<b>Column</b>	C18 Inertsil ODS-3 (4.6x250mm,5um I.D.)
<b>Oven</b>	ambient
<b>Detector Wavelength</b>	UV 254 nm
<b>Mobile phase</b>	A = 5% acetic acid in water, B = Absolute methanol
<b>Ratio of mobile phase</b>	A:B = 52.5:47.5
<b>Injection volume</b>	20 µL
<b>Flow rate</b>	1.0 mL/min
<b>Run time</b>	15 min
<b>Retention time</b>	6.620 min
<b>LOD</b>	3.24 µg/mL
<b>LOQ</b>	10.80 µg/mL
<b>Precision and accuracy</b>	RSD < 2%

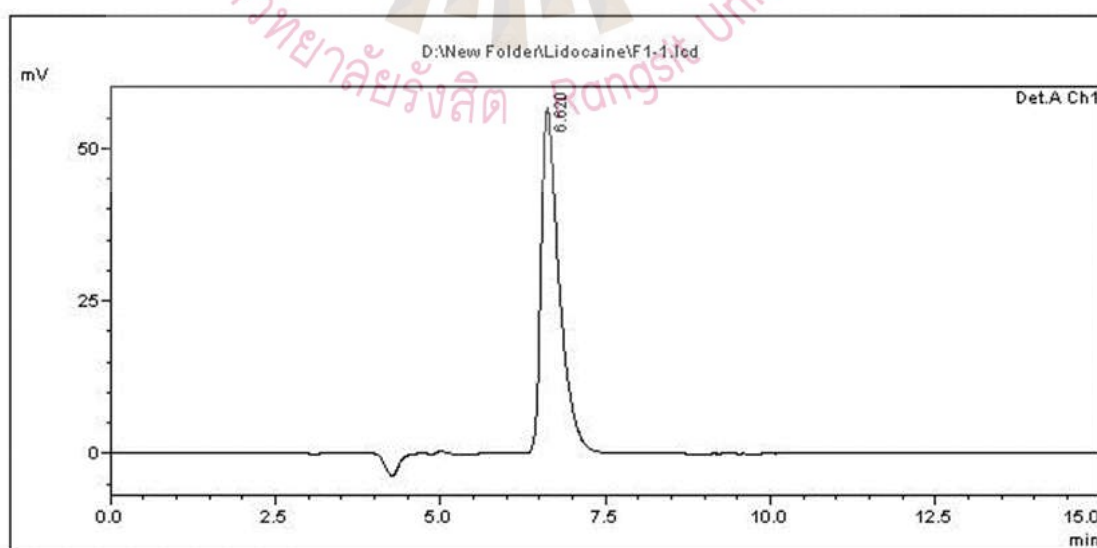


Figure A1 HPLC chromatogram of standard lidocaine hydrochloride.

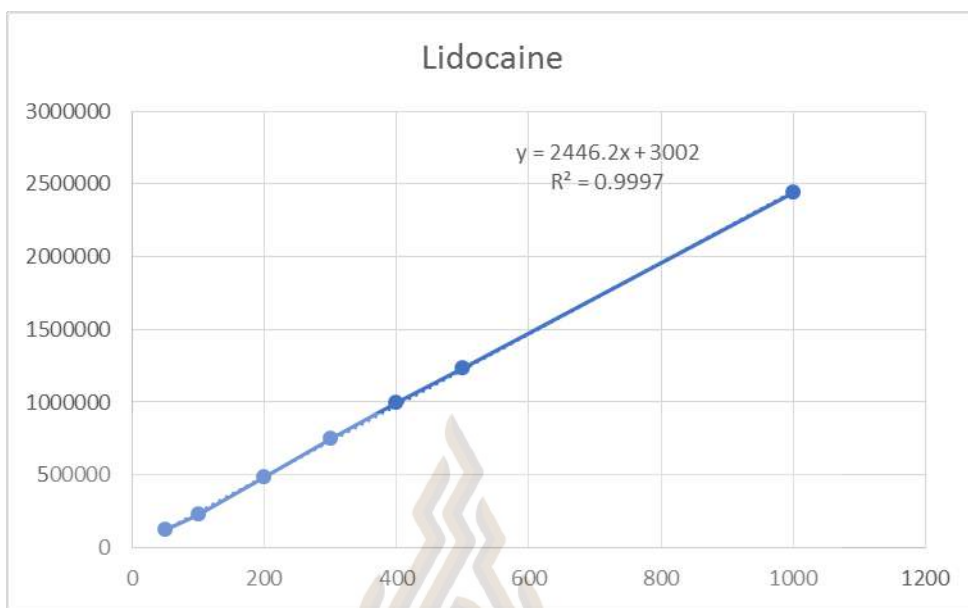


Figure A2 Calibration curve of lidocaine hydrochloride by HPLC analysis

#### Calibration curve of lidocaine hydrochloride in the release study

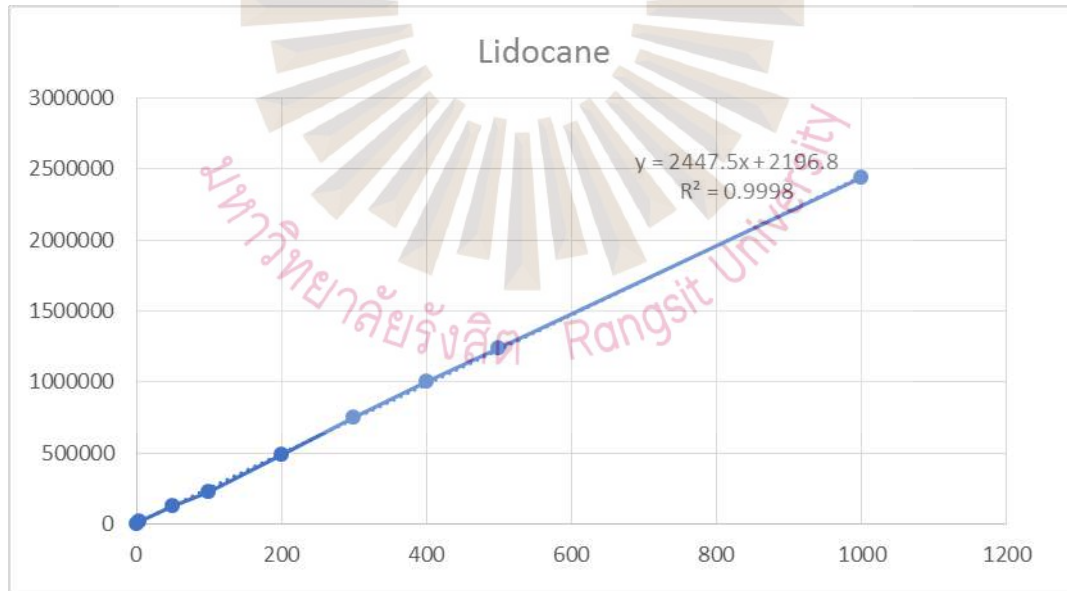


Figure A3 Calibration curve of lidocaine hydrochloride by HPLC analysis in the release study

The logo of Rangsit University is a circular emblem. At the top is a stylized flame or sunburst. Below it, a series of radiating lines form a sunburst pattern. In the center of this pattern, the text "Appendix B" is written in a bold, black, sans-serif font.

**Appendix B**

**Copies of Certified Documents Related to Human Clinical**

มหาวิทยาลัยรังสิต Rangsit University

		COA. No. RSUERB2022-038
<b>เอกสารรับรองโครงการวิจัย (Certificate of Approval)</b> โดย คณะกรรมการจริยธรรมการวิจัยในคน มหาวิทยาลัยรังสิต		
เอกสารรับรองเลขที่ :	COA. No. RSUERB2022-038	
ชื่อโครงการวิจัย :	ผลของการเปรียบเทียบประสิทธิภาพของยาชาเฉพาะที่ลิโดเคนไฮโดรคลอไรด์ในเทอร์โมเซตติงเจลและเบนโซเคนเจลในการทดลองทางคลินิก Comparison topical anesthetic efficacy of lidocaine hydrochloride loaded thermosetting gel (LG) and benzocaine gel (BG) in clinical trials study	
ชื่อหัวหน้าโครงการวิจัย :	อ.ทพ.ณัฐวุฒิ สุขขจรโรจน์	
หน่วยงานที่สังกัด :	วิทยาลัยทันตแพทย์ มหาวิทยาลัยรังสิต	
วิธีทบทวน :	พิจารณาจริยธรรมการวิจัยในคนประเภทเต็มคณะ (Full Board Review)	
เอกสารที่รับรอง :	1. แบบเสนอโครงการวิจัย 2. เอกสารชี้แจงผู้เข้าร่วมการวิจัย 3. หนังสือแสดงเจตนายินยอมเข้าร่วมการวิจัย 4. แบบสอบถาม/แบบสัมภาษณ์	
วันที่รับรอง :	8 เมษายน 2565	
วันที่หมดอายุ :	8 เมษายน 2567	
คณะกรรมการจริยธรรมการวิจัยในคน มหาวิทยาลัยรังสิต ได้พิจารณาและมีมติรับรองเอกสาร ดังที่ระบุไว้ข้างต้น โดยยึดหลักจริยธรรม Declaration of Helsinki, The Belmont Report, CIOMS Guideline และ International Conference on Harmonization in Good Clinical Practice หรือ ICH-GCP		
ลงนาม 		
( รองศาสตราจารย์ ดร. ปานนท์ กาญจนภูมิ ) ประธานคณะกรรมการจริยธรรมการวิจัยในคน มหาวิทยาลัยรังสิต		
<small>คณะกรรมการจริยธรรมการวิจัยในคน สำนักงานจริยธรรมการวิจัย ห้อง 504, ชั้น 5, อาคารอาทิตย์ อุไรรัตน์ (ตึก 1), มหาวิทยาลัยรังสิต โทร. 0-2791-5728 Email: ruethics@rsu.ac.th</small>		

Figure B1 Certificate of Ethic Committee Approval for Clinical Trial protocol

Trial

เอกสารบันทึกประวัติผู้ร่วมวิจัย  
 เลขที่วิจัย.....  
 วัน.....เดือน.....ปี.....

ชื่อ.....นามสกุล.....  
 เพศ.....อายุ.....น้ำหนัก.....  
 ประวัติโรคประจำตัว Past medical history  
 .....Congenital idiopathic methemoglobinemia  
 .....Radiation, Chemotherapy  
 .....Hypertension  
 .....อื่น ๆ  
 .....  
 .....  
 .....  
 การแพ้ Allergy  
 .....Lidocaine hydrochloride  
 .....Sea foods  
 .....อื่น ๆ  
 .....  
 .....  
 .....  
 Allergy and imitating test (inner lower lip)  
 .....Allergy  
     ( ) urticaria  
     ( ) Angioedema  
     ( ) rash  
     ( ) อื่น ๆ  
 .....  
 .....  
 .....Irritate  
     ( ) Wound  
     ( ) Eczema

Figure B2 Participant information form

เอกสารบันทึกผลการวิจัยส่วนที่ 1 หน้า 1

รหัสหมายเลขผู้เข้าร่วมวิจัย.....

การทดลองระยะเวลาและการออกฤทธิ์ของยาชา

Place a vertical mark on the line below to indicate how bad you feel your pain is today

No pain	_____	Worst pain imaginable	15 sec.
No pain	_____	Worst pain imaginable	30 sec.
No pain	_____	Worst pain imaginable	45 sec.
No pain	_____	Worst pain imaginable	1 min.
No pain	_____	Worst pain imaginable	1 min. 15 sec.
No pain	_____	Worst pain imaginable	1 min. 15 sec.
No pain	_____	Worst pain imaginable	1 min. 30 sec.
No pain	_____	Worst pain imaginable	2 min.

Figure B3 VAS form for pinprick test

เอกสารบันทึกผลการวิจัยส่วนที่ 1 หน้า 2  
 รหัสหมายเลขผู้เข้าร่วมวิจัย.....  
 การทดลองระยะเวลาและการออกฤทธิ์ของยาชา

Place a vertical mark on the line below to indicate how bad you feel your pain is today

No pain	_____	Worst pain imaginable	2 min. 15 sec.
No pain	_____	Worst pain imaginable	2 min. 30 sec.
No pain	_____	Worst pain imaginable	2 min. 45 sec.
No pain	_____	Worst pain imaginable	3 min.
No pain	_____	Worst pain imaginable	3 min. 15 sec.
No pain	_____	Worst pain imaginable	3 min. 30 sec.
No pain	_____	Worst pain imaginable	3 min. 45 min
No pain	_____	Worst pain imaginable	4 min.

Figure B3 VAS form for pinprick test (Continue.)

เอกสารบันทึกผลการวิจัยส่วนที่ 2

การทดลองการเปรียบเทียบผลของยาชา

รหัสหมายเลขผู้เข้าร่วมวิจัย.....

ชนิดของยาชา A / B

**Place a vertical mark on the line below to indicate how bad you feel your pain is today**

No pain  Worst pain imaginable

.....

เอกสารบันทึกผลการวิจัยส่วนที่ 2

การทดลองการเปรียบเทียบผลของยาชา

รหัสหมายเลขผู้เข้าร่วมวิจัย.....

ชนิดของยาชา A / B

**Place a vertical mark on the line below to indicate how bad you feel your pain is today**

No pain  Worst pain imaginable

Figure B4 VAS form for anesthetic comparison



## RESEARCH PUBLICATIONS

### Publication: International publication

Supachawaroj, N., Limsitthichaikoon, S. Factors Affecting Gelation of Lidocaine Hydrochloride-Loaded Polyelectrolyte Complex Thermosensitivity Gel for Dry Socket Treatment. *Key Engineering Materials*, 901(1), 111-116.

Supachawaroj, N., Damrongrungruang, T., Limsitthichaikoon, S. Formulation development and evaluation of lidocaine hydrochloride loaded in chitosan-pectin-hyaluronic acid polyelectrolyte complex for dry socket treatment. *Saudi Pharmaceutical Journal*, 29(9), 1070-1081.



## Biography

Name	Nuttawut Supachawaroj
Date of birth	January 16, 1976
Place of birth	Bangkok, Thailand
Education background	Mahidol University Diploma in Clinical Sciences (Oral and Maxillofacial Surgery), 2002 Chulalongkorn University, Thailand Doctor of Dental Surgery, 1999 Rangsit University, Thailand Doctor of Philosophy in Pharmacy, 2022
Address	299/225 Burasiri, Onnut, Bangna Bangkok Thailand 10250
Place of work	College of dental medicine, Rangsit university
Work position	Lecturer

